

INFORMATION TO USERS

This manuscript has been reproduced from the microfilm master. UMI films the text directly from the original or copy submitted. Thus, some thesis and dissertation copies are in typewriter face, while others may be from any type of computer printer.

The quality of this reproduction is dependent upon the quality of the copy submitted. Broken or indistinct print, colored or poor quality illustrations and photographs, print bleedthrough, substandard margins, and improper alignment can adversely affect reproduction.

In the unlikely event that the author did not send UMI a complete manuscript and there are missing pages, these will be noted. Also, if unauthorized copyright material had to be removed, a note will indicate the deletion.

Oversize materials (e.g., maps, drawings, charts) are reproduced by sectioning the original, beginning at the upper left-hand corner and continuing from left to right in equal sections with small overlaps.

Photographs included in the original manuscript have been reproduced xerographically in this copy. Higher quality 6" x 9" black and white photographic prints are available for any photographs or illustrations appearing in this copy for an additional charge. Contact UMI directly to order.

ProQuest Information and Learning
300 North Zeeb Road, Ann Arbor, MI 48106-1346 USA
800-521-0600

UMI[®]

**PRECIPITATION OF NICKEL SULPHATE
FROM DECOPPERISED ACID SOLUTION BY
SOLVENT DISPLACEMENT CRYSTALLISATION**

Georgiana A. Moldoveanu

**Department of Mining and Metallurgical Engineering
McGill University
Montreal, Canada**

September, 1999

**A Thesis submitted to the Faculty of Graduate Studies and Research
in partial fulfillment of the requirements of the degree of Master of
Engineering**

© Georgiana A. Moldoveanu, 1999



National Library
of Canada

Acquisitions and
Bibliographic Services

395 Wellington Street
Ottawa ON K1A 0N4
Canada

Bibliothèque nationale
du Canada

Acquisitions et
services bibliographiques

395, rue Wellington
Ottawa ON K1A 0N4
Canada

Your file *Votre référence*

Our file *Notre référence*

The author has granted a non-exclusive licence allowing the National Library of Canada to reproduce, loan, distribute or sell copies of this thesis in microform, paper or electronic formats.

The author retains ownership of the copyright in this thesis. Neither the thesis nor substantial extracts from it may be printed or otherwise reproduced without the author's permission.

L'auteur a accordé une licence non exclusive permettant à la Bibliothèque nationale du Canada de reproduire, prêter, distribuer ou vendre des copies de cette thèse sous la forme de microfiche/film, de reproduction sur papier ou sur format électronique.

L'auteur conserve la propriété du droit d'auteur qui protège cette thèse. Ni la thèse ni des extraits substantiels de celle-ci ne doivent être imprimés ou autrement reproduits sans son autorisation.

0-612-64238-0

Canada

ABSTRACT

Nickel constitutes the major impurity encountered during copper electrorefining (Cu ER) operations. Continuous nickel build-up in the electrolyte is controlled by withdrawing a fraction of solution from the tankhouse and separate nickel as crude $\text{NiSO}_4 \cdot 2\text{H}_2\text{O}$ via *Evaporative Crystallisation*. The energy required to evaporate water is high, increasing thus the operation costs; moreover, the product thus obtained is of poor quality in terms of purity and crystal size.

As part of an ongoing research project launched at McGill University, the *Solvent Displacement Crystallisation* (SDC) technique is investigated as an attractive alternative to the conventional method. SDC involves the addition of low-boiling point, water-miscible organic solvents (MOS) to aqueous solutions to cause salt precipitation based on the "salting out" effect. The crystals are separated by filtration whereas the solvent is subsequently recovered for reuse by low-temperature distillation.

The present work describes the successful application of SDC method to the precipitation of $\text{NiSO}_4 \cdot 6\text{H}_2\text{O}$ from Cu ER spent electrolytes. Tests have been performed on synthetic and industrial electrolytes (courtesy of Canadian Copper Refineries), using Isopropanol as precipitant. By maintaining a low supersaturation (i.e. controlled addition of the solvent to the electrolyte) and heterogeneous crystallisation conditions (use of seed/product recycling), crystal growth is favoured while impurity uptake/contamination is minimised.

RESUMÉ

Le nickel représente la plus importante impurité présente dans les opérations de raffinage électrolytique du cuivre. L'accumulation graduelle du nickel dans l'électrolyte est contrôlée en retirant une fraction de la solution et en séparant le nickel comme un sulfate impur $\text{NiSO}_4 \cdot 2\text{H}_2\text{O}$ par *Evaporation - Crystallisation*. L'énergie nécessaire pour vaporiser l'eau est élevée, ce qui augmente les coûts de l'opération. De plus, le produit ainsi obtenu est d'une mauvaise qualité (en termes de pureté et dimension des particules).

Dans le cadre d'un projet de recherches débuté à McGill, la technique de *Crystallisation par Remplacement du Solvant* (CRS) est examinée comme une alternative intéressante à la méthode conventionnelle. La CRS implique l'addition à la solution aqueuse d'un solvant organique miscible à l'eau, avec un bas point d'ébullition, pour causer la précipitation du composé inorganique par l'effet de "salting-out". Les cristaux sont séparés par filtration et le solvant est récupéré par distillation à basse température.

La présente thèse décrit l'utilisation de la CRS pour précipiter le $\text{NiSO}_4 \cdot 6\text{H}_2\text{O}$ de l'électrolyte usagé issu de les opérations de raffinage électrolytique du cuivre. Des tests ont été effectués sur des solutions synthétiques et industrielles (de Canadian Copper Refineries) en employant l'Isopropanole comme agent de précipitation. Une basse supersaturation (i.e. addition contrôlée du solvant à l'électrolyte) et des conditions hétérogènes de cristallisation (l'emploi d'une germe cristallin) favorisent la croissance des cristaux en même temps que la contamination avec certaines impuretés est minimisée.

ACKNOWLEDGEMENTS

First of all I would like to express my deepest appreciation and respect to my supervisor, Prof. George P. Demopoulos, who started up this novel work and let me be part of it. He always had time and patience to answer numerous questions but also gave me room to learn on my own. And, most important, I've learned that time management is the key of success in any enterprise.

I am indebted to Canadian Copper Refineries, in particular Jack Stafiej, David Tracy and Tom Whitton for all their help and their willingness to provide materials and information.

Extremely thankful I am to Monique Riendeau for her invaluable skills and patient assistance for XRD and AA analyses and to Helen Campbell for kindly helping me every time I needed SEM imaging and technical expertise. I am most grateful for all the help Purnima and Carol provided whenever I had administrative issues to solve.

A huge thanks to everyone in the hydromet lab, especially Frank and Niels for providing a great working environment, for enthusiasm and patiently answering lots of my (not always so clever) questions.

Special thanks to my parents for their permanent support, love and for their wisdom in letting me go across the Atlantic to find my way.

Last but certainly not least, I wish to acknowledge my friends Raluca and Radu, whose contagious optimism and *joie de vivre* boosted up my morale every time we met.

Finally, I am happy to dedicate this work to my husband Corneliu, who has so much confidence in me, continuously encouraged me when I was discouraged and always patiently put up with me through all the hard times.

TABLE OF CONTENTS

ABSTRACT	ii
RESUMÉ	iii
ACKNOWLEDGEMENTS	iv
TABLE OF CONTENTS	v
LIST OF FIGURES	viii
LIST OF TABLES	x
1. INTRODUCTION	1
1.1 Industrial Practice of Electrolyte Purification in Cu ER	1
1.2 Nickel Sulphate Precipitation by SDC	2
1.3 Research Objectives	3
2. LITERATURE REVIEW AND THEORY	5
2.1 Industrial Practice of Nickel Sulphate Removal in CuER	5
2.1.1 General description of Cu ER process	5
2.1.2 Impurity behaviour in Cu ER	6
2.1.3 Electrolyte purification in Cu ER	9
2.1.4 Nickel sulphate removal by Evaporative Crystallisation	12
2.2 Solvent Displacement Crystallisation	15
2.2.1 Salting-out effect	15
2.2.2 SDC into historical perspective	17
2.2.3 Conceptual flowsheet and advantages	19
2.2.4 Criteria for Miscible Organic Solvent selection	20
2.3 Solubility Data for Nickel Sulphate	21
2.3.1 Influence of temperature	21
2.3.2 Influence of H ₂ SO ₄	22
2.3.3 Influence of organic solvents	22
2.4 Crystallisation from Solution	23
2.4.1 Crystallisation driving force	23
2.4.2 Nucleation	25

2.4.3 Growth	28
2.4.4. Effect of impurities	30
3. EXPERIMENTAL	32
3.1 Materials	32
3.2 Experimental Set-up	33
3.2.1 Crystallisation tests	33
3.2.2 Distillation	34
3.3 Experimental Procedure	35
3.3.1 Crystallisation tests	35
3.3.2 Distillation	36
3.4 Analytical Methods	37
3.4.1 Aqueous samples	37
3.4.2 Solid product	37
4. RESULTS AND DISCUSSION	39
4.1 Preliminary Tests	39
4.1.1 Solubility of nickel sulphate in IP-H ₂ O-H ₂ SO ₄ system	39
4.1.2 Anatomy of a SDC test	40
4.1.3 SDC using the azeotrope	44
4.1.4 Effect of temperature	46
4.1.5 Final acidity of aqueous phase	48
4.2 Homogeneous Crystallisation Tests at 20°C	50
4.2.1 Tests conducted at high supersaturation	50
4.2.1.1 Influence of O/A ratio on [Ni] _{aq}	50
4.2.1.2 Equilibrium concentration of Ni and Induction time	51
4.2.1.3 Kinetics study	54
4.2.2 Tests conducted at low supersaturation	55
4.2.2.1 Critical supersaturation line	55
4.2.2.2 SDC tests at low supersaturation	57
4.2.3 Influence of supersaturation	59

4.2.3.1 Final nickel concentration in aqueous	60
4.2.3.2 Crystal quality	61
4.3 Heterogeneous Crystallisation Tests	63
4.3.1 Comparative SDC tests	63
4.3.2. Effect of product recycling	66
4.3.2.1 Crystal quality	66
4.3.2.2 Settling velocity	69
4.3.2.3 Solids density	70
4.4 Impurity Behaviour	73
4.4.1 Effect of impurities on crystal growth	73
4.4.2 Behaviour of Calcium	74
4.4.3 Crystal quality: Solvent Displacement Crystallisation vs. Evaporative Crystallisation	77
4.4.3.1 Particle size	77
4.4.3.2 Crystal purity	79
4.5 Flow-sheet Development	82
4.5.1 Production of NiSO ₄ ·6H ₂ O from industrial electrolyte	82
4.5.2 Control of gypsum precipitation	83
5. CONCLUSIONS AND RECOMMENDATIONS	85
5.1 Conclusions	85
5.2 Recommendations for Future Work	86
REFERENCES	87
APPENDICES	91
Appendix A: Free Acid Determination in Strong NiSO₄-H₂SO₄-H₂O solutions	91
Appendix B: Isopropanol Properties	94
Appendix C: Fractional Distillation	97
Appendix D: Hydrates of Nickel Sulphate	101

LIST OF FIGURES

Figure 2.1	Copper electrorefinery flowsheet	5
Figure 2.2	Influence of H ₂ SO ₄ concentration on the solubility of nickel sulphate at different temperatures	12
Figure 2.3	Evaporative crystallisation flowsheet	13
Figure 2.4	Evaporative crystallisers	14
Figure 2.5	Excess enthalpies of mixing of alcohols and water at 25°C	16
Figure 2.6	Metal solubility in aqueous-organic solutions	18
Figure 2.7	Conceptual flowsheet of nickel removal via SDC	19
Figure 2.8	Effect of temperature on the solubility of nickel sulphate	21
Figure 2.9	Nickel sulphates solubility in H ₂ O-CH ₃ OH at 15°C	23
Figure 2.10	Solubility-supersaturation diagram	24
Figure 2.11	Interfacial tensions at the boundaries between three phases	26
Figure 2.12	Supersaturation-controlled crystallisation process	28
Figure 2.13	Growth models	29
Figure 2.14	Sited for impurity adsorption on a growing crystal	31
Figure 3.1	Experimental set-up for the SDC test	33
Figure 3.2	Fractional distillation set-up	34
Figure 4.1	Nickel sulphate solubility in IP-H ₂ O-H ₂ SO ₄ system at 20°C	40
Figure 4.2	Preliminary SDC test (20°C, pure IP)	41
Figure 4.3	Influence of O/A on [Ni] _{aq} during SDC	41
Figure 4.4	XRD spectrum of crystals obtained from a preliminary SDC test	43
Figure 4.5	Comparative SDC tests using IP and azeotrope (20°C)	45
Figure 4.6	Effect of temperature on SDC (MOS=IP)	46
Figure 4.7	SEM images of nickel sulphate crystals (preliminary tests)	47
Figure 4.8	Influence of O/A on [Ni] _{aq}	51
Figure 4.9	Influence of O/A on the induction time	52
Figure 4.10	Equilibrium values of Ni function of O/A	53
Figure 4.11	Comparative kinetics study	54
Figure 4.12	Critical supersaturation line for the synthetic electrolyte	56

Figure 4.13	Critical supersaturation line for the industrial electrolyte	57
Figure 4.14	Comparative SDC tests at low supersaturation.....	58
Figure 4.15	Final nickel concentration as a function of supersaturation, compared to equilibrium values	60
Figure 4.16	Images of crystals obtained via homogeneous SDC	62
Figure 4.17	Heterogeneous crystallisation test for synthetic electrolyte	63
Figure 4.18	Heterogeneous crystallisation test for industrial electrolyte	65
Figure 4.19	SEM images of NiSO ₄ .6H ₂ O produced from synthetic solution via heterogeneous SDC	67
Figure 4.20	SEM images of NiSO ₄ .6H ₂ O produced from industrial solution via heterogeneous SDC	68
Figure 4.21	Influence of crystallisation strategy on settling velocities	70
Figure 4.22	Influence of crystallisation approach on solids density	71
Figure 4.23	Gypsum particles separated during SDC process of nickel sulphate	75
Figure 4.24	EDS spectrum of NiSO ₄ .6H ₂ O containing the white precipitate	75
Figure 4.25	EDS spectrum of gypsum	76
Figure 4.26	Particles of nickel sulphate produced from the industrial solution	78
Figure 4.27	XRD spectrum of NiSO ₄ .2H ₂ O produced via EC at CCR	80
Figure 4.28	XRD spectrum of NiSO ₄ .6H ₂ O produced via SDC	80
Figure 4.29	SDC of nickel sulphate from industrial decopperised electrolyte	82
Figure 4.30	SDC of nickel sulphate with gypsum partial removal option	84
Figure C.1	Isopropanol-water phase diagram	100

LIST OF TABLES

Table 2.1	Typical copper anode data	7
Table 2.2	Standard electrochemical potentials of elements involved during Cu ER process	7
Table 2.3	Nickel phases and their behaviour during electrorefining	8
Table 2.4	Typical nickel contents of copper anodes, cathodes and cellhouse electrolytes	9
Table 3.1	Chemicals used in experimental work	32
Table 3.2	Industrial electrolyte composition	32
Table 4.1	Development of a fractional distillation experiment following SDC	43
Table 4.2	Materials mass balances	44
Table 4.3	Initial and final parameters during SDC ($T = 20^{\circ}\text{C}$)	45
Table 4.4	Initial and final parameters during SDC at different temperatures	46
Table 4.5	Sulphuric acid concentration before and after distillation	48
Table 4.6	Influence of O/A on nickel concentration in aqueous phase	50
Table 4.7	Influence of O/A on some process parameters	53
Table 4.8	Comparative SDC results at low supersaturation ($O/A_{\text{total}}=1.5$)	58
Table 4.9	Final nickel concentration in homogeneous SDC tests	60
Table 4.10	Chemical compositions of nickel sulphate solutions	73
Table 4.11	Chemical composition of nickel sulphate crystals	79
Table A.1	Preparation of $\text{H}_2\text{SO}_4\text{-NiSO}_4$ standard solutions	92
Table B.1	Physical properties of isopropanol	94
Table C.1	Theoretical plates required to separate liquid mixtures	98
Table D.1	Nickel sulphate hydrates	102

1. INTRODUCTION

1.1 Electrolyte Purification in Copper Electrorefining

The majority of the world's copper production (more than 8×10^6 tonnes/year) originates from the smelting of copper sulphide concentrates and occasionally the pyrometallurgical treatment of copper scraps. During this pyrometallurgical processing, many impurities report to the copper anodes.

Marketable copper (99.99+% Cu) essentially free of any deleterious elements (less than 20 ppm impurities) is produced by **electrorefining**. The procedure entails:

- (a) dissolving copper from impure anodes (99% Cu) into $\text{CuSO}_4\text{-H}_2\text{SO}_4\text{-H}_2\text{O}$ electrolyte;
- (b) selectively electroplating pure copper without the anode impurities onto cathode.

The impurities in anodes occur in solid solution in the copper metal matrix and in discrete inclusions at the copper grain boundaries. During electrorefining, all the impurities undergo chemical and/or morphological changes that impact significantly on anode passivation, cathode quality, electrolyte purification and recovery of by-products from the anode slimes.

Cathode contamination as well as anode passivation (hence the cessation of the ER operation) can be avoided by maintaining a strict control of impurities (both soluble and insoluble) in the electrolyte. The conventional practice of impurity control consists of continuously withdrawing a certain volume of electrolyte from the circulation system to recover its copper content and isolate/remove the soluble impurities. The steps involved are:

- (a) Decopperising: practised by electrowinning in liberator cells;
- (b) Removal of As, Bi, Sb: by EW or, more recently, combining IX/SX;
- (c) Nickel recovery: by *evaporative crystallisation*.

Nickel is said to be one of the worst elements in contributing to decreased copper electrical conductivity as it forms a solid solution with copper. Its concentration in copper anodes ranges from 14 to 6700 ppm whereas the maximum permissible level of nickel in copper cathodes must be less than 7 ppm. Much of the nickel dissolves along with the copper during electrolysis and accumulates as nickel sulphate in the electrolyte. Nickel recovery from the decopperised electrolyte is the last step of impurity control process. The current procedure to remove nickel sulphate from copper sulphate electrolytes is by *evaporative*

crystallisation. This technique is both difficult and expensive. Evaporative crystallisation involves the evaporation of water until H_2SO_4 concentration has increased sufficiently to ensure almost complete precipitation of $\text{NiSO}_4 \cdot 2\text{H}_2\text{O}$ (the solubility of nickel sulphate decreases with increasing acid concentration). After cooling, the solids are recovered by centrifugation, water-washed and packaged without further purification. The residual solution is a very concentrated, impure, sulphuric acid (referred as "black acid"), which can be either returned to the refinery for acid control or used to leach anode slimes.

Although practised for long time, nickel sulphate removal by evaporative crystallisation shows nevertheless some major disadvantages:

- (a) the residual solutions are extremely corrosive, resulting in high operating and maintenance costs;
- (b) the evaporation step required to remove water is highly energy intensive, increasing therefore the operating costs;
- (c) the final product ($\text{NiSO}_4 \cdot 2\text{H}_2\text{O}$) is of poor quality in terms of purity and crystal-size.

1.2 Solvent Displacement Crystallisation

Research conducted by Cohen in the eighties (Cohen, 1987) suggested that an alternative crystallisation process could be developed that would recover nickel sulphate with less energy consumption. The method is referred as *Solvent Displacement Crystallisation* (SDC) and involves the addition of low-boiling point, water-miscible organic solvents (MOS) to aqueous solutions to cause the crystallisation of inorganic salts, based on the concept of "salting out effect". This enables the separation of electrolytes from their aqueous solutions via precipitation and filtration. A general explanation of this effect indicates that there is a competition between the polar organic molecules and inorganic ions for the water molecules. Since the organic solvent exhibits a higher affinity for water, this will lead to capture of part of the hydration water molecules, causing thus salt precipitation. The solvent is subsequently recovered for reuse by employing relatively inexpensive low-temperature or vacuum distillation.

This novel technique appears to offer a number of advantages over the conventional method:

- (a) the potential to reduce energy costs in the recovery of inorganic salts from aqueous process streams;
- (b) a high solute recovery yield may be obtained by selecting the appropriate water-miscible solvent;
- (c) fine $\text{NiSO}_4 \cdot 6\text{H}_2\text{O}$ (as opposed to crude $\text{NiSO}_4 \cdot 2\text{H}_2\text{O}$) can be produced directly from decopperised electrolyte.

The integration of this crystallisation method into the conventional electrolyte purification flowsheet would comprise:

- (a) addition of a low-boiling point, water-miscible organic solvent to the decopperised electrolyte that leaves the liberator cells;
- (b) separation of crystals by filtration
- (c) recovery of organic solvent by low-temperature or vacuum distillation;

1.3 Research Objectives and Thesis Outline

Research Objectives:

- Confirm Cohen's work (Cohen, 1987) by employing isopropanol (IP) as water-miscible organic solvent to homogeneously precipitate nickel sulphate from a synthetic electrolyte solution ($\text{NiSO}_4\text{-H}_2\text{SO}_4\text{-H}_2\text{O}$)
- Design a SDC procedure that yields clean, well-grown crystals and achieves low final nickel concentration in the aqueous phase by controlling supersaturation via the regulated mixing of the organic solvent with the electrolyte and using seed/product recycling.
- Test the newly designed SDC method with industrial electrolyte solutions and compare the product quality with that obtained by the conventional procedure.

Thesis Outline

- Chapter 2 critically reviews the industrial practice of nickel sulphate removal, as practised in copper electrorefineries. As the conventional method involves the precipitation of $\text{NiSO}_4 \cdot 2\text{H}_2\text{O}$ from the system $\text{NiSO}_4\text{-H}_2\text{SO}_4\text{-H}_2\text{O}$, a special attention will be given to nickel sulphate solubility data and the factors affecting it. The same chapter

describes the principles of the SDC method and briefly presents the Crystallisation Theory applied in conjunction to this technique.

- Chapter 3 describes the experimental set-ups and procedures used to achieve the objectives proposed as well as the analytical methods employed.
- Chapter 4 summarises and discusses the results yielded by the SDC tests. The influence of several factors are presented (temperature, volume of organic solvent, supersaturation), with respect to the crystal quality on one hand (in terms of purity and size) and to the final nickel concentration in the aqueous phase on the other hand. Parallel experiments performed on synthetic and industrial solutions are outlined and their results comparatively discussed.
- Chapter 5 provides conclusions and suggestions for future work.
- The Appendices constitute the last section. They provide information on analysis, properties of nickel sulphate hydrates, properties of isopropanol and fractional distillation.

2. LITERATURE REVIEW AND THEORY

2.1 Industrial Practice of Nickel Sulphate Removal in Copper Electrorefining

2.1.1. General description of copper electrorefining process

Almost all copper is treated electrochemically during its production from ore; considerable copper scrap is also electrorefined (figure 2.1). In either case, many impurities report to the copper anodes. Marketable copper, melted and cast must contain less than 20 ppm impurities (Biswas and Davenport, 1994).

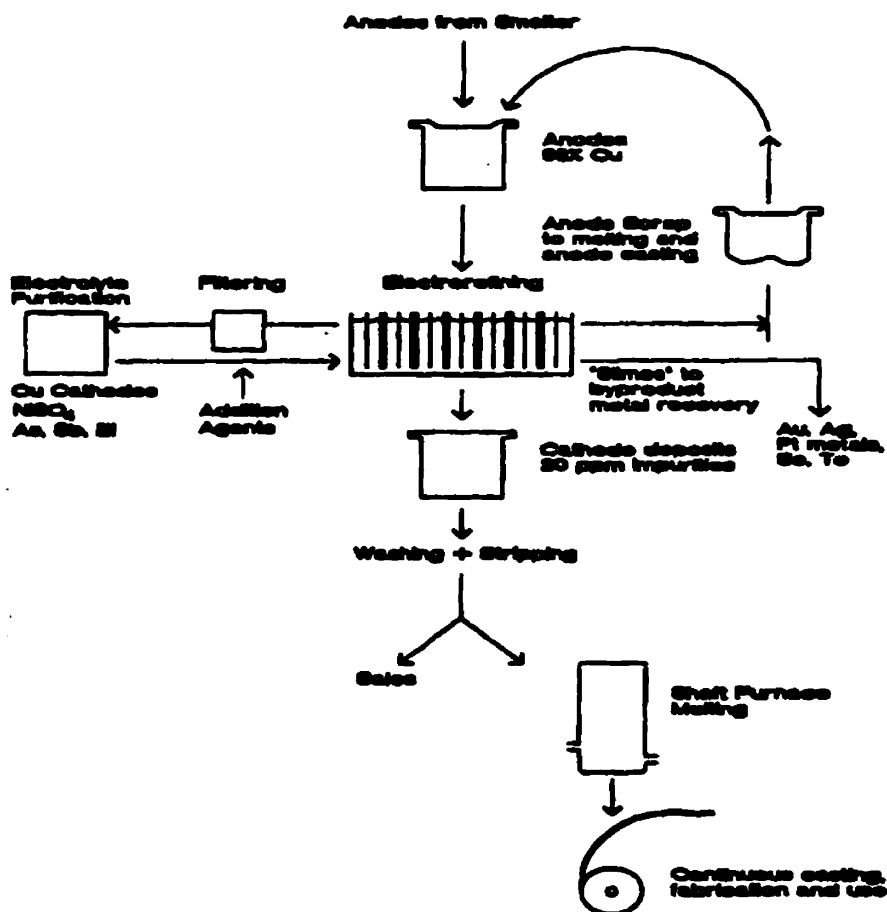


Figure 2.1 Cu ER flowsheet (Biswas and Davenport, 1994)

The Cu ER procedure entails the application of an electrical potential between an impure copper anode and a metal cathode in a $\text{CuSO}_4\text{-H}_2\text{SO}_4\text{-H}_2\text{O}$ electrolyte, so that:

(a) Copper is electrochemically dissolved from the anode into the solution, producing cations and electrons:
$$\text{Cu}^0_{\text{anode}} \rightarrow \text{Cu}^{2+} + 2\text{e}^-, \quad e^0 = 0.34 \text{ V} \quad (2.1)$$

(b) The electrons produced by reaction (1) are conducted towards the cathode through the external circuit and power supply;

(c) The Cu^{2+} cations migrate to the cathode by convection and diffusion/migration;

(d) The electrons and Cu^{2+} recombine at the cathode surface to produce copper metal which plates on the cathode:
$$\text{Cu}^{2+} + 2\text{e}^- \rightarrow \text{Cu}^0_{\text{cathode}}, \quad e^0 = 0.34 \text{ V} \quad (2.2)$$

The overall Cu ER reaction is:
$$\text{Cu}^0_{\text{anode}} \rightarrow \text{Cu}^0_{\text{cathode}}, \quad E_{\text{int}} = 0 \text{ V}. \quad (2.3)$$

Impurities are prevented from plating on the cathode by:

(a) choosing an electrolyte ($\text{CuSO}_4\text{-H}_2\text{SO}_4\text{-H}_2\text{O}$) in which some anode components do not dissolve;

(b) keeping soluble impurities at low concentrations in the electrolyte so that they do not affect the process.

Item (b) is accomplished by withdrawing and purifying an electrolyte bleed stream.

Copper electrorefining serves two purposes:

- it produces copper essentially free of deleterious impurities;
- it separates valuable elements (e.g. gold, silver, PGM) from the copper for subsequent recovery as by-products.

2.1.2 Impurity behaviour in copper electrorefining

As mentioned above, electrorefining in a $\text{CuSO}_4\text{-H}_2\text{SO}_4\text{-H}_2\text{O}$ electrolyte is universally employed to produce the required high-purity copper from the impure anodes. The impurities in copper anodes occur both in solid solution in the copper metal matrix and in discrete inclusions at the copper grain boundaries. During ER, all impurities undergo extensive chemical and/or morphological changes that impact significantly on anode passivation and cathode quality. Table 2.1 presents the typical composition for anodes and the form in which each element occurs (Chen and Dutrizac, 1990-a).

Table 2.1 Typical copper anode data (Chen and Dutrizac, 1990-a)

ELEMENT	COMPOSITIONAL RANGE (%)	OCCURRING FORM
Cu	>99	Cu, Cu ₂ O, Cu ₂ (Se,Te), complex oxides
Ni	0.02 - 0.67	Ni solid solution, NiO, complex oxides
Pb	0.006 - 0.27	Pb solid solution, complex oxides
Se	0.034 - 0.22	Cu ₂ (Se,Te) and Ag ₂ (Se,Te)
Te	0.001 - 0.007	Cu ₂ (Se, Te) and Ag ₂ (Se,Te)
As	0.004 - 0.039	As solid solution, complex oxides
Sb	3 ppm - 0.022	Complex oxides
Bi	5 ppm - 0.007	Complex oxides
Ag	0.035 - 0.21	Ag solid solution, Cu-Ag alloy
Au	6 ppm - 47 ppm	Au solid solution
Fe	0.001 - 0.006	NiFe ₂ O ₄ , Cu-Ni-Fe complex oxide
O ₂	0.11 - 0.15	oxide

Isakov (1973) divides anodic impurities into three groups according to their behaviour during electrolysis, which depends on their standard reduction potential as compared to that of copper (Table 2.2):

- **First group:** metals more electronegative than Cu that are not deposited and pass almost completely into solution where accumulate: **Ni, Fe, Zn, Co.**
- **Second group:** metals more electropositive than Cu that do not dissolve in the electrolyte and pass almost completely into the slime: **Au, Ag, Se, Te, PGM.** Insoluble salts such as: **PbSO₄** or **Sn(OH)₂SO₄** report also to the slimes.
- **Third group:** metals that have potentials similar to that of Cu: **As, Sb, Bi.** They pass into solution when the anode dissolves and can be deposited under the appropriate conditions (high concentration of these elements, low Cu concentration). **AsO₃⁻⁴** can also react with Sb and Bi to form insoluble compounds known as "floating slimes".

Table 2.2 Standard electrochemical potentials of elements involved during Cu ER

(Biswas and Davenport, 1994)

ELEMENT	ELECTROCHEMICAL REACTION	E ⁰ _{RED} (V)
Cu	$\text{Cu}^{2+} + 2\text{e}^- \rightarrow \text{Cu}^0$	0.34
Zn	$\text{Zn}^{2+} + 2\text{e}^- \rightarrow \text{Zn}^0$	-0.7
Ni	$\text{Ni}^{2+} + 2\text{e}^- \rightarrow \text{Ni}^0$	-0.23
Co	$\text{Co}^{2+} + 2\text{e}^- \rightarrow \text{Co}^0$	-0.28
Fe	$\text{Fe}^{2+} + 2\text{e}^- \rightarrow \text{Fe}^0$	-0.45

Pb	$\text{Pb}^{2+} + 2\text{e}^- \rightarrow \text{Pb}^0$	-0.13
Au	$\text{Au}^{3+} + 3\text{e}^- \rightarrow \text{Au}^0$	1.42
Ag	$\text{Ag}^+ + \text{e}^- \rightarrow \text{Ag}^0$	0.8
As	$\text{HAsO}_2 + 3\text{H}^+ + 3\text{e}^- \rightarrow \text{As}^0 + \text{H}_2\text{O}$	0.25
Sb	$\text{SbO}^+ + 2\text{H}^+ + 3\text{e}^- \rightarrow \text{Sb}^0 + \text{H}_2\text{O}$	0.21
Bi	$\text{BiO}^+ + 2\text{H}^+ + 3\text{e}^- \rightarrow \text{Bi}^0 + \text{H}_2\text{O}$	0.32
O ₂	$1/2\text{O}_2 + 2\text{H}^+ + 2\text{e}^- \rightarrow \text{H}_2\text{O}$	1.23

▪ **Behaviour of Nickel during Cu ER**

Nickel is a common impurity in copper anodes; its concentration ranges from 14 to 6700 ppm. Chen and Dutrizac (1990-b) have reported detailed experimental studies on Ni-bearing copper anodes. They concluded that all of the nickel in copper anodes containing less than 0.3% Ni (wt) occurs in solid solution in the copper matrix, regardless of the oxygen content and the presence of other impurities. When the anodes contain more than 0.3% Ni, NiO forms (as crystals present at the copper grain boundaries); if the antimony is present, some kupferglimmer ($\text{Cu}_3\text{Ni}_{2-x}\text{SbO}_{6-x}$, $x = 0.1-0.3$) is also produced. Both these phases are considered undesirable, as they report to the anode slimes.

The common presence of nickel in commercial copper anodes creates a number of problems during the electrorefining process and the subsequent treatment of the slimes.

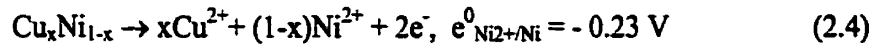
Table 2.3 presents the main nickel carriers in copper anodes and offers a general perspective of the behaviour of nickel during Cu ER.

Table 2.3 Nickel phases and their behaviour during Cu ER (Chen and Dutrizac, 1990-b)

Anode	Electrolyte	Anode Slimes
Ni in solid solution in the Cu matrix	Dissolves as NiSO_4 (*)	Partly precipitates as $\text{NiSO}_4 \cdot n\text{H}_2\text{O}$, $(\text{Cu}, \text{Ni})\text{SO}_4 \cdot 5\text{H}_2\text{O}$
Kupferglimmer ($\text{Cu}_3\text{Ni}_{2-x}\text{SbO}_{6-x}$)	Partly dissolves as NiSO_4	Refractory as $\text{Cu}_3\text{Ni}_{2-x}\text{SbO}_{6-x}$
NiO	- (refractory)	NiO
Mixed Ni-M oxides (M = Fe, Cu, Sn, Sb, Zn) Cu-Ni silicates	- (refractory)	Mixed Ni-M oxides (M = Fe, Cu, Sn, Sb, Zn) Cu-Ni silicates

(* species in bold indicate the final phases)

As the copper anode corrodes electrochemically, nickel present in solid solution dissolves along with Cu but do not plate (less noble than copper - Table 2.2) thus accumulating in the solution:



Although most of the dissolved Ni accumulates in solution (> 99%), a small amount re-precipitates as $\text{NiSO}_4 \cdot x\text{H}_2\text{O}$ or $(\text{Cu},\text{Ni})\text{SO}_4 \cdot 5\text{H}_2\text{O}$ in the anodic slimes layer. The refractory phases such as NiO, mixed oxides and kupferglimmer pass into the slimes.

The concentration of Ni in the electrolyte is largely a function of the nickel content of the anode (table 2.4), as exemplified for some copper refineries. Cathode contamination as well as anode passivation (hence the cessation of the ER operation) can be avoided by maintaining a strict control of impurities in the electrolyte.

Table 2.4 Typical nickel contents of Cu anodes, cathodes and cellhouse electrolytes (Chen and Dutrizac, 1990-b)

Refinery	Ni in Anodes (ppm)	Ni in Cathodes (ppm)	Ni in Electrolyte (g/l)
Rio Tinto Minera, Spain	150	-	0.7
Kidd Creek, Canada	200	0.4	8.0
CCR, Canada	2100	5.5	17
Inco, Canada	6700	1.5	20 - 50
IMI Refiners, England	2800	5	20 - 30

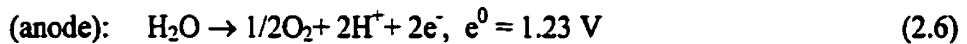
2.1.3. Electrolyte purification in copper electrorefining

For optimum electrorefining conditions, the electrolyte must contain less than 40 g/l Cu, 15 g/l Ni and the lowest possible amount of other impurities (Hoffmann, 1997). Conventional practice for impurity control consists of withdrawing a certain volume of electrolyte from the tank house to recover its copper content and isolate the impurities:

- (1) Cu recovery by **electrowinning**;
- (2) Removal of **As, Sb, Bi** by **electrowinning** or, more recently, by **IX/SX** (Ando and Tsuchida, 1997; Bravo, 1997);
- (3) Ni recovery as nickel sulphate via **evaporative crystallisation** process.

- **Recovery of Copper**

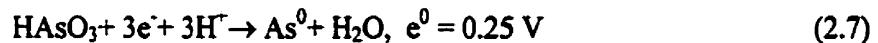
Decopperising is usually practised in stages, by electrowinning in “liberator cells”, using an insoluble Pb alloy anode and copper or stainless steel blanks for the cathode. The electrolyte is impoverished in three sections, starting from ~50 g/l Cu to an intermediate value of ~10 g/l and a final content of less than 1 g/l Cu.



Some of the electrowon Cu is sufficiently pure to be processed as electrolytic cathode. The deposit becomes progressively rougher as the concentration of Cu in the electrolyte decreases. Cathodes produced when the Cu levels are fairly high (15-45 g/l) can be recycled to the anode furnace. As the Cu concentration decreases, through the final EW stages, As, Sb and Bi begin to deposit so those cathodes are sent to the smelter (Braun et al., 1976).

- **Control of Arsenic**

Arsenic concentration is usually controlled by As electrowinning in liberator cells, along with Sb and Bi, after Cu has been electrodeposited. The electrodes used are of the same nature as for Cu EW. The cathodic reaction is:



Because all of these impurities are less noble than copper, their removal also removes any remaining Cu. The product is an impure cathode that is recycled to the smelter.

The main risk of this procedure is the generation of elemental arsenic and arsine (AsH_3), a highly poisonous gas. Several techniques can be employed to reduce arsine generation (Hoffmann, 1997):

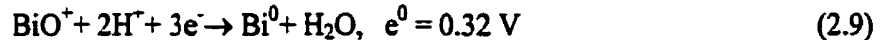
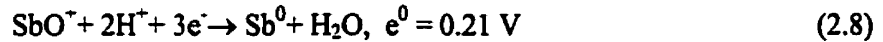
- (1) Periodic reversal of current during impurity removal and gas cooling in order to decompose the hydrides before leaving the stack.
- (2) Maintaining approx. 5 g/l Cu in solution during As EW to recover arsenic as cuprous arsenide (Cu_3As).
- (3) Use of solvent extraction (more recent).

SX practice, while reducing the As concentration in the electrolyte, is incapable of removing all arsenic (Conrad, 1990). However, this technique is efficient enough to keep

impurity levels below refinery specifications (arsenic final concentration is lowered to 6 g/l As).

- ***Control of Antimony and Bismuth***

Electrolytic deposition of Sb and Bi occurs after Cu EW in liberator cells, when the cathode potential becomes sufficiently electronegative. The relative proportions of Sb and Bi in the cathodic deposit increase as the Cu content in the electrolyte decreases so those cathodes are sent to the smelter. The cathodic reactions are:



Chelating resins such as MX-2 (Miyoshi Oil and Fat Company), C-467 (Sumitomo Chemicals Company) and UR-3300 (MESCO) are currently used in plant practice to control Sb and Bi levels during Cu ER (e.g. Hitachi, Tamano or Caraiba Metais refineries) (Ando and Tsuchida, 1997).

- ***Control of Nickel Concentration***

Nyirenda and Phiri (1998) theoretically evaluated the most important species separation and solution purification hydrometallurgical methods that could be applied to nickel control process in Cu ER spent electrolyte.

- (1) Solvent extraction, ion exchange and sulphide precipitation were ruled out as they would have required electrolyte dilution from over 200 g/l sulphuric acid to high pH levels. For example, favourable Ni extraction using LIX 984 requires addition of ammonia to reach pH 9 (Cole and Feather, 1997), which means severe acid loss.
- (2) Cementation was also excluded as would have introduced another element (the cementing agent) into electrolyte. The method would also require neutralisation plus the complete removal of Cu^{2+} ions from solution prior to Ni cementation.
- (3) Chemical (reactive) precipitation of Ni as crystalline nickel ammonium sulphate – $(\text{NH}_4)_2\text{SO}_4 \cdot \text{NiSO}_4 \cdot 6\text{H}_2\text{O}$ – using aqueous ammonia was considered an option. Although able to remove Ni from foul electrolyte, ammonia solution was found unsuitable on account of the low residual acid in the remaining electrolyte. Furthermore, the method would be costly if it had to achieve substantial Ni removal.
- (4) Evaporative crystallisation involves the evaporation of part of water from the bled-off foul electrolyte so that the solubility limit of nickel sulphate in the remaining acid-

enriched liquor is exceeded. As this method is almost universally used for Ni control in copper tankhouses, it will be described in some detail in the next section.

2.1.4. Nickel sulphate removal by evaporative crystallisation

• Principles

When the solubility of a solute in a solvent is not appreciably decreased by a reduction in temperature, supersaturation of the solution can be achieved by the removal by some of the solvent (usually water), inducing thus salt precipitation. This technique is called **Evaporative Crystallisation** and it is employed to recover Ni as crude (impure) nickel sulphate ($\text{NiSO}_4 \cdot 2\text{H}_2\text{O}$) from decopperised electrolytes. The crystallisation occurs according to the reaction (Nyirenda and Phiri, 1998):



(x = number of crystallisation water molecules, depends on temperature and possible presence of dehydrating agents in the medium).

The solution contains components in sulphate forms and free sulphuric acid (>200 g/l, corresponding to ~20% H_2SO_4), which considerably influences the solubility of individual species. From figure 2.2 it is evident that nickel sulphate solubility increases with elevated temperature and decreases with sulphuric acid concentration in solution.

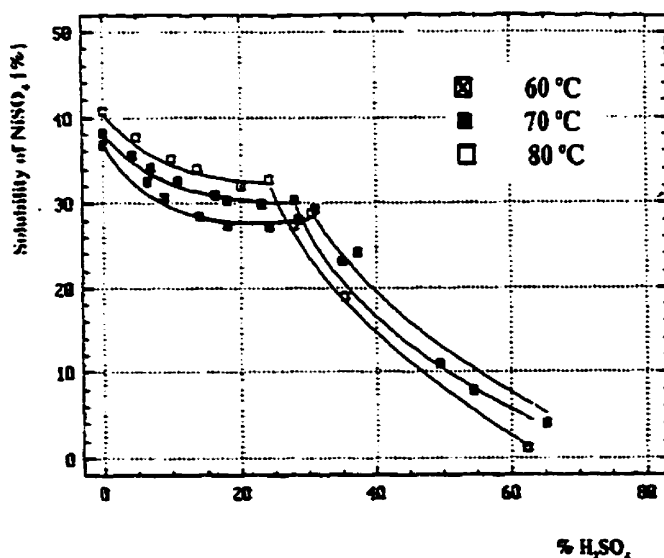


Figure 2.2 Influence of H_2SO_4 concentration on the solubility of nickel sulphate at different temperatures (Havlik et al., 1996)

- **Practical Procedure**

The solution from electrolytic treatment (at this point, the electrolyte contains less than 1 g/l Cu, 17-20 g/l Ni and >200 g/l H₂SO₄.) passes to an evaporator where water is removed (figure 2.3). Evaporation continues until H₂SO₄ concentration has increased sufficiently to ensure complete precipitation of the Ni content as NiSO₄·2H₂O. The crystals are separated by centrifuging, water-washed to displace H₂SO₄ and packaged.

The evaporative crystallisation technique targets a final nickel concentration of ~6-7 g/l in the residual solution. The residual solution (referred as “Black Acid”), containing more than 1000 g/l H₂SO₄, can be either returned to the refinery for acid control or used to leach anode slimes (Hoffmann, 1997).

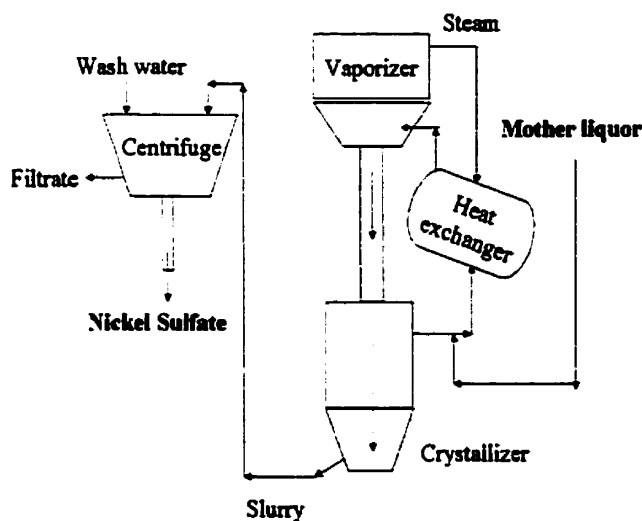


Figure 2.3 Evaporative Crystallisation flowsheet (adapted from Busch et al., 1961)

It was demonstrated (Nyirenda and Phiri, 1998) that evaporative crystallisation of nickel sulphate could achieve 81% and 100% salt removal at 66.5% and 80% electrolyte evaporation, respectively. However, the acid concentration in the purified electrolyte exceeded 1000 g/l, meaning high operation and maintenance costs due to the extreme corrosiveness of the final solutions.

Examples of evaporative crystallisers are shown in figure 2.4. Each of these designs utilizes evaporation to generate supersaturation of the solute. Supersaturation in industrial crystallisers is relieved by two basic mechanisms: nucleation of new crystals and growth of existing crystals (Mullin, 1993).

To minimise the production of unwanted nuclei, crystallisers are designed for maximum slurry circulation; in this manner, excessive high supersaturation is avoided and solute deposition on existing crystals is maximised. For the forced circulation crystalliser, the circulation arises by an external circulation pump whereas for the DTB, an internal circulator is provided. Typically, crystals of less than 0.5 mm are produced.

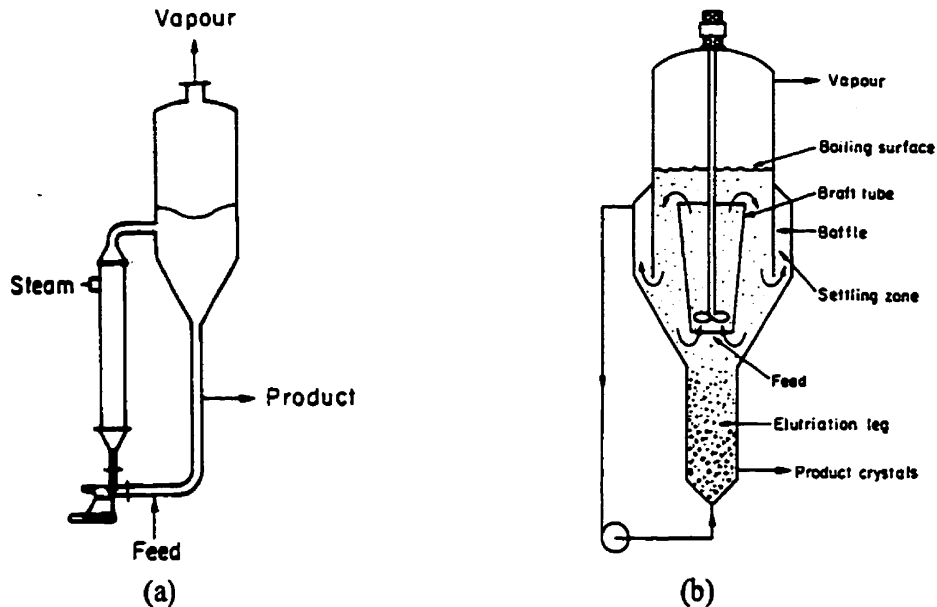


Figure 2.4 Evaporative crystallisers: (a) Forced Circulation; (b) Draft-Tube-Baffled
(Mullin, 1993)

- ***Disadvantages of Evaporative Crystallisation Technique***

Although employed for long time, the conventional nickel removal technique shows nevertheless some major disadvantages:

- (1) final product of poor physical (crystal size) and chemical (purity) quality.
- (2) water evaporation process is highly energy-intensive, increasing thus operating costs;
- (3) final solutions (“black acid”) of extremely corrosiveness.

The operation should be reviewed to determine if new or different technologies would provide greater operating economies, reduce recycle streams or enhance the purity of the products. Next section will introduce the “Solvent Displacement Crystallisation”, a new method to recover nickel sulphate from spent electrolytes based on the principle that water-miscible organic solvents cause a decrease in the solubility of salts when added to their aqueous solutions.

2.2. Solvent Displacement Crystallisation

A solution can be made supersaturated, with respect to a given solute, by the addition of another miscible liquid phase that reduces the solubility of the solute in the initial solvent and causes precipitation/crystallisation. The process is commonly referred to as “salting-out”, although it applies to electrolytes and non-electrolytes alike. The separation technique based on this phenomenon is designed as “*Solvent Displacement Crystallisation*” (SDC). A slow addition of the salting-out agent can change a fast precipitation of a solute into a more controlled crystallisation process.

2.2.1. Salting-out effect

The descriptions “quenching” and “solventing-out” have both been applied to the precipitation of electrolytes from aqueous solutions by the addition of a water-miscible organic solvent (Mullin, 1993). However, despite the fact that no single designation can be appropriate for all cases, the term “salting-out” will be used for convenience throughout this thesis. The characterisation of an experiment by salting-out means an increase in the activity coefficient of the electrolyte with increasing organic solvent concentration or, inversely, a decrease in water activity (Demopoulos, 1997).

Schneider (1969) reviews the first attempts to explain salting-out phenomena in the mid-twenties, which treated the solute as a substance soluble only in “free water”, i.e. the water that is not bonded to the hydration shell of the ions or to other substances. It was also suggested that the specific effects of water-miscible organic solvents (MOS) on the salt solubility might be explained by the dipole orientation of the water molecules in the hydration shell and by the dipole orientation toward the organic solvent.

There are many exceptions to the rule that “like dissolves like”, but this rough empiricism can still serve as a useful guide. In order to dissolve, the solute must break the solvent’s bonds and replace them with bonds of similar strength. The closer the chemical similarity between two substances, the higher their mutual solubility (Mullin, 1993).

In polar protic solvents (such as water and alcohols), the solvent molecules interact by forming hydrogen bonds. To have a reasonable solubility, a certain solute must be capable of forming hydrogen bonds with the solvent’s molecules. Franks (1967) studied

the excess enthalpies of mixing of alcohols and water at 25°C (figure 2.5). The negative enthalpies are generally explained in terms of preferential hydrogen bonding between alcohol and water, at the expense of the bonds among water molecules (i.e. there is decrease in the number of “free water” molecules that would be available to hydrate a potential electrolyte dissolved in the mixture).

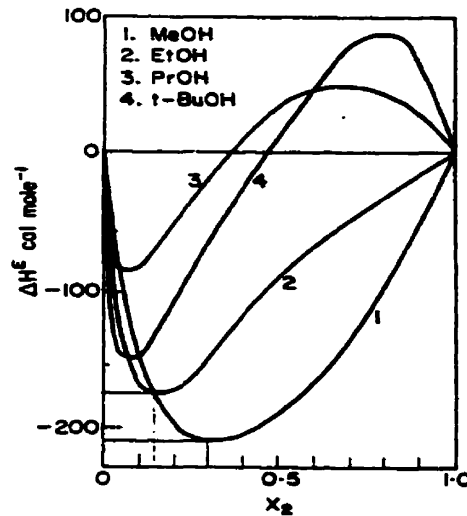


Figure 2.5 Excess enthalpies of mixing of alcohols and water at 25°C (Franks, 1967)

It can be thus inferred that the addition of polar organic molecules to aqueous solutions of electrolytes will lead to capture part of water molecules and subsequently reduce the solubility of salt. Alfassi and Mosseri (1984) described this process as a competition between the inorganic salt and the polar organic solvent on the water molecules on one hand and of preferential bonding between MOS and water on another hand.

Alfassi (1979) has found that the solubility of a solute in a homogeneous mixture of water and MOS can be represented as a function of the MOS concentration by:

$$S = S^w \exp(-\lambda f), \text{ (g/l)} \quad (2.11)$$

where S^w is the solubility in pure water (g/l), f is the volume fraction of MOS and λ is a constant characteristic of the salt and the solvent termed “the precipitating constant”.

Neglecting the change of volume with mixing, the amount of salt precipitated by the addition of V ml of MOS to 1 ml of saturated aqueous solution is given by:

$$P = S^w \{1 - (V + 1) \exp[-\lambda V / (V + 1)]\} \quad (2.12)$$

This is a maximum type function; increasing V always leads to a smaller solubility per unit volume but a larger volume of solution. The maximum fraction of salt that can be precipitated is obtained for $V = \lambda - 1$:

$$P_{\max} = 1 - \lambda \exp(1 - \lambda) \quad (2.13)$$

One important conclusion of these equations is that if $\lambda \leq 1$ for a salt–MOS system, no precipitation occurs when the MOS is added to the aqueous solution ($P_{\max} = 0$). On the other hand, for a $\lambda = 10$, $P_{\max} = 0.999$, meaning that all the salt was precipitated.

2.2.2. Solvent Displacement Crystallisation into historical perspective

The SDC technique is common practice in organic chemistry for the recovery of dissolved solids from solution and is frequently used for commercial purification in the biochemical and pharmaceutical industries. Despite its potential wide range of uses in inorganic processing and hydrometallurgy, relatively few industrial and laboratory applications have been reported in the literature.

In 1979, Alfassi reported acetone, tetrahydrofuran, dioxane and low molecular weight alcohols as the most efficient MOS to induce salt precipitation (mostly sulphates and halides). Mosseri and Alfassi (1984) reported also the separation of $KX-KXO_3$ ($X = \text{Cl, Br, I}$) using 1,4-dioxane and acetone as MOS, to precipitate KXO_3 while KX remains in solution; however, this is not a commercially important system.

The recovery of inorganic salts from concentrated aqueous solutions by addition of MOS is considered by Weingaertner, Lynn and Hanson (1991), who propose a process in which the filtered mother liquor is regenerated into two separate phases, organic and aqueous, by change of temperature and addition of more feedstock. Both phases are then recycled. Thus, NaCl is precipitated using isopropanol or diisopropyl amine, whereas Na_2CO_3 is removed adding propanol or butanol.

Potential applications of SDC to hydrometallurgical systems have been reported only recently but the studies were not expanded beyond the laboratory scale.

Thus, in 1998 Sato et al. used ethanol to selectively recover Nd from a sulphuric acid solution containing Nd, Fe and B, generated from rare earth magnet scraps. 41.7% ethanol (of total solution amount) achieved 97.4% Nd recovery ratio, as $\text{Nd}_2(\text{SO}_4)_3 \cdot 8\text{H}_2\text{O}$ of 96.8% purity.

Cohen (1987) presented experimental data for two systems of practical importance:

- $\text{CuSO}_4\text{-H}_2\text{O-H}_2\text{SO}_4$

The solutions studied simulated aqueous streams in copper processing (EW, ER, leaching) containing 5 g/l Cu, 1 g/l Fe^{3+} and ~1.8 g/l H_2SO_4 .

$\text{CuSO}_4\cdot 5\text{H}_2\text{O}$ was precipitated by the addition of different MOS to the leach liquor. Of the solvents investigated, acetone was the most effective in depressing Cu solubility (figure 2.6 a).

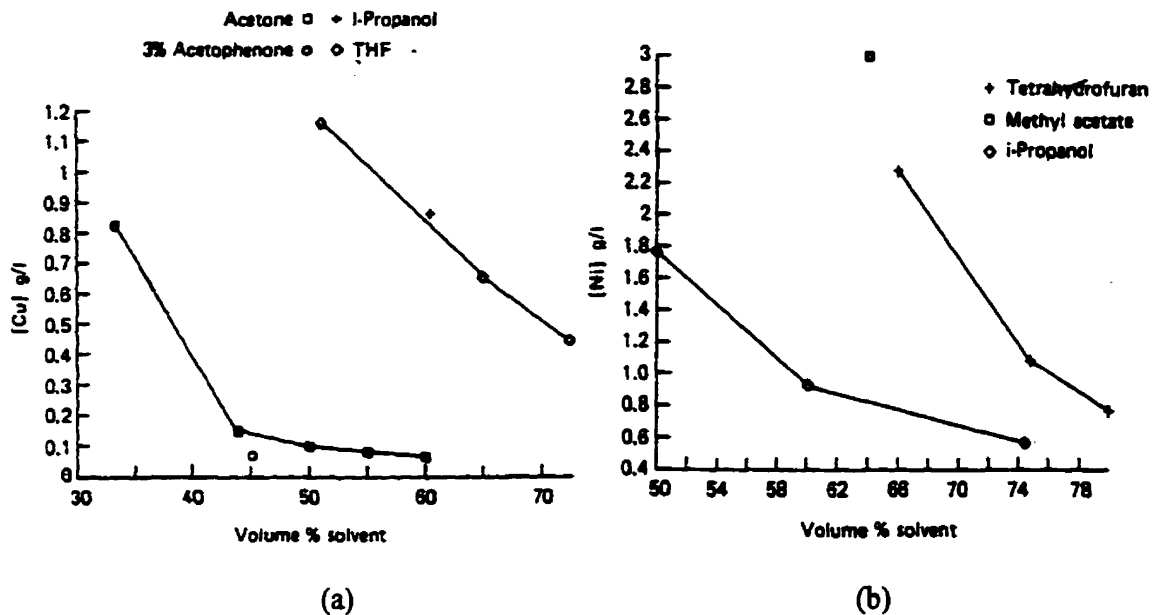


Figure 2.6 Metal solubility in aqueous-organic solutions: (a)-Cu; (b)-Ni (Cohen, 1987)

- $\text{NiSO}_4\text{-H}_2\text{O-H}_2\text{SO}_4$

SDC can be successfully employed to remove Ni from Cu ER spent electrolytes, becoming thus an attractive alternative to the conventional method of evaporative crystallisation. Cohen worked on synthetic solutions that reproduced the actual composition of decopperised electrolytes (16 g/l Ni, 10 g/l As, 0.5 g/l Cu, 200 g/l H_2SO_4). From the solvents tested, isopropanol was selected as being the most effective at depressing Ni solubility and precipitating crystalline $\text{NiSO}_4\cdot 6\text{H}_2\text{O}$ (figure 2.6 b).

On the basis of Cohen's work, the SDC technique for nickel sulphate production was further investigated and expanded because of its potential to make a significant improvement in metal recovery operations in Cu ER.

2.2.3 Conceptual flowsheet and Advantages

As already mentioned, the addition of water-miscible organic solvents to aqueous solutions of electrolytes may be used to cause solute crystallisation. SDC method is developed based on this phenomenon and enables hence the separation of salts from their aqueous solution by precipitation and filtration. The organic solvent is subsequently recovered for reuse by distillation. By selecting a low-boiling point MOS, its recovery by distillation would require less energy consumption than a similar process involving water (as it is performed in the conventional evaporative crystallisation (EC) method), as indicated by Cohen (1987).

The integration of SDC technique (instead of EC for Ni removal) into the actual electrolyte purification flowsheet, as practised in Cu ER, would comprise:

- Controlled addition of a low-boiling point, water-miscible organic solvent to the decopperised electrolyte that leaves the liberator cells;
- Separation of nickel sulphate crystals by filtration;
- Recovery of MOS by low-temperature or vacuum distillation.

Figure 2.7 illustrates the conceptual flowsheet of SDC employed to remove Ni from decopperised electrolytes in Cu ER.

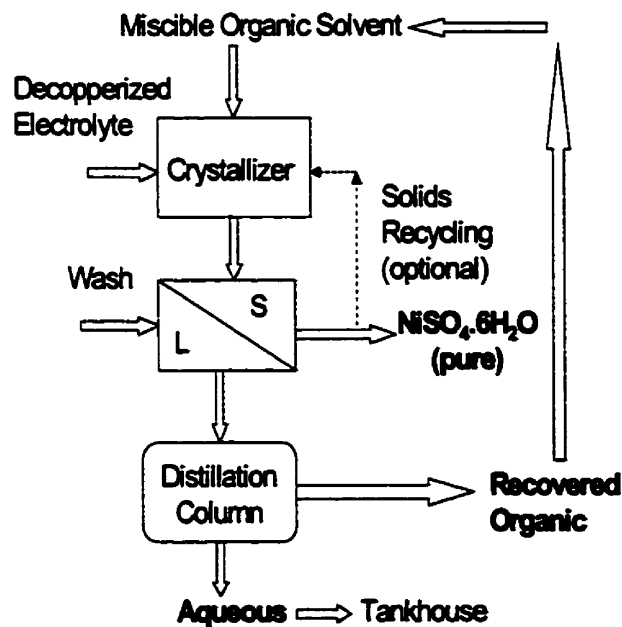


Figure 2.7 Conceptual flowsheet of nickel removal via SDC

This novel technique may prove an attractive alternative to the highly energy-intensive conventional method by its many advantages:

- (a) The potential to reduce energy costs in the recovery of inorganic salts from aqueous process streams. The rationale for energy saving via SDC can be stated as follows: a salt can be recovered from an aqueous solution by evaporating water thus increasing its concentration above its solubility. However, the specific heat of vaporisation is high and therefore the energy required for evaporation is also. As many common organic solvents have specific heats of vaporisation lower than that of water, more volume of MOS can be distilled for the same energy.
- (b) A high solute recovery yield may be obtained by selecting the appropriate water-miscible solvent. Furthermore, Mullin (1993) explained that better purification is often obtained than that from a straightforward evaporative crystallisation method since the mixed mother liquor retains more of the undesirable impurities than does the original solvent.
- (c) Controlled addition of MOS maintains a low supersaturation, yielding thus larger crystals with high solids density.

2.2.4 Criteria for the Miscible Organic Solvent selection

The selection of “the best” MOS for the SDC process is not always an easy matter; there are countless organic liquids that are potentially capable of acting as a crystallising agent, but many factors must be considered in order to achieve optimum performance.

- (1) It is necessary for the added organic solvent to be miscible with water in all proportions, in other words to have a polar protic nature, being thus able to establish same nature bonds (i.e. hydrogen) with water molecules.
- (2) Normal boiling point and specific heat of vaporisation lower than those of water, in order to decrease the energy consumption during evaporation.
- (3) Not reactive with aqueous phase elements, to avoid valuable metal loss through new compounds/complexes formation.
- (4) Low toxicity, inexpensive, available, if the SDC method is to be implemented at industrial scale.

- (5) Electrochemically inert in the e_h -pH operating window of copper electrorefining/electrowinning.
- (6) A relatively small volume of MOS precipitates a large fraction of salt.

2.3 Solubility Data for Nickel Sulphate

The “power” of a solvent is usually expressed as the mass of solute that can be dissolved in a given mass of pure solvent (usually water) at one specified temperature (Mullin, 1993). The extent to which a substance will dissolve in another varies greatly with different substances and depends on the nature of the solute and solvent, the temperature and the presence of other components.

2.3.1 Influence of temperature

The influence of temperature on the solubility of a solute in a particular solvent is, in general, quite pronounced. Because most substances absorb heat in solution (endothermic process) they tend to become more soluble at higher temperatures.

Figure 2.8 indicates the solubility curve of nickel sulphate in water function of temperature, based on solubility data compiled by Linke and Seidell (1958).

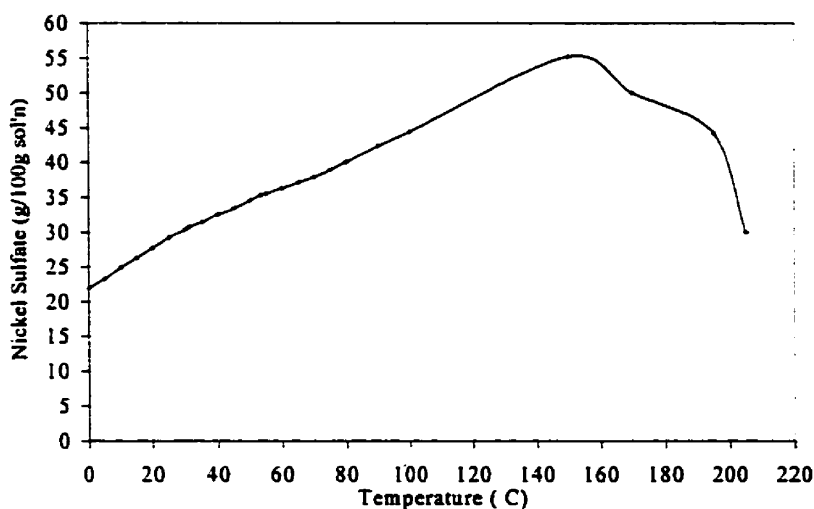


Figure 2.8 Effect of temperature on the solubility of nickel sulphate
(adapted from Linke and Seidell, 1958)

As shown, the solubility of nickel sulphate in water increases with increasing temperature up to approx. 150°C then presents a net decrease in spite of increasing temperature. Since in the interval 20-60°C any sharp decrease in temperature does not translate in a sensible decrease in solubility, it becomes obvious why nickel sulphate crystallisation should be achieved by other means (i.e. water evaporation, addition of MOS).

2.3.2 Influence of sulphuric acid concentration

In Cu ER, the spent electrolyte contains, besides nickel sulphate and minor impurities, free sulphuric acid, which considerably influences the solubility of individual species. From the dependence of the nickel sulphate solubility on the H₂SO₄ concentration, as shown in figure 2.2 (section 2.1.4), it is evident that, with increasing sulphuric acid concentration in solution, the salt's solubility decreases. Rohmer (1939) and Linke and Seidell (1958) assert that for more than 600 grams H₂SO₄ per 100 g solution, nickel solubility tends to zero (~1.13 g/l Ni at 25°C and 0.3 g/l Ni at 50°C). The temperature values selected are that of practical interest in Cu ER.

2.3.3 Influence of organic solvents

In general, compounds of similar chemical character are more readily soluble in each other than are those whose chemical character is entirely different. Since the chemical nature of MOS and nickel sulphate is quite different, there is no possibility of MOS solvating the ionic compound; therefore the solubility of electrolytes in water gradually decreases due to the addition of organic solvents miscible with water. As explained in section 2.2, the effects of the solvent composition (weight %) on chemical phenomena affecting dissolved solutes are thought to be a combination of critical solvation and solvent structure effects. Linke and Seidell, in their exhaustive compilation (1958), offer some data on solubility of NiSO₄.xH₂O (x = 6,7) in the system water-methanol.

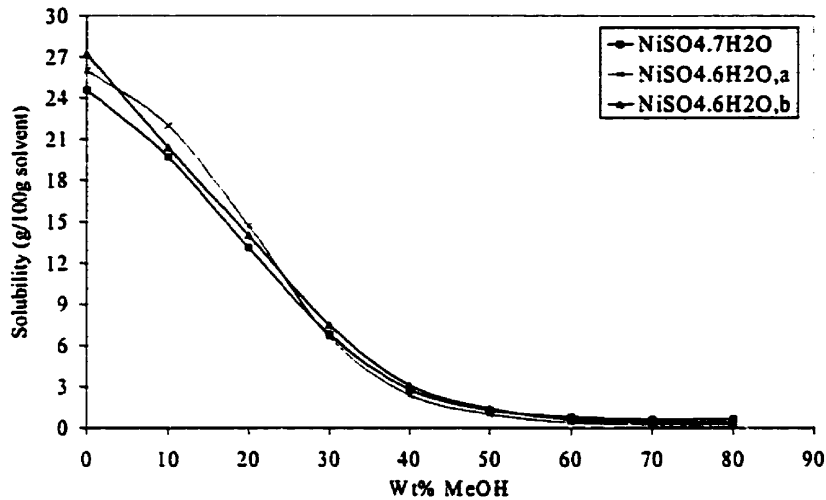


Figure 2.9 Nickel sulphates solubility in H₂O-CH₃OH at 15°C (Seidell and Linke, 1958)

As observed in figure 2.9, the solubility for three most stable NiSO₄ hydrates decreases in a similar way with increasing methanol fraction, at constant temperature. Similar trends have been noticed in isopropanol (Cohen, 1987 and section 2.2.2 of this thesis), reinforcing thus the conclusion that the solubility of nickel sulphate in mixed aqueous – organic solvents decreases with increasing organic fraction; the larger the organic molecule, the lower the fraction required to initiate precipitation.

2.4 Crystallisation from Solution

2.4.1 Crystallisation driving force

The state of supersaturation is essential for all crystallisation operations; supersaturation is the concentration of component ions in excess of the saturated concentration. Supersaturated solutions can be described using solubility-supersaturation diagrams (figure 2.10), which are divided into three zones (Mullin, 1993):

- (1) The stable (unsaturated) zone, where crystallisation is impossible;
- (2) The metastable (supersaturated) zone, where homogeneous crystallisation is improbable; however, if a crystal seed were placed in such a solution, growth would occur on it (heterogeneous crystallisation);
- (3) The labile (unstable) zone where spontaneous (homogeneous) crystallisation is probable;

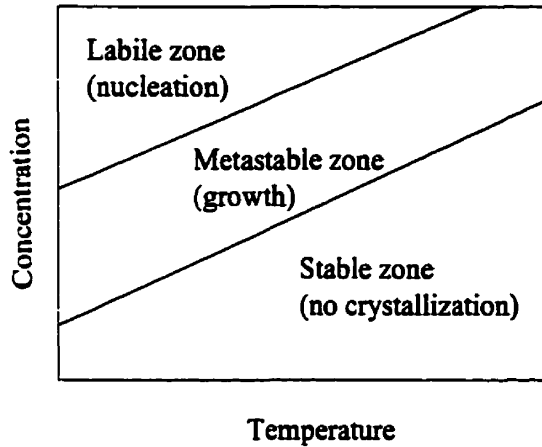


Figure 2.10 Solubility – supersaturation diagram

There are several ways to induce supersaturation in a solution. For systems in which the solubility is not a strong function of temperature, evaporation is used (see section 2.1). Cooling is employed when the solubility increases with temperature while heating is used when the solubility decreases with temperature. The most common method used is that of adding another reagent to the solution to suppress the solubility of the solute (e.g. reactive crystallisation, solvent displacement crystallisation).

The thermodynamic driving force for crystallisation is the difference between the chemical potential of the solute in solution (state 1) and crystal (state 2) (Nielsen, 1984):

$$\Delta\mu = \mu_1 - \mu_2 = \mu_1^0 + RT\ln(a_1) - \mu_2^0 - RT\ln(a_2) \quad (2.14)$$

or, in terms of Gibbs free energy:

$$\Delta G = -RT\ln(a/a^*) = -RT\ln(S) \quad (2.15)$$

μ^0 =standard chemical potential (J/mol), R=universal gas constant (J/molK), T=absolute temperature (K), a=activity of the solute, a^* =activity of the pure solute in equilibrium with a macroscopic crystal, S=supersaturation.

Supersaturation acts as crystallisation driving force, any $S > 1$ inducing $\Delta G < 0$ (hence spontaneous process).

$$S = a/a^* = C/C_{eq} \quad (2.16)$$

(when activity coefficients are assumed to be = 1)

C=solute concentration (mol/l), C_{eq} =equilibrium solubility of the solute at the temperature and pressure of the system (mol/l).

For ionic crystals, supersaturation can be expressed with the aid of solubility product:



$$K_{sp} = [A^+]_{eq} \cdot [B^-]_{eq} \quad (2.18)$$

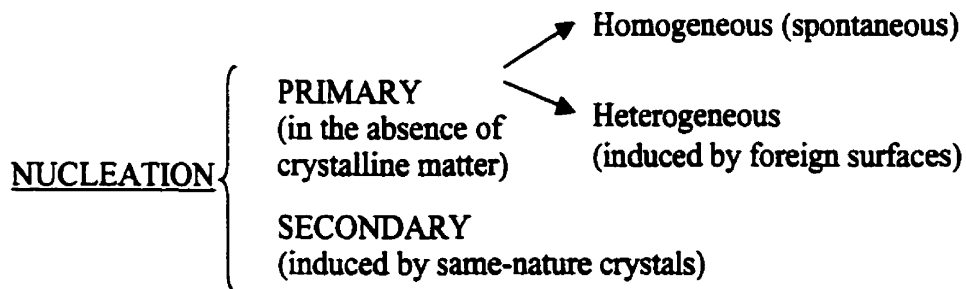
$$S = [A^+] \cdot [B^-] / K_{sp} \quad (2.19)$$

$[A^+]$ and $[B^-]$ are ionic concentrations in supersaturated solutions; for simplicity, concentrations are considered to be equal to activities.

2.4.2 Crystal nucleation

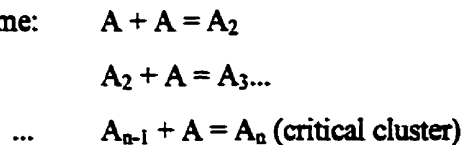
The condition of supersaturation alone does not suffice to cause crystallisation. Before crystals can develop, there must exist in the solution a number of microscopic solid bodies (embryos, nuclei or seeds) that act as centres of crystallisation. Nucleation may occur spontaneously or it may be induced artificially by agitation, mechanical shock, friction and extreme pressures within solutions (Mullin, 1993).

Nucleation processes can be classified according to the following scheme:



- ***Homogeneous Primary Nucleation***

Exactly how a stable crystal nucleus is formed within a homogeneous fluid is not known with any degree of certainty. Mullin (1993) proposes a sequence of bimolecular additions according to the scheme:



Further additions to the critical cluster would result in nucleation and subsequent growth of the nucleus. Short chains or flat monolayers may be formed initially and eventually a crystalline lattice is built up. The construction process, which occurs very rapidly, can only continue in local regions of very high supersaturation; many embryos fail to achieve maturity and re-dissolve because they are extremely unstable.

An empirical approach to the nucleation process is described by Nielsen (1984), expressing a relationship between the induction period τ (sec) and the initial concentration of the supersaturated solution C (mol/l):

$$\tau = k \cdot C^{1-p} \quad (2.20)$$

where k = constant and p is the number of molecules in a critical nucleus.

The induction period represents the time interval between mixing two solutions and the appearance of crystals (i.e. the time needed for the assembly of a critical nucleus); τ may range from microseconds to days, depending on the supersaturation.

- **Heterogeneous Primary Nucleation**

The rate of nucleation of a solution can be increased considerably by the presence of mere traces of impurities in the system (dust particles, insoluble particles); even some particular spots on the reactor's walls or on the impeller can act as catalysts for crystallisation. As the presence of a foreign surface can induce nucleation at degrees of supersaturation lower than those required for spontaneous nucleation, the overall free energy change associated with the formation of a critical nucleus under heterogeneous conditions (ΔG_{hetero}) must be less than the corresponding value associated with the homogeneous conditions (ΔG_{homo}):

$$\Delta G_{\text{hetero}} = \phi \cdot \Delta G_{\text{homo}} \quad (2.21)$$

where $\phi < 1$.

Mullin (1993) indicated that the interfacial tension, γ , is an important factor in controlling the nucleation process. Figure 2.11 shows an interfacial energy diagram for three phases in contact.

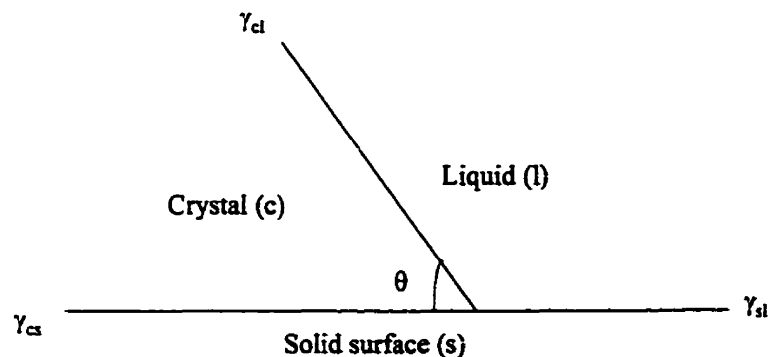


Figure 2.11 Interfacial tensions at the boundaries between three phases (Mullin, 1993)

The factor ϕ in equation (23) can be expressed as:

$$\phi = [(2 + \cos\theta)(1 - \cos\theta)^2]/4 \quad (2.22)$$

Three cases can be identified, according to θ values.

- (1) $\theta = 180^\circ$, $\phi = 1$ and $\Delta G_{\text{hetero}} = \Delta G_{\text{homo}}$: complete non-affinity between the crystalline solid and the foreign surface. The overall free energy for nucleation is the same as of that required for homogeneous (spontaneous) nucleation.
- (2) $0 < \theta < 180$, $\phi < 1$ and $\Delta G_{\text{hetero}} < \Delta G_{\text{homo}}$: partial affinity between the two solids. Nucleation is easier to achieve on the foreign surface than homogeneously.
- (3) $\theta = 0$, $\phi = 0$ and $\Delta G_{\text{hetero}} = 0$: complete affinity between the two solids. This corresponds to the seeding of a supersaturated solution with crystals of the same nature as the solute.

- **Secondary Nucleation**

Probably the best methods for inducing crystallisation are to inoculate or seed a supersaturated solution with crystals of the solute. Deliberate seeding is often employed in industrial crystallisation to maintain a control over the product size and size distribution.

Mullin (1993) reviews several possible mechanisms of secondary nucleation, such as:

- "initial" breeding: crystalline dust swept off a newly introduced seed crystal;
- "needle" breeding: the detachment of weak outgrowths;
- "polycrystalline" breeding: the fragmentation of a weak polycrystalline mass;
- "collision" breeding: fragmentation resulting from the interactions of crystals with one another or with parts of the reactor.

Fragmentation processes can occur either by collision or by the development of internal stresses in crystals, which lead to crack formation and subsequent crack propagation due to adsorption of impurity species at defects on crystal surface.

Production of crystalline, well-grown solids can be favoured by either applying a high temperature or a lower supersaturation ($S < S_{\text{cr,homo}}$); the latter approach is employed in the present work. As Demopoulos et al. demonstrated (1995), crystalline products can be obtained by controlling S below $S_{\text{cr,homo}}$ via a staged addition of the precipitating agent (figure 2.12). During the first step seed material is added to the solution to induce growth

and to avoid homogeneous nucleation. In this fashion supersaturation is maintained at a sufficient low value throughout the whole experiment.

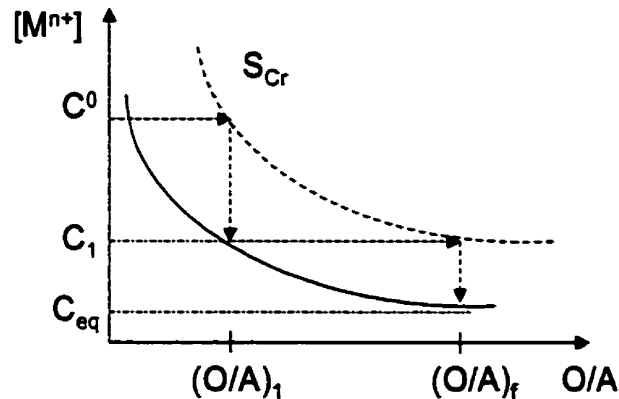


Figure 2.12 Supersaturation – controlled crystallisation process (adapted from Demopoulos et al., 1995)

2.4.3. Crystal growth

As soon as stable nuclei have been formed in a supersaturated system, they begin to grow into crystals of visible size. Any accurate analysis of the growth process must consider the combined effects of diffusion and surface adsorption.

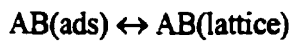
For an electrolyte crystallising from an aqueous solution, the following processes may all be taking place (Mullin, 1993):

- (1) Bulk diffusion of hydrated ions through the diffusion boundary layer and through the adsorption layer: the process depends linearly on the concentration gradient and inversely on diffusion layer thickness or crystal size (Chiang and Donohue, 1987).
- (2) Surface diffusion of hydrated or dehydrated ions: the distance a particle must diffuse in the adsorbed layer to a kink or growth site depends on crystal size and supersaturation.
- (3) Partial or total dehydration of ions.
- (4) Integration into the lattice
- (5) Counter-diffusion of released water through the adsorption and boundary layers.

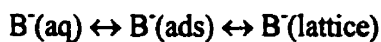
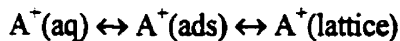
Ionic crystals can grow either by the addition of neutral molecules or by the addition of individual ions that subsequently react and become incorporated into the lattice.

Chiang and Donohue (1987) propose three mechanisms of growth in the case of ionic species:

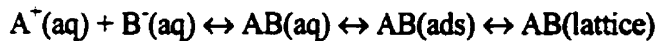
- **Mechanism I: Surface Reaction/Molecule Integration**



- **Mechanism II: Sequential Ionic Integration**



- **Mechanism III: Molecular Growth**



Independent of the growth mechanism (i.e. the incorporation of individual ions or molecules), the model of a growing crystal face is essentially the same. As Mullin (1993) describes the Kossel–Frank theory, it appears that a flat crystal surface is in fact made up of moving layers (steps) of monoatomic height, which may contain one or more kinks (figure 2.13 a). In addition, there will be loosely adsorbed growth units (atoms, molecules or ions) on the crystal surface and vacancies in the surfaces or steps. Growth units are most easily incorporated into the crystal at a kink; the kink moves along the step and the face is completed. A fresh step could be created by surface nucleation at the corners.

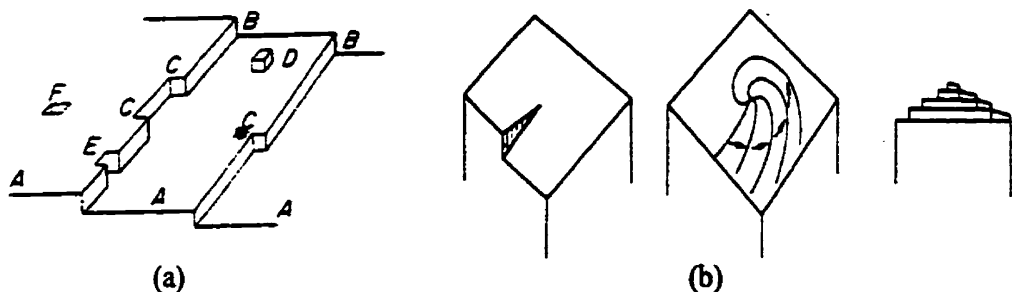


Figure 2.13 Growth models (Mullin, 1993)

(a) Kossel's model of a growing crystal: A-flat surfaces; B-steps; C-kinks; D-surface-adsorbed particle; E-edge vacancies; F-surface vacancies.

(b) Development of a growing spiral starting from a screw dislocation

Moreover, crystals may contain edge or screw dislocations that cause steps to be formed on the faces and promote growth. Once a screw dislocation has been formed, the crystal face can grow up following a spiral pattern (figure 2.13 b). The curvature of the spiral cannot exceed a certain maximum value, determined by the critical radius for a two-dimensional nucleus under the conditions of supersaturation in the medium in which the crystal grows.

2.4.4 Influence of impurities

- ***Effect on Nucleation***

The presence of impurities in a system can considerably affect nucleation behaviour. The higher the charge on the impurity cation, the more powerful the inhibiting effect, e.g. $\text{Cr}^{3+} > \text{Fe}^{3+} > \text{Al}^{3+} > \text{Ni}^{2+} > \text{Na}^+$. The heteronuclei are rendered inactive by impurity adsorption on their surfaces. Mullin (1993) suggested that if the impurity suppresses primary nucleation, secondary nucleation could occur if the uptake of impurity by the growing crystals is significant. The seed crystal creates an impurity concentration gradient about itself; the concentration of impurity near the crystal surface becomes lower than that in the bulk solution and if it is reduced low enough, nucleation can occur. Another possibility is that certain impurities induce secondary nucleation by adsorbing at defects on existent crystal surfaces and initiating crack propagation and subsequent fragmentation.

- ***Effect on Growth***

Impurities can influence crystal growth rates in a variety of ways. They can change the structural properties of solutions or the equilibrium saturation concentration and hence the supersaturation. They can alter the characteristics of the adsorption layer at the crystal – solution interface and influence the integration of growth units or may be even built into the crystal (especially if there is some degree of lattice similarity).

Impurities are often adsorbed selectively on to different crystal faces and retard their growth rates. To effect retardation, it is not necessary for the impurity to achieve total face coverage. As seen in figure 2.14 (Mullin, 1993), three sites may be considered at which impurity species may become adsorbed and disrupt the flow of growth layers

across the faces: a kink, a step or an edge. If kink site adsorption is possible, growth retardation may be affected at very low impurity levels in the solution. More impurity would be necessary if step site adsorption is the preferred mode while much higher levels may be required if adsorption only occurs on face site.

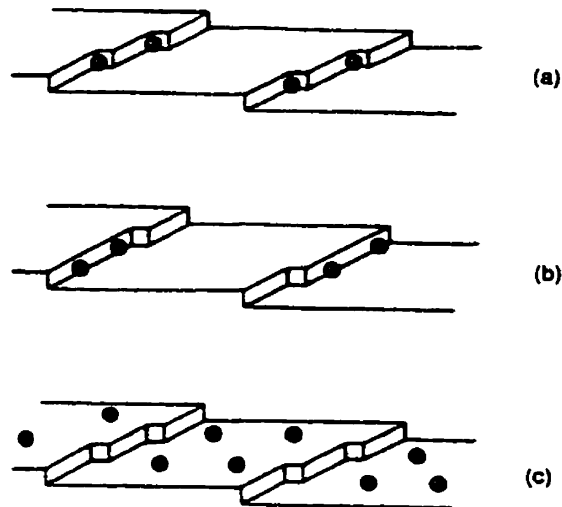


Figure 2.14 Sites for impurity adsorption on a growing crystal: (a) kink; (b) step; (c) face
(Mullin, 1993)

3. EXPERIMENTAL

3.1 Chemicals

Reagent grade chemicals were used in all the experiments, except when the industrial electrolyte was employed. The synthetic solutions were prepared with de-ionised water, by the dissolution of suitable amounts of $\text{NiSO}_4 \cdot 6\text{H}_2\text{O}$ and H_2SO_4 .

Chemicals are listed in table 3.1 while the composition for the industrial electrolyte is given in table 3.2.

Table 3.1 Chemicals used in experimental work

Compound	Formula	Supplier	Typical Concentration in Solution
Nickel Sulphate Hexahydrate	$\text{NiSO}_4 \cdot 6\text{H}_2\text{O}$	A&C American Chemicals Ltd.	17-20 g/l Ni
Sulphuric Acid	H_2SO_4	Fisher Scientific	200-250 g/l
Sodium Hydroxide	NaOH	Anachemia	1N
2-Propanol	$\text{C}_3\text{H}_8\text{O}$	Fisher Scientific	Varies

Table 3.2 Industrial electrolyte composition (*)

Element	Concentration (g/l)
Ni	18.7
H_2SO_4	250.5
Al	0.11
As	0.99
Bi	0.02
Ca	0.39
Cd	0.003
Co	0.02
Cu	1.14
Fe	0.29
Mg	0.08
Sb	0.002
Sn	0.11
Zn	0.14

(*) from CCR private communications

3.2 Experimental Set-up

3.2.1 Crystallisation tests

SDC tests were performed at ambient temperature (20-21°C), in a cylindrical 1-litre Pyrex reactor (A) with a separate glass lid containing 4 holes (B). Each hole was plugged with rubber stoppers (C) to prevent solution loss or to allow insertion of a stirrer, manual burette, sampling pipette (D) (or thermometer, when required). An axial-mixing type plastic-coated metal impeller (E) (diameter of 4.5 cm, with 3 blades inclined at 45°) agitated the solution; a Dayton stirrer was used with variable speed control (F). The MOS was added to the aqueous solution via a 100 ml manual burette (G) (figure 3.1).

For the single experiment conducted at 40°C, the reactor was immersed in a Cole-Parmer water bath; the water was mixed, heated and maintained at the desired temperature with an accuracy of ~2°C.

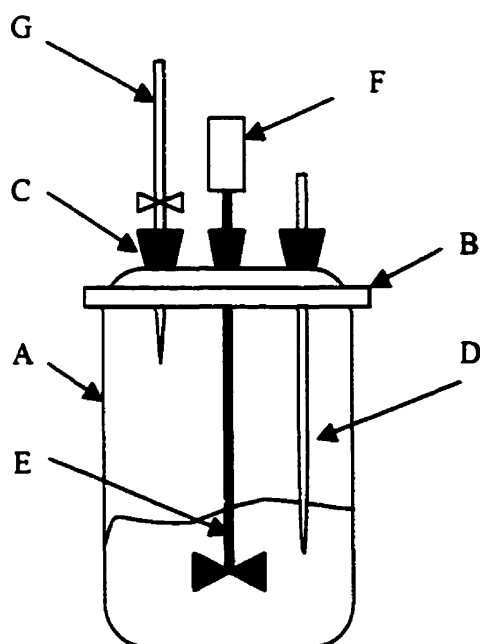


Figure 3.1 Experimental set-up for the SDC tests: A-reactor; B-lid; C-rubber stoppers; D-sampling pipette or thermometer; E-impeller; F-motor; G-manual burette.

3.2.2 Fractional distillation

Fractional distillation experiments were performed employing the set-up presented in figure 3.2. The water-organic mixture was brought to boiling point in a 1000-ml Pyrex round-bottom flask heated by a Glas-Col hemispherical heating mantle; the temperature was controlled by a Dayton variable autotransformer. The vapour phase was enriched in the lower-boiling point component through an insulated Kimax brand distillation column (300mm in length) packed with Pyrex glass beads ($\phi = 4$ mm) while the temperature was read using a thermometer inserted into the distilling head. The organic phase was condensed in a water-cooled, Kimax brand, Liebig-type condenser (400 mm in length) and collected in a 1000-ml Pyrex round-bottom receiving flask.

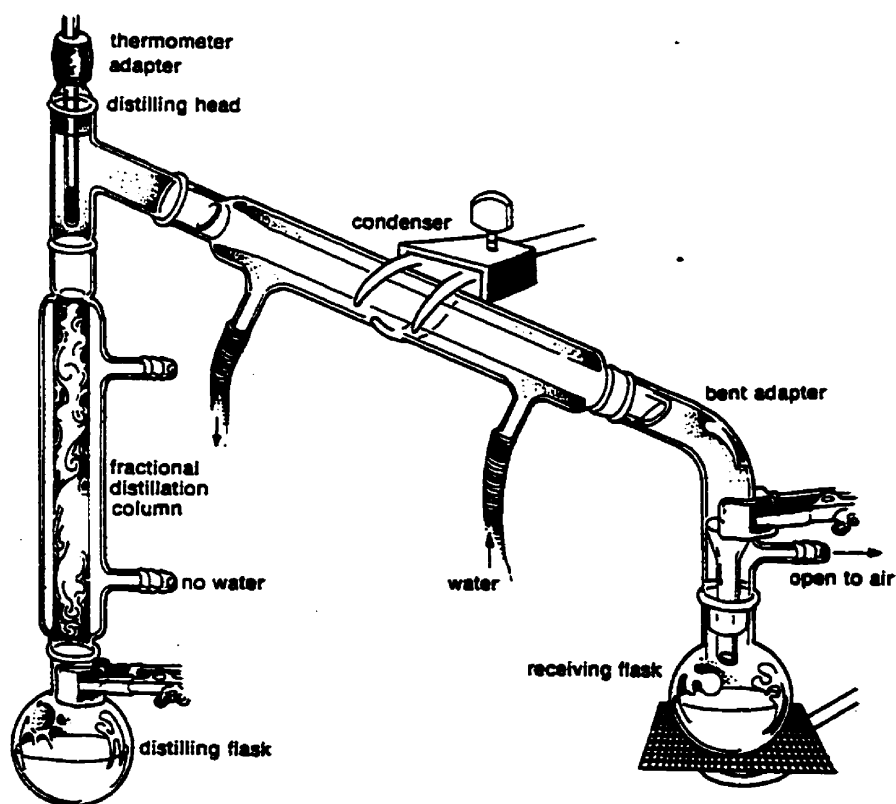


Figure 3.2 Fractional distillation set-up (Pavia, Lampman and Kriz, 1982)

3.3 Experimental Procedure

3.3.1 Crystallisation tests

- ***Nickel Sulphate Solubility Line in $H_2O-H_2SO_4$ -Isopropanol System***

100 ml of pre-made mixtures containing 250 g/l H_2SO_4 aqueous solution and different amounts of IP were agitated in conical Pyrex flasks while $NiSO_4 \cdot 6H_2O$ crystals were added to the system. When nickel sulphate concentration in solution exceeded its solubility (crystals in equilibrium with solution), salt's addition stopped and the system was allowed to equilibrate for 24 hours. The next day the crystals were separated by filtration and each filtrate was analysed for Ni content.

- ***Determination of Critical Supersaturation for $NiSO_4$ in $H_2O-H_2SO_4$ System***

Pure 100 ml solutions of 10, 20, 30, 40, 50 and 60 g/l Ni and 250 g/l H_2SO_4 were agitated with a magnetic stirrer in Pyrex flasks. Small volumes of IP were slowly added to the aqueous solutions by the means of a manual burette; after each addition, a 15-minutes equilibration period was allowed. At the moment a "cloud" was seen (initiation of the homogeneous crystallisation process), the volume of IP that induced the $S_{cr,homo}$ was recorded and the solutions were stirred for 24 hours, to reach complete equilibrium. The next day the crystals were separated by filtration and the Ni content in solution was determined with atomic adsorption spectroscopy.

- ***Solvent Displacement Crystallisation***

In a typical SDC test, 200 ml aqueous solution (either synthetic or industrial electrolyte) were agitated at ambient temperature (20-21°C) while isopropanol was added from a 100 ml manual burette (usually, organic/aqueous total ratio = O/A = 1.5, meaning 300 ml of IP were used in each SDC experiment).

The duration of standard SDC tests was 60-90 minutes, unless otherwise mentioned.

- ***Homogeneous Crystallisation:*** to homogeneously precipitate nickel sulphate, IP was added at once to the aqueous phase. The mixture was agitated for 120 minutes and samples were taken every 2, 5, 10, 15 minutes, then every 15 minutes, in order to monitor Ni content and hence the kinetics of the process. Samples taken by pipette were diluted 10 times immediately with 5% HCl solution to prevent further precipitation within the sample.

- *Heterogeneous Crystallisation*: low S was maintained via a slow IP delivery; for a certain volume of IP corresponding to a supersaturation $S < S_{cr,homo}$, organic addition was stopped and nickel sulphate seed was provided to the system, in order to favour the secondary nucleation process and hence crystal growth. After a 15-minutes equilibration period, IP addition was resumed in a controlled, step-wise manner, small volumes at a time, followed by 15-minutes equilibration periods, as to maintain $S < S_{cr,homo}$ throughout the whole experiment. After each addition/stirring period the agitation was stopped and 2-ml samples were taken, diluted and analysed for Ni.

When the precipitation tests were over, the crystals were separated by filtration, washed with IP to displace water and sulphuric acid, air-dried at room temperature, weighted and collected for further analysis. The filtrate was measured and subjected to fractional distillation in order to recover the organic phase.

3.3.2 Fractional distillation

When the boiling-point differences of components to be separated are not too large (i.e. $< 20^{\circ}\text{C}$), fractional distillation as opposed to simple distillation is required to achieve good separation (more information in appendix C).

The filtrate from the SDC tests was distilled employing the set-up depicted in figure 3.2. As the distilling flask was slowly heated, the vapour mixture of IP and water raises in the packed column and is subjected continuously to many vaporisation-condensation cycles; with each cycle within the column, the composition of the vapour is progressively enriched in the lower-boiling point component. Finally, nearly pure organic emerges from the top of the column, condenses and passes into the receiving flask as first fraction. The liquids to be separated in this research project were water (b.p.= 100°C) and isopropanol (b.p.= 82°C). However, due to strong intermolecular attractions, H_2O -IP mixtures behave non-ideally and Raoult's law is not followed. Hence, upon distillation a constant boiling point mixture called an *azeotrope* is collected, with a fixed composition (87.8% IP, 12.2% H_2O , wt/wt) and a fixed boiling point (80.4°C) which cannot be altered by simple or fractional distillation.

The duration of a typical distillation experiment was ~3 hours, starting with ~450 ml aqueous-organic mixtures.

3.4 Analytical Methods

3.4.1 Aqueous sample

- ***Atomic Adsorption Spectroscopy (AA)***

The nickel content in solution was determined with an Instrumental Laboratory model 357 AA spectrometer. The linear range of measurement for Ni is between 0 and 5 mg/l; the detection limit for Ni by AA is 0.06 mg/l. The machine was calibrated using 1, 3 and 5 mg/l standards prepared from 1000 mg/l certified Ni standard (Fisher).

- ***Acid Titration***

Since direct pH measurements in highly concentrated sulphuric acid solutions cannot offer an accurate and reproducible value of acid content, sulphuric acid values at different stages of the experiments were monitored by titration with NaOH 1N (Appendix A). An automatic titrator was used (Radiometer Copenhagen Titalab™90), equipped with a high precision ABU 900 Autoburette System and glass pH electrode (Fisher Accu-pHast).

- ***Inductively Coupled Plasma Spectroscopy (ICP)***

ICP offers several advantages over measurement with AA:

- lower detection limit
- lower inter-element interference due to higher flame temperature
- determination of several elements simultaneously

The latter feature was employed to monitor the impurity uptake during SDC (i.e. the impurity content of nickel sulphate product). Analytical department of CCR performed the ICP analysis of nickel sulphate crystals on a Thermo Jarrell Ash ICP-MS.

3.4.2 Crystalline product

- ***X-Ray Diffraction (XRD)***

The confirmation of crystalline phases and the determination of the number of crystallisation water molecules were achieved by XRD analysis, using a Phillips PW1710 machine. The spectrum obtained for a certain sample was matched to different standard spectra ($\text{NiSO}_4 \cdot x\text{H}_2\text{O}$, $x=2,4,6,7$) contained in the computer's database.

- ***Scanning electron Microscopy (SEM)***

The solids produced were analysed using a JEOL 840A scanning microscope at 10kV; prior to that, the samples were gold-coated in a Hummer VI plasma sputter coater. The images obtained were used to establish particle size and morphology.

The SEM was also equipped with a Noran *Energy-Dispersive Spectroscopy (EDS)* which could determine the quantitative analysis of the solids (overall analysis) or the quantitative composition of the individual particles (spot analysis).

4. RESULTS AND DISCUSSION

4.1 Preliminary Tests

In this research thesis, the effectiveness of IP to cause the crystallisation of nickel sulphate as suggested by Cohen (1987) is investigated. The solvent is added gradually into the aqueous solution while periodic sampling and AA analysis monitor the concentration of nickel. Following the precipitation of $\text{NiSO}_4 \cdot 6\text{H}_2\text{O}$, the organic phase is recovered by fractional distillation at 80°C and the solvent is separated as an azeotrope, containing 88% IP (wt/wt).

Since in industry the azeotrope as opposed to pure organic solvent may have to be used (for economical reasons), a test was performed to evaluate the effectiveness of the IP- H_2O azeotrope mixture to precipitate nickel sulphate.

Finally, since the industrial spent electrolyte leaves the tankhouse at elevated temperature of -40 - 50°C , a SDC test at 40°C was also performed.

4.1.1 Solubility of $\text{NiSO}_4 \cdot 6\text{H}_2\text{O}$ in isopropanol-water-sulphuric acid system at 20°C

Since no data are reported in literature, the solubility of nickel sulphate had to be determined as a function of IP fraction prior to performing any SDC test (figure 4.1). Details about the working procedure are given in section 3.3.1.

As observed, nickel concentration decreases with increasing IP fraction, from a value of 67.14 g/l Ni for $O/A=0.1$ to 1.33 g/l Ni corresponding to $O/A=2.3$.

Nevertheless, these values are higher than those reported by Cohen (1987): for example, at $O/A=1$ (meaning equal volumes of organic to aqueous) Cohen reports a concentration of 1.8 g/l Ni as opposed to 7.28 obtained in this research project. However, based on the consistency of results obtained during this work, Cohen's data seem questionable.

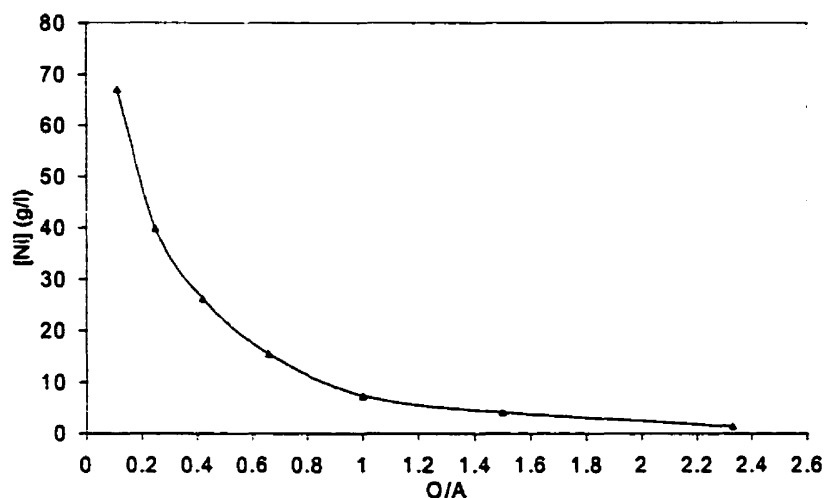


Figure 4.1 Nickel sulphate solubility in IP-H₂O-H₂SO₄ system (250 g/l H₂SO₄, T=20°C)

Once the solubility line established, the next step was to conduct preliminary SDC tests in order to validate the effectiveness of IP and azeotrope as salting-out agents for nickel sulphate, to study the influence of temperature and to determine the optimum experimental procedure for further SD tests.

4.1.2 Anatomy of a SDC test

Due to the lack of information in Cohen's article concerning the experimental procedure, the preliminary tests were performed following a gradual organic addition to the aqueous phase. Before the influence of other parameters (temperature, azeotrope) is investigated, a typical SDC tests is described (20°C, pure IP).

- **Crystallisation**

In a typical SDC test 100 ml aqueous solution containing ~25 g/l Ni and ~200 g/l H₂SO₄ (as in Cohen's work, these value simulate industrial conditions) were agitated at ambient temperature (20°C). Isopropanol was added from a 100 ml manual burette; an organic/aqueous total ratio (O/A)_{total} of 1.5 was selected, meaning 150 ml of IP were used. After each IP addition, an equilibration period of 15 minutes was allowed, then the solution was sampled to monitor nickel concentration.

Figure 4.2 presents the progression of a SDC experiment in time: nickel concentration reports on the left-side y-axis while the amount of IP (expressed as O/A ratio) is read off the right-handed y-axis.

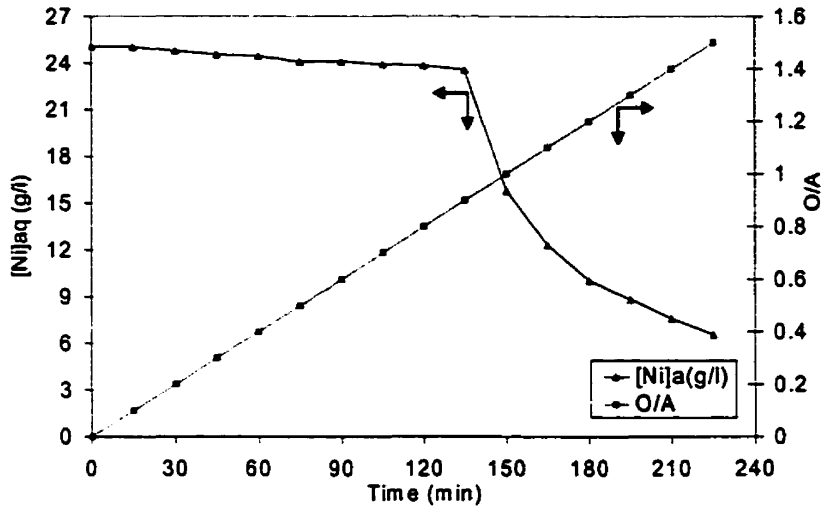


Figure 4.2 Preliminary SDC test (200 g/l H₂SO₄, T=20°C, IP)

The total duration of the experiment was 225 min; as observed, the massive drop in nickel concentration occurred after 135 min, corresponding to a O/A=0.9. For a better understanding of the influence of IP fraction on [Ni]_{aq}, the previous figure is re-plotted:

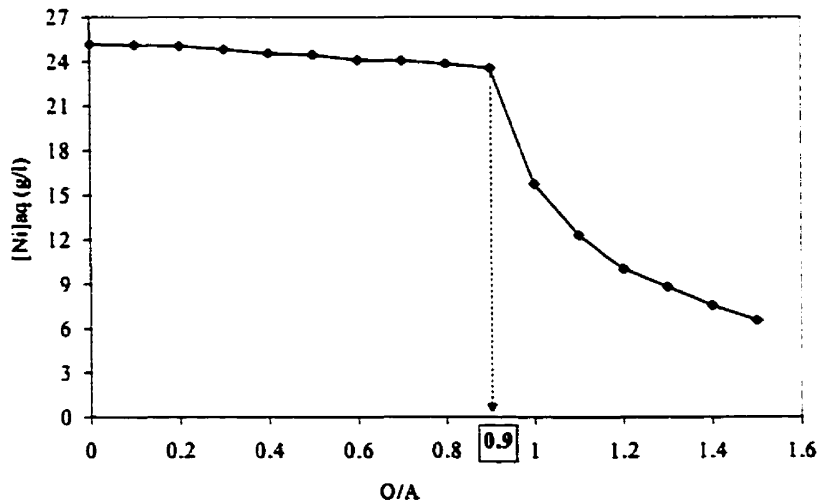


Figure 4.3 Influence of O/A on [Ni]_{aq} during SDC (200 g/l H₂SO₄, T=20°C, IP)

The precipitation process requires a certain O/A ratio, depending on the initial nickel concentration. In the initial stages, IP addition to the aqueous has no visible effect on nickel solubility: the appearance of the solution remains unchanged (clear, deep green) and $[\text{Ni}]_{\text{aq}}$ is constant. As more solvent is added, water molecules are induced to hydrate the organic instead of the inorganic salt, provoking thus an increase in nickel sulphate saturation (decrease in solubility). For a certain IP volume, corresponding to an O/A ratio of 0.9, there is no more water available to solvate the electrolyte hence nickel sulphate crystals form. Nevertheless, this process does not occur instantaneously: as the 0.9 fraction is added under mild stirring, a certain "induction period" elapses (approx. 10 minutes) until changes are observed. The turbidity increases as the clear solution become opaque (denoting the initiation of the nucleation process) then fine light-green crystals start to separate. The crystallisation process continues through the rest of the experiment as more O/A fractions are added, followed by 15 min stirring periods and sampling.

The final $[\text{Ni}]_{\text{aq}}$ was 6.55 g/l Ni (corresponding to $O/A_{\text{total}}=1.5$) meaning that ~74% of nickel was precipitated. The duration of the experiment can be considerably shortened by adding IP at once up to $O/A=0.9$ to start the crystallisation process.

The selected O/A_{total} ratio was considered effective enough to lower nickel concentration to values comparable to those obtained in industry via evaporative crystallisation (Dobner 1997, Hoffmann 1997). Addition of more solvent (i.e. raising O/A above 1.5) can further reduce the final nickel concentration.

• **Filtration**

Following the SDC test, the crystals were separated by filtration (good filterability), washed with small volumes of IP (25 ml) to displace water and sulphuric acid, air-dried at room temperature, weighted and collected for further analysis. 5.41 grams of fine, light-green crystals were separated from 100 ml aqueous solution containing 25 g/l Ni.

To confirm the crystallinity of the product and to determine the number of crystallisation water molecules, XRD analysis was performed. The spectrum obtained for this sample was matched to different standard spectra ($\text{NiSO}_4 \cdot x\text{H}_2\text{O}$ $x=2,4,6,7$) contained in the computer's database. The sharp peaks indicated crystalline status; moreover, it was found that $\text{NiSO}_4 \cdot 6\text{H}_2\text{O}$ offered the best match to the sample studied (figure 4.4).

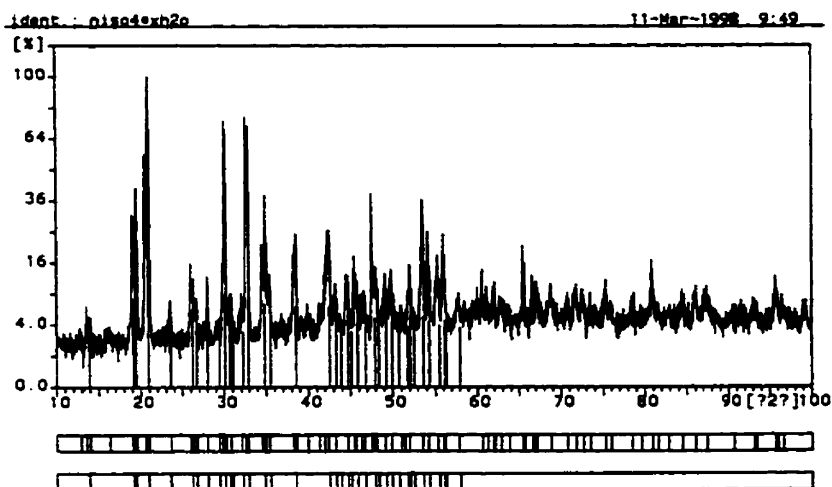


Figure 4.4 XRD spectrum of crystals obtained from a preliminary SDC test
(200 g/l H₂SO₄, T=20°C, IP, standard comparison spectrum: NiSO₄·6H₂O)

- **Distillation**

Following filtration, the organic phase was recovered by fractional distillation employing the set-up presented in figure 3.2, section 3.2.2 (details on fractional distillation in appendix C). The aqueous-organic mixture is heated until the first fraction, containing the azeotrope, distils at 80°C; the vaporisation-condensation process continues at constant temperature as long as the same fraction is collected. When all IP is removed as azeotrope (88% IP, 12% H₂O), the temperature rises again and the next fraction vaporises. The process is stopped and the two phases are measured after cooling. Table 4.1 summarises distillation data derived from a preliminary test in which were employed 100 ml aqueous and 150 ml IP+25 ml IP for washing = 175 ml IP. From the total volume of 275 ml mixture, 220 ml were subjected to distillation (the balance represents 30-ml samples taken during the test, crystallisation water and moisture retained in the cake).

Table 4.1 Development of a fractional distillation experiment following SDC

Time (min) (*)	Comments
t=0	Start heating; in for distillation: 220 ml IP-H ₂ O mixture
t=20	Boiling process begins at T=80°C
t=25	T=80°C, distillation of azeotrope, continuous process
t=95	Separation of azeotrope ends; T raises at 97°C Out from distillation: 160 ml azeotrope (88% IP) and 60 ml aqueous

(*) the duration depends on the volume of mixture distilled

- **Material balances**

Table 4.2 gives general material balances for nickel, isopropanol and water as employed in this preliminary test.

Table 4.2 Materials mass balances

NICKEL		
IN	100 ml NiSO ₄ .6H ₂ O solution at 25 g/l Ni = 2.5 g Ni	Total in: 2.5 g Ni
OUT	98 ml aqueous at 6.55 g/l Ni = 0.64 g Ni 5.41 g NiSO ₄ .6H ₂ O = 1.20 g Ni Samples taken during SDC = 0.35 g Ni	Total out: 2.19 g Ni Nickel closure: 87.6%
ISOPROPANOL		
IN	150 ml for SDC = 117 g IP 25 ml for cake wash = 19.5 g IP	Total in: 175 ml = 136.5 g IP
OUT	160 ml azeotrope (88%wt IP) = 114.04 g 12.27 ml samples taken during SDC = 9.57 g	Total out: 123.61 g IP IP closure: 90.55%
WATER		
IN	100 ml = 100 g H ₂ O	Total in: 100 g
OUT	2.22 g H ₂ O as crystallisation water 60 ml = 60 g H ₂ O after distillation 15.55 g in azeotrope 18.73 g in aqueous samples	Total out: 96.5 g H ₂ O Water closure: 96.5%

The losses of IP and Ni/water/solution can most likely be assigned to a combination of causes such as: moisture retained in the cake, sampling and column hold up during distillation. The problem of sulphuric acid concentration in the aqueous phase prior and after distillation will be addressed in section 4.1.5.

4.1.3 SDC using the azeotrope

Since in a potential industrial implementation of the SDC technique it will be preferably to recover by distillation the azeotrope mixture as opposed to pure solvent, a test was performed to determine the effectiveness of the former in causing NiSO₄ crystallisation. The experiment was conducted in the manner described in section 4.1.2 with the difference that azeotrope was employed instead of IP.

Table 4.3 gives comparative data from SDC tests performed with pure IP and azeotrope, respectively. The same data are graphically represented in figure 4.5.

It must be mentioned that "O" in the case of the azeotrope does not represent the organic component only (IP), but the whole azeotrope addition (88% IP wt/wt or 91.6% vol/vol).

Table 4.3 Initial and final parameters during SDC ($T = 20^{\circ}\text{C}$)

CONDITIONS	INITIAL		FINAL	
	Isopropanol	Azeotrope	Isopropanol	Azeotrope
$[\text{Ni}]_{\text{aq}}$, g/l	18.91	18.34	6.15	8.03
O/A_{crystall}	-	-	1.1	1.9
O/A_{total}	-	-	1.5	2.5
$[\text{H}_2\text{SO}_4]$, g/l	198.32	201.14	305.17 (*)	206.78 (*)

(*) after distillation, see section 4.1.5

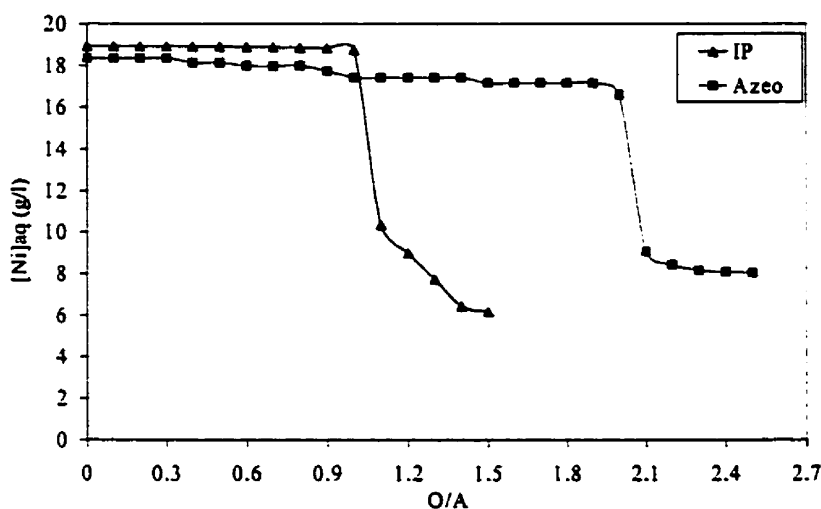


Figure 4.5 Comparative SDC tests using IP and azeotrope (200 g/l H_2SO_4 , $T=20^{\circ}\text{C}$)

Since the azeotrope contains only 88% (wt/wt) IP it is clear that more azeotrope must be added to start crystallisation. As observed, when working with aqueous solutions of similar nickel content (~ 18 g/l Ni), an O/A ratio of 1.9 (where O represents the **whole** azeotrope) was required to precipitate nickel sulphate as opposed to 1.1 for the pure IP. Nevertheless, if O/A_{crystall} for the azeotrope is recalculated on the basis of IP content only, the converted value is 1.16, very close to O/A_{crystall} when using pure IP (table 4.3). These results indicate that more azeotrope must be employed if a similar $[\text{Ni}]_{\text{aq,final}}$ to that obtained with pure IP is desired, meaning increased volumes to be handled and separated by distillation. However, since the boiling point of the azeotrope is 80°C (lower than

those of IP and water) separating the azeotrope brings the additional advantage of less energy consumption for evaporation.

Another observation derived from this test is that the use of azeotrope does not lead to an increased acidity in the aqueous phase following distillation.

4.1.4 Effect of temperature

To simulate the industrial working conditions (the spent electrolyte leaves the tankhouse at elevated temperatures: 40-50°C), a SDC test at 40°C was also performed.

Table 4.4 Initial and final SDC parameters at different temperatures (MOS = IP)

CONDITIONS	INITIAL		FINAL	
	T = 20°C	T = 40°C	T = 20°C	T = 40°C
[Ni] _{aq} , g/l	25.09	24.45	6.55	7.19
O/A _{crystall.}	-	-	1.0	1.5
O/A _{total}	-	-	1.5	2
[H ₂ SO ₄], g/l	198.3	200.7	305.17*	331.15*

*- after distillation

As indicated in table 4.4, SDC performed at 40°C requires a higher O/A ratio to initiate crystallisation (since nickel sulphate solubility increases with temperature); consequently, more IP must be employed in order to reach a similar [Ni]_{aq} as for 20°C (figure 4.6).

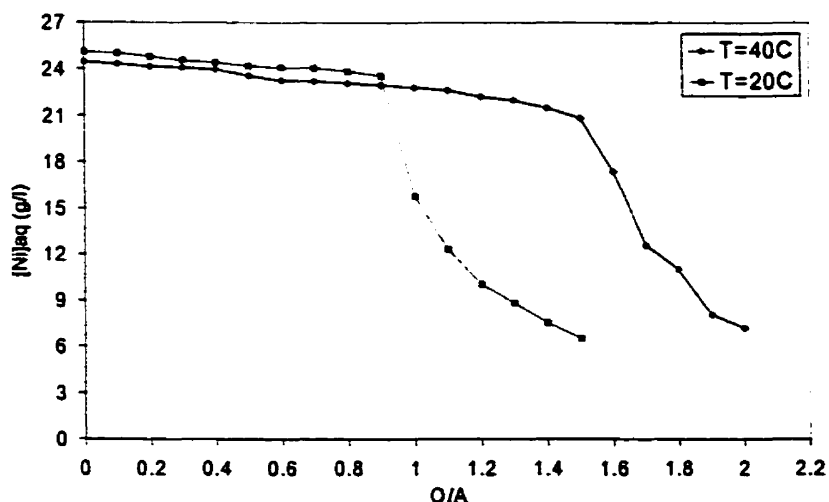


Figure 4.6 Effect of temperature on SDC (200 g/l H₂SO₄, IP)

- **Crystal morphology**

Images obtained from SEM were used to evaluate particle size and morphology of crystals produced by preliminary SDC tests under different conditions (IP, azeotrope, 20°C and 40°C respectively) and to compare them with pure, reagent-grade $\text{NiSO}_4 \cdot 6\text{H}_2\text{O}$ from Fisher (figure 4.7).

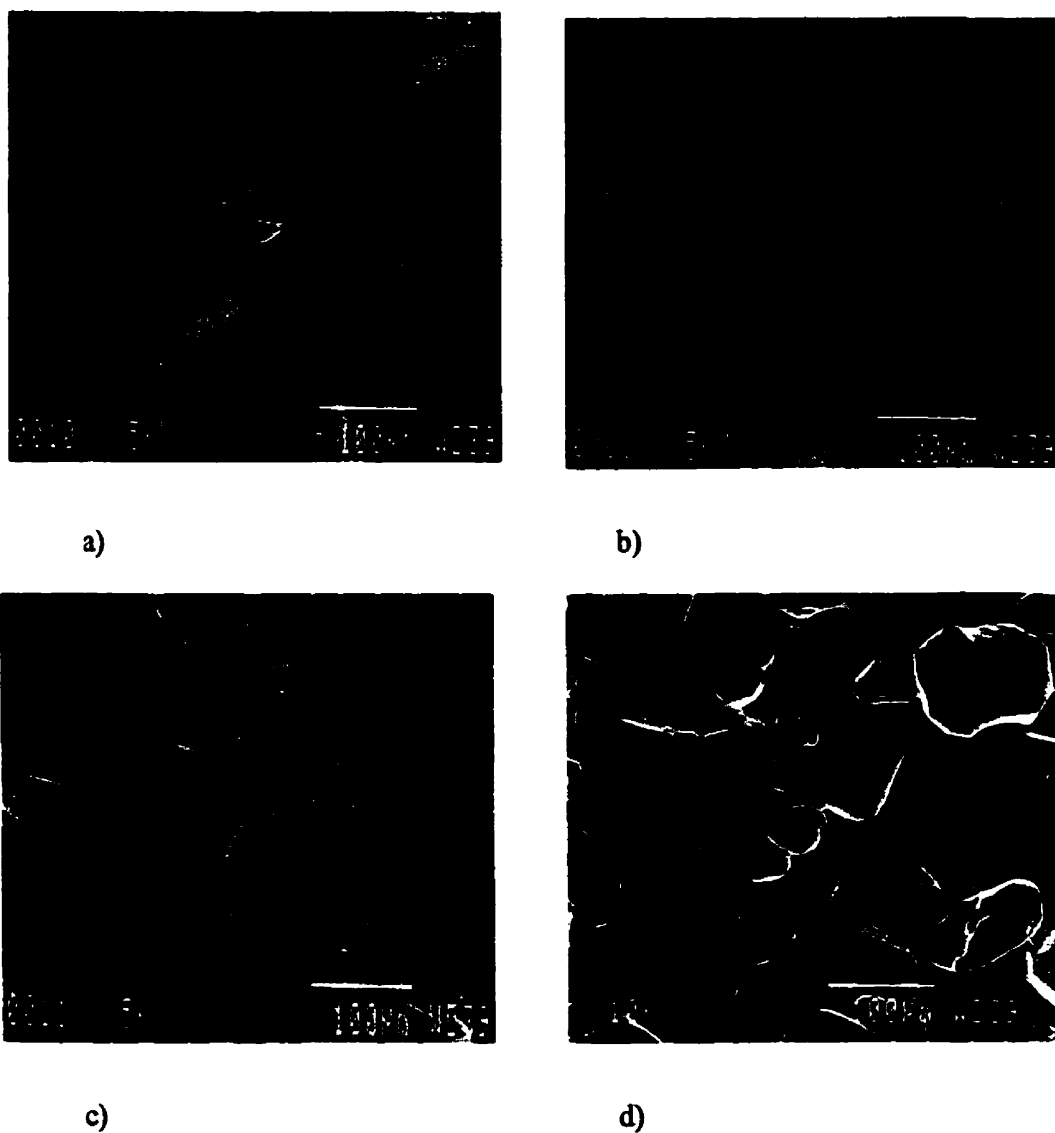


Figure 4.7 SEM images of $\text{NiSO}_4 \cdot 6\text{H}_2\text{O}$ crystals (preliminary tests, $\times 200$ magnification)

- a) pure $\text{NiSO}_4 \cdot 6\text{H}_2\text{O}$ (Fisher); b) SDC: 20°C, IP;
- c) SDC: 20°C, azeotrope; d) SDC: 40°C, IP.

Compared to pure $\text{NiSO}_4 \cdot 6\text{H}_2\text{O}$, which exhibits very coarse particles (figure 4.7 a), the crystals obtained via SDC have a smooth surface and an average size of $\sim 100 \mu\text{m}$ or less. Agglomerated particles are obtained at ambient temperature (figure 4.7. b) whereas the use of azeotrope as opposed to pure IP produces rougher crystals (figure 4.7 c). The quality and morphology of crystals (cleaner, larger) seem to be better at elevated temperatures (figure 4.7 d).

4.1.5 Final acidity of aqueous phase

As already explained, IP is recovered by fractional distillation at 80°C , although its boiling point is 82°C . This behaviour (better explained in appendix C) is due to its property to form strong hydrogen bonds with water hence it distils out not as pure solvent but as a mixture. This mixture is called “*azeotrope*” and behaves as a pure compound containing 88% IP and 12% H_2O (wt/wt). The direct consequence of this fact is that, upon distillation, some water is removed from the aqueous phase and carried to the azeotrope, provoking thus an increase in H_2SO_4 concentration in the final aqueous solution.

The variation of sulphuric acid concentration during SDC under different conditions is summarised in table 4.5. The method used to measure sulphuric acid concentration is described in some detail in appendix A.

Table 4.5 Sulphuric acid concentration before and after distillation

SDC Conditions	[H_2SO_4] (g/l)	
	Initial (before distillation)	Final (after distillation)
20°C, IP	198.3	305.17
40°C, IP	200.7	331.15
20°C, azeotrope	201.14	206.78

As observed, sulphuric acid concentration in the aqueous solution after distillation is increased with approx. 50% when IP is employed as salting out agent whereas the use of azeotrope has no effect on $[\text{H}_2\text{SO}_4]_{\text{aq}}$. From an energy point of view, the azeotrope is preferred. However, returning dilute acid ($\sim 200 \text{ g/l}$) to the tankhouse needs to be

evaluated by employing the water balance of the plant. This issue is not considered here, as no plant data were available to the author.

Partial Conclusions

- Nickel sulphate solubility in IP-H₂O system was determined and found to be strongly dependent on the fraction of IP, expressed as organic/aqueous (O/A) ratio.
- Preliminary SDC tests have been performed to validate similar work reported by Cohen (1987), employing IP as salting out agent for nickel sulphate. SDC method, as described in literature, can be successfully applied to the recovery of nickel (as **crystalline NiSO₄·6H₂O**) from aqueous electrolytes.
- The amount of NiSO₄·6H₂O to be precipitated depends on the temperature and volume of isopropanol.
- The use of **pure** isopropanol (as opposed to azeotrope) translates in lower [Ni]_{aq,final} and smaller amounts of precipitant employed but leads of an increased acidity of the aqueous solution upon distillation, as the organic phase is recovered as an **azeotrope** (88% w/w IP, 12% H₂O).

4.2 Homogeneous Crystallisation Tests

The main objective of this section is to assess the influence of supersaturation value on crystal product quality and $[\text{Ni}]_{\text{aq,final}}$ and to perform comparative SDC tests on the synthetic and industrial electrolyte in order to evaluate the kinetics of the process.

4.2.1 Tests conducted at high supersaturation

As the crystallisation theory indicates (Demopoulos, 1997), precipitation under high supersaturation conditions (i.e. nucleation prevails over growth) leads to very fine particles, usually difficult to separate by filtration. The value of supersaturation relates to the amount of precipitant added and its rate of addition. In the present research work, the amount of organic precipitant is expressed as "organic to aqueous ratio" (O/A).

4.2.1.1 Influence of O/A ratio on nickel concentration in the aqueous phase

Since IP acts as salting-out agent for nickel sulphate, it was important to determine the relation between the amount of IP and the decrease in nickel concentration in the aqueous phase. Hence, the optimum experimental conditions could be determined (i.e. the minimum amount of IP that would achieve an acceptable final value of Ni).

Table 4.6 gives the values of $[\text{Ni}]_{\text{aq}}$ as a function of O/A for both synthetic and industrial electrolytes. It must be mentioned that these are not true equilibrium values as the stirring intervals between IP additions were short: 15 minutes in duration.

Table 4.6 Influence of O/A on $[\text{Ni}]_{\text{aq}}$ (250 g/l H_2SO_4 , $T=20^\circ\text{C}$, IP)

O/A	$[\text{Ni}]_{\text{SYNTH}} \text{ (g/l)}$	$[\text{Ni}]_{\text{IND}} \text{ (g/l)}$
0	19.04	20.78
1	19.04	12.39
2	7.85	6.53
3	5.09	3.07
4	0.99	1.32
5	0.79	0.8
6	0.6	0.59
7	0.47	0.47
8	0.43	0.35
9	0.31	0.24
10	0.25	0.20

Figure 4.8 illustrates the trend observed from the previous table.

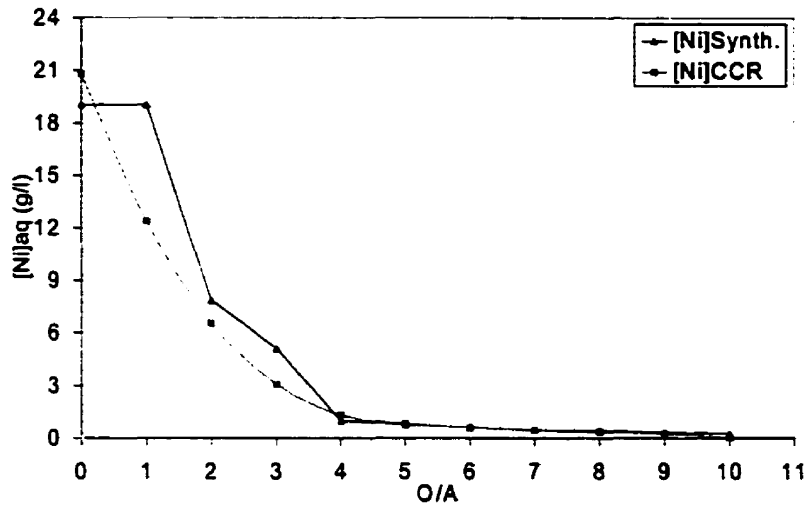


Figure 4.8 Influence of O/A on $[Ni]_{aq}$

This chart indicates that $O/A=1$ has no effect on synthetic electrolyte but triggers homogeneous crystallisation in the industrial one. This different behaviour can be explained by the presence of impurities in the industrial solution (gypsum and other particles), which act as seed for nucleation.

For $O/A>1$, rapid homogeneous crystallisation occurs as the critical supersaturation is reached (section 2.4 of this thesis), resulting in a sharp decrease in nickel concentration. At $O/A>4$ only slight decrease in $[Ni]$ is obtained (table 4.6), since over 90% of the aqueous nickel content is already precipitated at $O/A=4$.

Depending on the target value of nickel concentration in the final solution, an appropriate O/A has to be chosen.

4.2.1.2 Equilibrium value of Nickel and Induction Time function of O/A

Nielsen (1984) defines the *induction time* (τ) as “the time interval between mixing two reacting solutions and the appearance of the first crystals that can be visually observed”. Although this is an over-simplification, induction time represents the time needed for the assembly of a critical nucleus and depends on supersaturation (Mullin, 1993). The efficiency of a precipitating agent (expressed as O/A) can be qualitatively evaluated through τ values (figure 4.9). The left-hand y-axis shows the induction times

for the industrial electrolyte, the values for the synthetic solution are read off the right-hand axis.

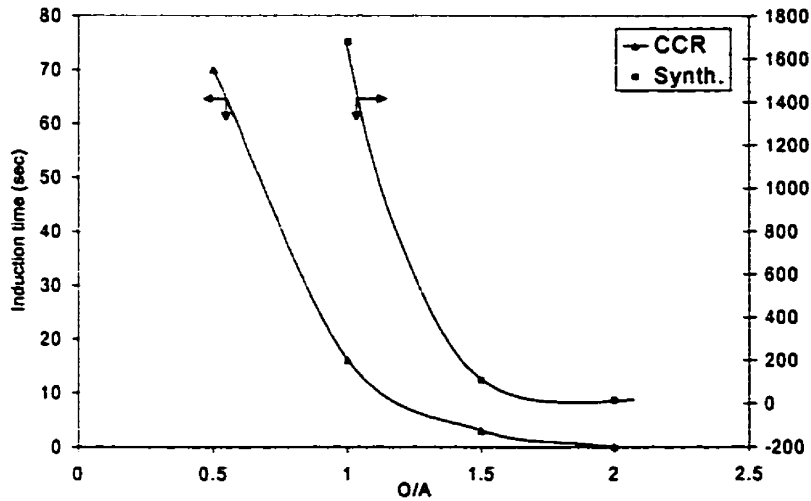


Figure 4.9 Influence of O/A on the induction time (250 g/l H₂SO₄, T=20°C, IP)

Crystallisation occurs much more rapidly in the industrial electrolyte as compared to the synthetic one (lower τ), for the same O/A ratio; this behaviour has already been correlated to the impurities that act as nucleation sites in the industrial solution. For example, at O/A=1, the synthetic, pure, electrolyte requires 28 minutes to initiate homogeneous crystallisation, as compared to 16 seconds in the case of industrial one!

Any O/A>2 induces practically instantaneous crystallisation, therefore τ is considered to become zero (table 4.7). The induction time is a subjective value, since it relates on the observer's eye; moreover, air bubbles formed during the incorporation of IP in the aqueous phase prevent the visualisation of the first crystals at high O/A ratios.

Typical SDC tests were performed allowing an equilibration period of only 15 minutes between IP additions; hence it was considered interesting to determine the *minimum* ("true" equilibrium) nickel concentration achievable in the aqueous phase for a certain O/A value by extending the equilibration time to 24 hrs. Different O/A ratios were prepared with synthetic and industrial solutions containing ~20 g/l Ni and 250 g/l sulphuric acid, followed by continuous stirring (24 hrs). Then the solutions were filtered and AA was performed on the filtrate to determine [Ni]_{eq} (table 4.7).

Table 4.7 Influence of O/A on some process parameters

O/A	SYNTHETIC		INDUSTRIAL	
	τ (sec)	$[\text{Ni}]_{\text{eq}}$ (g/l)	τ (sec)	$[\text{Ni}]_{\text{eq}}$ (g/l)
0	No ppt	20.66	No ppt	20.68
0.5	No ppt	20.66	70	17.15
1.0	1680	16.53	16	14.71
1.5	107	5.68	3	6.65
2.0	15	4.33	0	5.04

Equilibrium values of nickel in the aqueous phase (i.e. minimum Ni concentration for a certain O/A) can be also visualised on the chart depicted in figure 4.10.

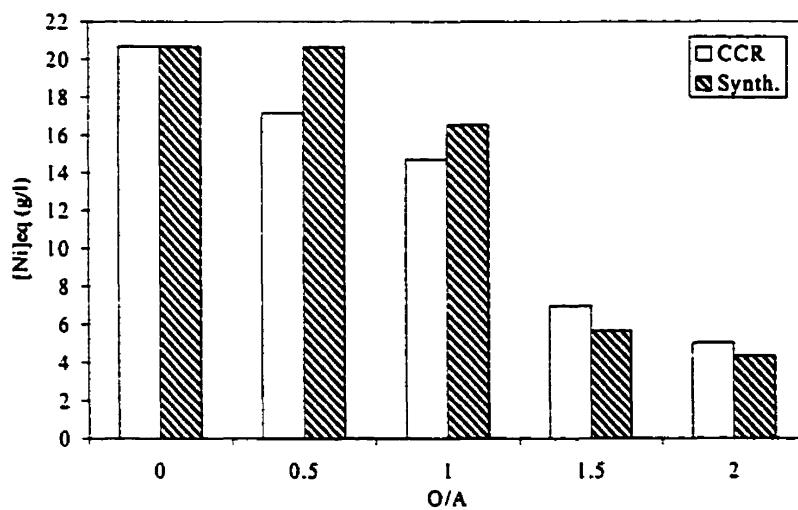


Figure 4.10 Equilibrium values of Ni function of O/A (time elapsed: 24 hr, 250 g/l H_2SO_4 , $T=20^\circ\text{C}$, IP)

The chart confirms the fact that nickel concentration decreases with increasing O/A and sub-unit values of O/A do not induce crystallisation in the synthetic electrolyte, as already discussed. Even for O/A=1, the nucleation process is slow, hence the lower nickel concentration in the synthetic electrolyte as opposed to the industrial one, where the impurities promote nucleation.

4.2.1.3 Kinetics study

The aim of this study was to determine the comparative kinetics for the two solutions considered, which is illustrated below (figure 4.11).

High supersaturation was ensured by the instantaneous addition of IP ($O/A=1.5$) to the aqueous phases which contained ~ 20 g/l Ni and 250 g/l sulphuric acid, under moderate stirring, at room temperature (20°C). Sampling was performed at 2, 5, 10, then every 15 minutes, for a 180-minutes total period, in order to analyse for nickel.

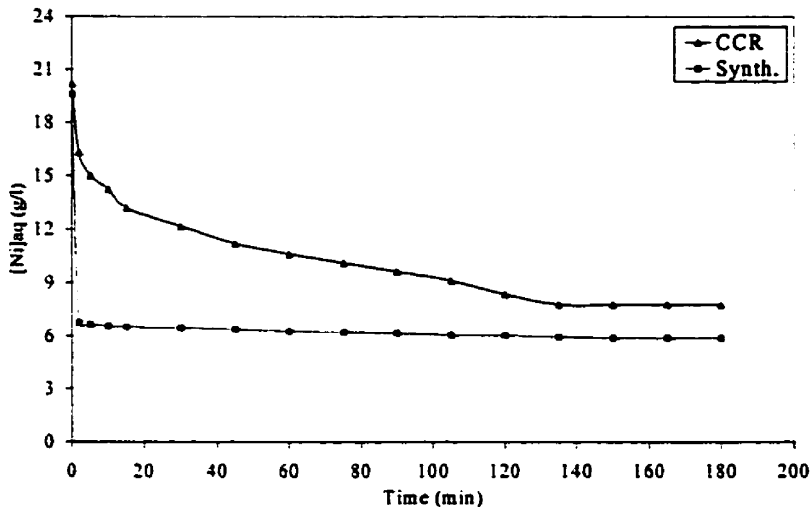


Figure 4.11 Comparative kinetics study (250 g/l H_2SO_4 , $O/A=1.5$, $T=20^\circ\text{C}$)

Crystallisation/precipitation kinetics are very fast with the synthetic solution but slow with the industrial one. This is exactly the opposite of nucleation kinetics (refer to induction times in table 4.7). Approximately 5 minutes are required by the synthetic electrolyte to attain a concentration of 6.7 g/l Ni; the subsequent decrease to the final value of 6.15 g/l (corresponding to a supersaturation of 3.25) shows a plateau over the remaining time interval. This value, compared to the equilibrium concentration of 5.68 g/l Ni (section 4.2.1.2), suggests that an interval of less than 30 minutes should suffice to perform efficient homogeneous SDC tests on the synthetic system.

Industrial electrolyte requires more than 120 minutes to reach constant concentrations of 7.76 g/l Ni (corresponding to $S=2.57$) and these values are still higher than those obtained in the synthetic solution under similar conditions (behaviour already related to the amount of impurities). Nevertheless, they are relatively close to the equilibrium

concentration of 6.65 g/l, hence 120 minutes should suffice for a SDC test performed on the industrial weak acid.

4.2.2 Tests conducted at low supersaturation

In this section, the critical supersaturation lines are determined, in an effort to achieve a better supersaturation control during SDC.

4.2.2.1 Critical supersaturation line

As explained in section 2.4.1, supersaturation is the concentration of component ions in excess of the saturated concentration, usually expressed as $S=C/C_{eq}$ (C-solute concentration, C_{eq} -equilibrium solubility of the solute at the temperature and pressure of the system). Mullin (1993) defines the critical supersaturation line as the concentrations at which uncontrolled homogeneous (spontaneous) crystallisation occurs. Its position is not as well defined as that of solubility line because it is affected by the rate at which supersaturation is generated and the intensity of agitation.

In this research work, critical supersaturation lines were constructed for both electrolyte solutions, in order to establish the window in which the homogeneous crystallisation is prevented and low supersaturation is maintained. This was done in order to achieve better crystal quality and lower nickel concentrations in the aqueous phase.

Solutions of different amounts of Ni and 250 g/l H_2SO_4 were agitated in Pyrex flasks as small volumes of IP were slowly added to the aqueous solutions at ambient temperature; after each addition, a 15-minutes equilibration period was allowed. At the initiation of the homogeneous crystallisation process, the volume of IP was recorded and the solutions were stirred for 24 hours, to reach complete equilibrium. Ni content in solution was determined by AA analysis, as shown in figure 4.12 for the synthetic solution.

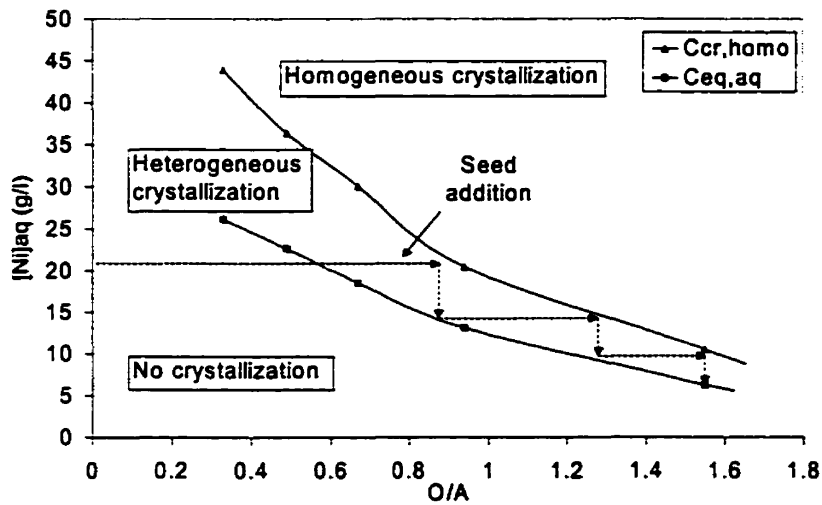


Figure 4.12 Critical supersaturation line for the synthetic electrolyte (250 g/l H_2SO_4 , $T=20^\circ\text{C}$, $S_{\text{cr}} \sim 1.6$)

As indicated by the chart, $S_{\text{cr}} \sim 1.6$; for any $S > 1.6$, homogeneous (spontaneous) crystallisation occurs in the synthetic solution, yielding fine precipitates (product characteristics addressed in section 4.2.3.2). On the other hand, $S < 1$ does not promote the specific conditions required for crystallisation.

For any supersaturation value in the range 1-1.6, crystallisation is thermodynamically possible but does not start (metastable equilibrium) because of unfavourable kinetics. In order to control supersaturation below S_{cr} but still achieve low nickel concentrations, IP should be added in a step-wise manner following the path indicated in figure 4.12, in accordance to Crystallisation Theory. Moreover, if, instead of increasing supersaturation by the addition of IP, nickel sulphate seed (crystals) is introduced to the aqueous solution in the previously-mentioned supersaturation interval, *heterogeneous crystallisation* starts, ensuring thus even more favourable conditions for crystal growth.

The next step of this comparative study was to establish in a similar manner the critical solubility line for the industrial weak acid (figure 4.13). It appears that $S_{\text{cr}} \sim 1.1$; for any $S > 1.1$, “homogeneous” (spontaneous) crystallisation occurs in the industrial solution, yielding fine precipitates.

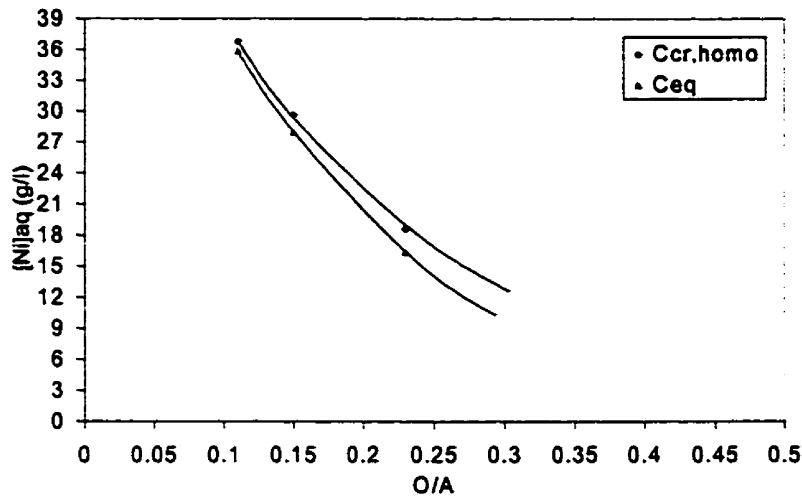


Figure 4.13 Critical supersaturation line for the industrial electrolyte (250 g/l H_2SO_4 , $T=20^\circ\text{C}$, $S_{\text{cr}} \sim 1.1$)

As observed, the heterogeneous crystallisation window is much narrower than that for the synthetic system, hence supersaturation control through step-wise addition of IP is difficult to perform. However, these results must be regarded with caution, since the premature formation of a white precipitate (later identified as gypsum, $\text{CaSO}_4 \cdot 2\text{H}_2\text{O}$) constitutes a major source of error for the evaluation of nickel sulphate homogeneous precipitation in the industrial electrolyte. Moreover, the critical concentrations to induce spontaneous precipitation are not truly “homogeneous”, due apparently to small gypsum and other impurity particles that act as nucleation seeds and cause crystallisation at low supersaturation, below “true” $S_{\text{cr,homo}}$.

Considering these, the only coherent means to maintain a low supersaturation in the case of the industrial electrolyte is to add IP in small O/A increments.

4.2.2.2 SDC tests at low supersaturation

SDC tests at low supersaturation have been performed in order to study and compare the behaviour of the two solutions and to monitor the nickel concentration in the aqueous phase.

A typical test was conducted as follows: 300 ml IP were added to 200 ml aqueous solutions (i.e. total O/A=1.5), under moderate stirring, (addition rate of 1ml/min).

Ni concentration in the aqueous phase was monitored by sampling every 15 minutes, for a total duration of 150 minutes. The results from comparative SDC tests performed on the synthetic and industrial electrolytes are presented in figure 4.14. The two solutions obviously behaved differently during SDC, despite same initial nickel and sulphuric acid concentration and same experimental conditions.

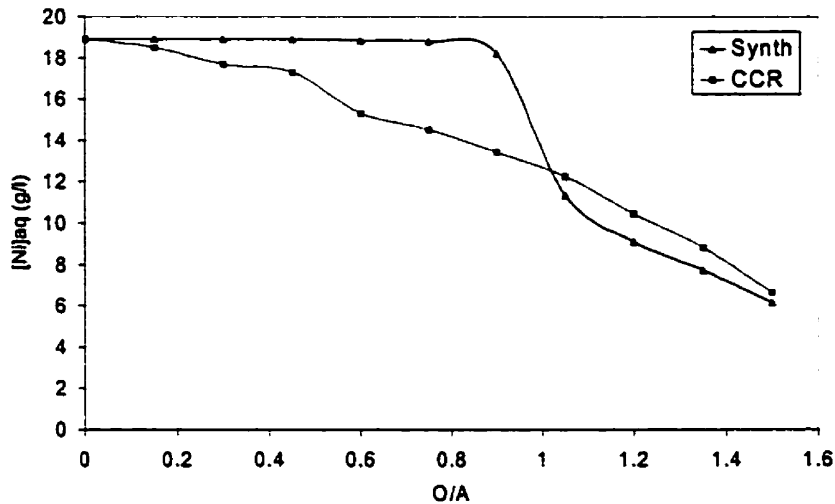


Figure 4.14 Comparative SDC tests at low supersaturation (250 g/l H_2SO_4 , $T=20^\circ C$, $O/A_{total}=1.5$)

Table 4.8 summarises the most important parameters monitored during the tests.

Table 4.8 Comparative SDC results at low supersaturation ($O/A_{total}=1.5$)

Solution	$[Ni]_{initial}$ (g/l)	$O/A_{cr,homo}$	Controlled low Supersaturation	$[Ni]_{final}$ (g/l)
SYNTHETIC	19.2	~ 1.05	1.4-1.6	5.88
INDUSTRIAL	18.7	0.27-0.3 (*)	1.08-1.1	6.78

(*) gypsum starts precipitating at $O/A=0.2-0.22$

As IP was gradually added to the synthetic solution, no precipitation occurred while $S < S_{cr,homo}$. Above a certain O/A value, identified as ~1.05 (corresponding to $S \sim 1.6$), homogeneous crystallisation started, resulting in a sharp decrease in $[Ni]$, trend that continued (although more moderately) as additional IP entered the system. The chart indicates that the duration of the process can be considerably shortened by adding at once the fraction of IP corresponding to $O/A=1$ (no precipitation yet, since $S < S_{cr,homo}$).

The remaining fraction of $O/A = 0.5$ will be subsequently added in a controlled manner, as indicated in section 4.2.2.1, to maintain a low supersaturation.

Homogeneous crystallisation of nickel sulphate was found to start at much lower supersaturation values in the case of the industrial electrolyte ($O/A \sim 0.3$, corresponding to $S \sim 1.1$). Moreover, gypsum precipitation was found to initiate at $O/A \sim 0.2$, which interferes severely with the crystallisation of nickel sulphate. It is believed that gypsum (and perhaps other trace impurities) acts as seed to promote heterogeneous nucleation hence early crystallisation of nickel sulphate. Since an exact $S_{cr,homo}$ could not be determined in this case, supersaturation control in subsequent tests is performed by step-wise IP addition from the start to the finish.

Final concentrations in aqueous phase were 5.88 g/l Ni for the synthetic solution and 6.78 g/l Ni for the industrial one, suggesting that the effect of selected O/A ratio (i.e. 1.5) is comparable with respect to nickel, despite different electrolyte behaviour.

Partial Conclusions

- Critical supersaturation line established for the synthetic solution allows the application of Crystallisation Theory principles in conjunction with nickel sulphate precipitation via SDC, in order to control supersaturation and produce good quality crystals.
- The similar line determined for the industrial solution should not be relied on since premature gypsum crystallisation interferes with nickel sulphate precipitation.
- The critical O/A that initiates homogeneous crystallisation under low supersaturation was determined for both electrolytes by performing comparative SDC tests.
- Although the two systems behave differently during SDC, the final nickel concentration in aqueous has comparable value for the same O/A and reaction time.

4.2.3 Influence of Supersaturation

As already explained, the Crystallisation Theory predicts that a low (controlled) supersaturation translates in improved crystal quality during homogeneous crystallisation tests as it creates more favourable conditions for growth as opposed to excessive nucleation.

The effects of supersaturation magnitude on $[\text{Ni}]_{\text{final}}$ and crystal morphology are assessed by comparing the results obtained from SDC performed on synthetic and industrial electrolytes.

4.2.3.1 Final nickel concentration in the aqueous phase

Table 4.9 depicts a summary of homogeneous crystallisation tests performed at 20°C, employing a total O/A=1.5 under high and low supersaturation conditions, respectively; the same data are graphically presented in figure 4.15.

Table 4.9 Final nickel concentration in homogeneous SDC tests (O/A_{total}=1.5, 20°C)

$[\text{Ni}]_{\text{aq}}$ (g/l)	Equilibrium ⁽¹⁾	High Supersaturation ⁽²⁾	Low Supersaturation ⁽³⁾
SYNTHETIC	5.68	6.15	5.88
INDUSTRIAL	6.65	7.76	6.78

⁽¹⁾ total reaction time=24 hr

⁽²⁾ total reaction time =180 min, IP added at once

⁽³⁾ total reaction time =150 min, IP added in doses

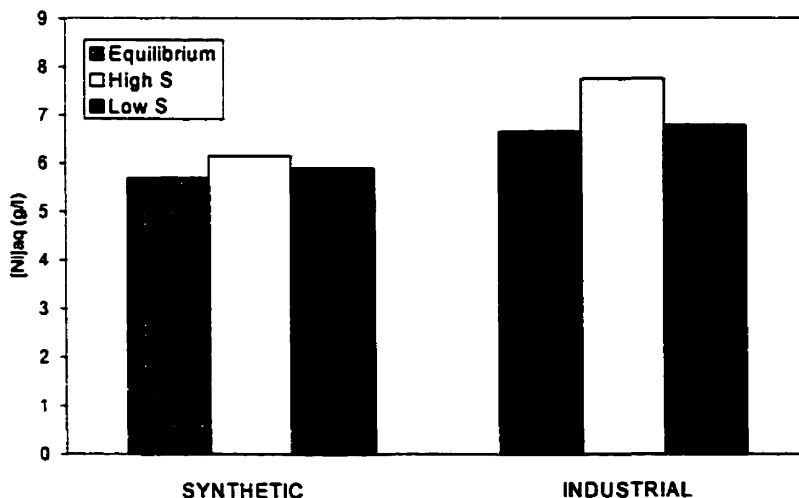


Figure 4.15 Final Ni concentration as a function of supersaturation, compared to equilibrium values (250 g/l H₂SO₄, O/A=1.5, T=20°C)

As expected, SDC tests performed in conditions of controlled supersaturation achieved lower nickel concentrations for both systems, compared to similar tests at high supersaturation, since the growth-controlled precipitation mechanism prevents the formation of colloidal particulates.

For the same SDC conditions (O/A, reaction time, temperature), final nickel concentrations were always higher for the industrial electrolyte than for the synthetic one. This may be explained by the presence of impurities in the industrial solution, which adsorb on the crystal's surface inhibiting further growth (section 2.4.4).

4.2.3.2 Crystal quality

SEM photos show distinct crystal morphology and size dependence on supersaturation magnitude. Tests conducted at high supersaturation yielded fine, irregular crystals of less than 50 μm average size for both electrolytes. However, the product from the synthetic solution shows smoother surfaces whereas the crystals from the industrial one have sharper contours and present cracks (figure 4.16 a and b). This can be related to impurities, which selectively adsorb on the growing particle's surface, as explained by Mullin (1993).

Tests conducted at low supersaturation show a certain increase in particle size. The crystals from synthetic electrolyte (average particle size 50-100 μm) preserve the smooth appearance, as the shape tends to become polygonal (figure 4.16 c). The product obtained from the impure system exhibits the same fractured, irregular shape; although the average size slightly increased for some particles, this growth process is not general. A large population of fine, acicular particles also formed despite the controlled supersaturation. Moreover, the product is largely contaminated by gypsum particles, which precipitate as extremely fine needles prior to and along with nickel sulphate (figure 4.16 d).

In conclusion, it can be stated that:

- SDC tests performed under controlled supersaturation lead to lower $[\text{Ni}]_{\text{aq}}$ and better crystal quality.
- The synthetic solution yielded lower $[\text{Ni}]_{\text{aq}}$ and larger crystals.
- For subsequent SDC tests, the control of supersaturation should be accompanied by use of seed/product recycling in order to achieve even better results in terms of crystal quality and final nickel concentrations.

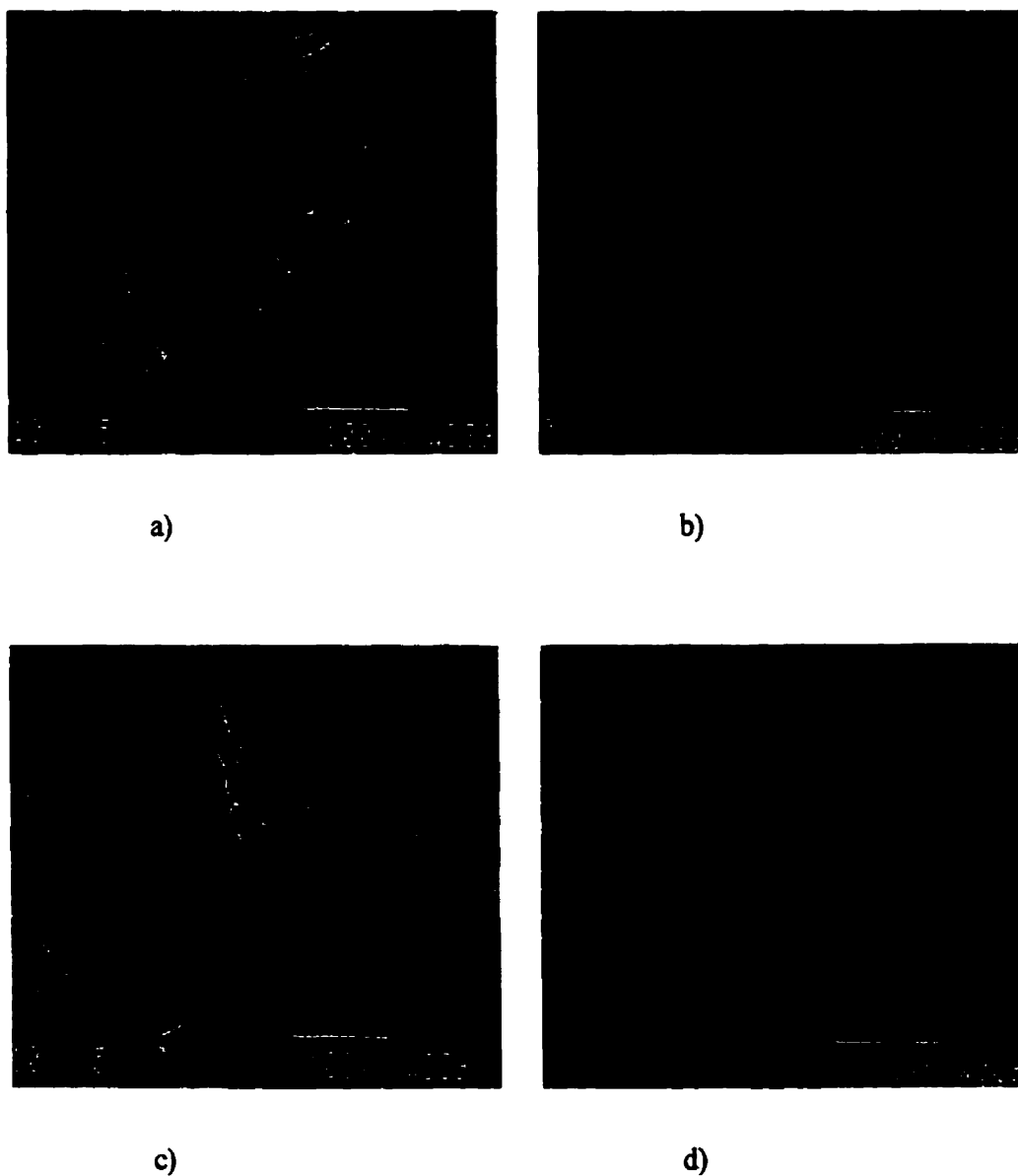


Figure 4.16 Crystals obtained via homogeneous SDC (SEM, x200 magnification)

- a) synthetic, high supersaturation; b) industrial, high supersaturation;
- c) synthetic, low supersaturation; d) industrial, low supersaturation.

4.3 Heterogeneous Crystallisation Tests

The previous section demonstrated that controlled (low) supersaturation has beneficial effects on crystals' quality, even for homogeneous crystallisation conditions. If same-nature crystalline seed is made available during the first stages of a precipitation process conducted under low supersaturation, larger particles will be produced (growth is favoured). The objective of this section is to perform comparative heterogeneous crystallisation tests on both electrolyte systems to produce large-sized nickel sulphate crystals and then to monitor the growth process by assessing some product properties.

4.3.1 Comparative SDC tests

In both cases, 300 ml IP are step-wise added to 200 ml aqueous solution ($O/A_{total}=1.5$) under moderate stirring, at 20°C. Each IP addition is followed by 15-min equilibration periods and sampling to analyse for Ni. The seeding step (50 g/l $NiSO_4 \cdot 6H_2O$ from previous SDC tests) occurs just prior to reaching $S_{cr,homo}$.

- **Synthetic Electrolyte**

Step-wise addition of IP follows the path shown in figure 4.12, section 4.2.2.1, maintaining thus low supersaturation; seed is added in the O/A range of $0.8 < O/A < 1$.

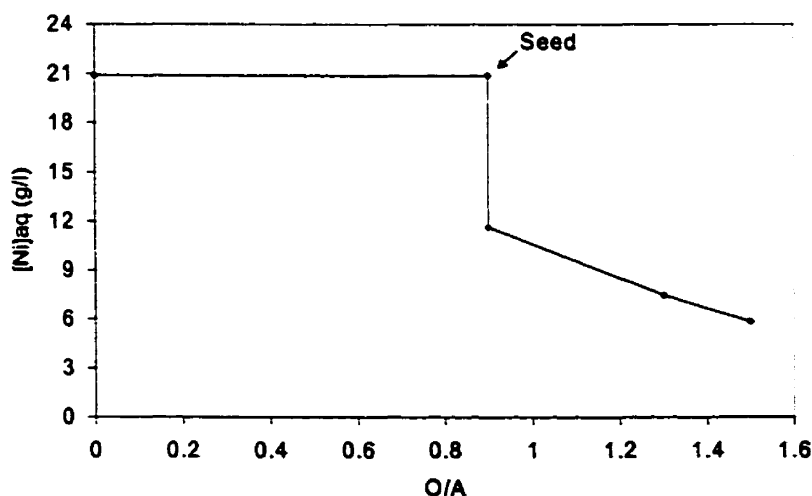


Figure 4.17 Heterogeneous crystallisation test for synthetic electrolyte

(250 g/l H_2SO_4 , $O/A_{total}=1.5$, $T=20^\circ C$, 50 g/l seed, duration=60 min)

Since the O/A ratio at which seed is added is just below $S_{cr,homo}$, there is no risk of inducing homogeneous crystallisation hence the duration of heterogeneous SDC experiments in the case of synthetic electrolyte is considerably reduced (t~60 min as opposed to 150 min for homogeneous crystallisation under low supersaturation).

Approximately 50 g/l seed ($NiSO_4 \cdot 6H_2O$) from previous SDC tests under low supersaturation in synthetic solution were added at $O/A=0.9$; since $S_{cr,homo}$ was not exceeded, secondary nucleation occurred, resulting in a sharp decrease in $[Ni]_{aq}$. A 30-min equilibration period was allowed after the seed addition step. The remaining IP was added in such a manner as to maintain a low supersaturation, according to figure 4.12.

The final metal concentration achieved in the aqueous phase was 5.85 g/l Ni, comparable to that of 5.88 g/l Ni obtained in an un-seeded test under low supersaturation. This information suggests that the selected O/A interval for seed addition was correct. Lower O/A values would provoke seed dissolution whereas higher ratios would induce spontaneous precipitation.

- ***Industrial Electrolyte***

The critical supersaturation for primary homogeneous crystallisation is system-specific; the industrial solution, despite similar composition in terms of Ni and H_2SO_4 as the synthetic solution, exhibits a different critical supersaturation line, due most probably to the presence of impurities (figure 4.13, section 4.2.2.1).

Concerning the aspect of the above-mentioned line, it was concluded that the results must be viewed with caution due to premature gypsum precipitation hence the impossibility to determine an exact O/A corresponding to $S_{cr,homo}$ for nickel sulphate. Moreover, the extremely narrow window that favours secondary nucleation offers no practical use, so the line thus established will not be employed during heterogeneous SDC tests performed on industrial electrolyte.

A certain O/A ratio that would allow addition of seed without dissolution or initiation of homogeneous crystallisation was established by trial and error. The remaining IP was step-wise added in such a manner as to maintain a low supersaturation (O/A increments of 0.2 were arbitrarily selected, corresponding to doses of 40 ml IP).

The schematic of a heterogeneous SDC test for the industrial system is depicted in figure 4.18.

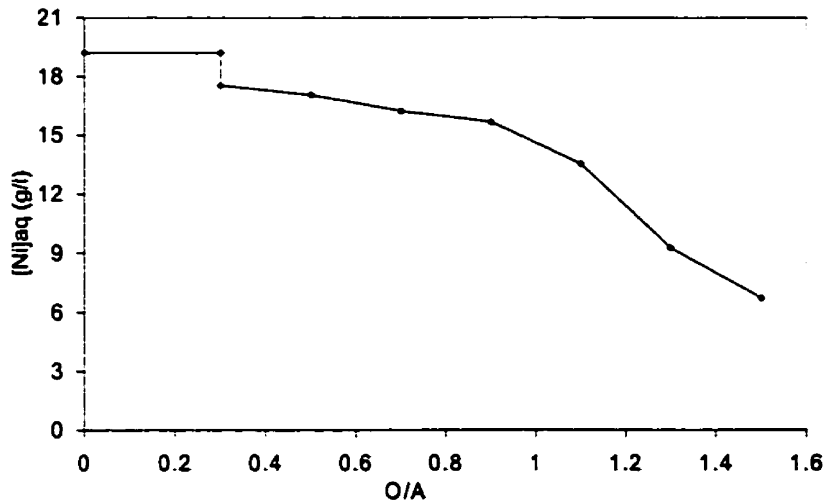


Figure 4.18 Heterogeneous crystallisation test for industrial electrolyte

(250 g/l H_2SO_4 , $O/A_{\text{total}}=1.5$, $T=20^\circ\text{C}$, 50 g/l seed, duration=120 min)

A ratio of $O/A=0.3$ was found adequate to allow seed addition without exceeding $S_{\text{cr,homo}}$; 50 g/l seed from a previously homogeneous SDC test under low supersaturation in industrial electrolyte were added then the solution was allowed to equilibrate for 30 min. To maintain controlled supersaturation, small O/A increments are employed, followed by 15-min stirring, translating thus in longer duration of the experiments performed on industrial electrolyte: 120 min as compared to 60 minutes for the synthetic system.

As observed, the decrease in nickel concentration is more moderate than for synthetic electrolyte at the same O/A_{total} ratio and quantity of seed (50 g/l $\text{NiSO}_4 \cdot 6\text{H}_2\text{O}$). The final metal concentration achieved in the aqueous phase was 6.71 g/l Ni, as opposed to 5.85 g/l Ni obtained in a similar experiment performed on the synthetic solution. Responsible for such difference appear to be the impurities present in the industrial system, which apparently adsorb on the crystals' surface, blocking thus further incorporation of nickel sulphate ions into the lattice.

An additional difficulty encountered while performing SDC tests on the industrial electrolyte was the premature precipitation of a white, fine product later identified as gypsum. The separation process starts at $O/A \sim 0.2$; although at that point the experiment

was interrupted to remove gypsum, further IP additions induce co-precipitation of remaining gypsum along with nickel sulphate, leading thus to an impure final product.

- ***Product Recycling Strategy***

Use of seed (heterogeneous crystallisation) and step-wise addition of IP (low supersaturation) should translate in better crystal quality (in terms of purity and size), as predicted by Crystallisation Theory.

If this strategy were to be repeated for a certain number of experiments, each test using as seed the product from the previous one, some increase in particle size is to be expected.

The advantages of producing well-grown crystals are obvious: better filterability, faster settling in thickeners, less amount of water retained, smaller uptake of impurities.

The number of product-recycling tests, following the initial seeding experiment, was arbitrarily chosen to be 5. All heterogeneous recycling tests were performed at 20°C, for $O/A_{\text{total}}=1.5$ and the procedure was generally the same for both solutions, similar to that previously described in this section.

The initial seeded experiment employed $\text{NiSO}_4 \cdot 6\text{H}_2\text{O}$ obtained via homogeneous SDC tests under low supersaturation (section 4.2.2.2) then part of the product from each test was used as seed for the following (corresponding to ~50 g/l seed).

4.3.2 Effect of product recycling

Since the final nickel concentration in the aqueous phase is always a function of O/A and temperature, the effect of product recycling will be monitored by those properties whose values are influenced by the growth process: crystal size and morphology, percent solids density, settling velocity.

4.3.2.1 Crystal Quality

SEM pictures offer accurate information about morphology and size of the particles. Figures 4.19 and 4.20 compare crystals obtained via SDC from synthetic and industrial solutions, respectively, after 5 recycling experiments following seeding.

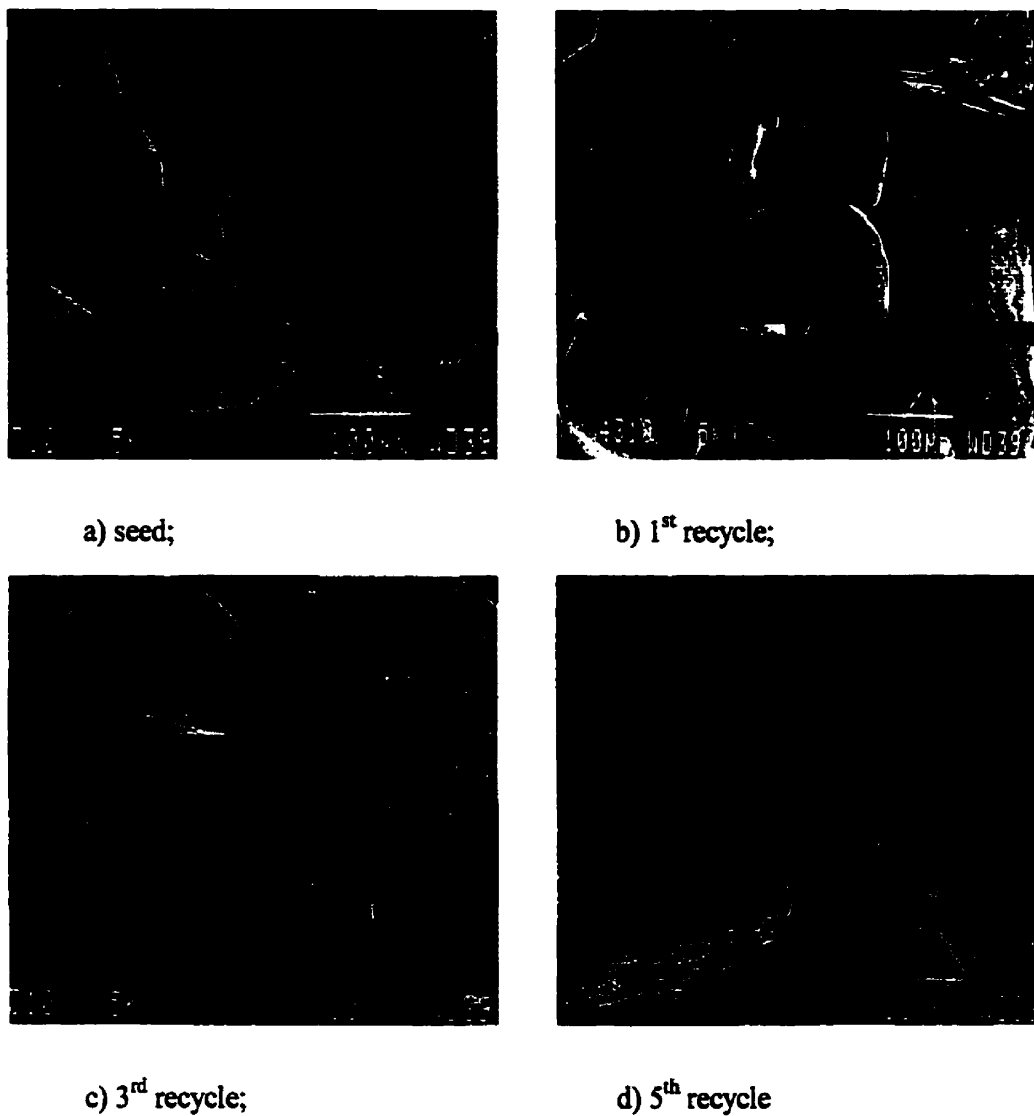


Figure 4.19 SEM images of $\text{NiSO}_4 \cdot 6\text{H}_2\text{O}$ produced from synthetic solution via heterogeneous SDC
(250 g/l H_2SO_4 , $T=20^\circ\text{C}$, $O/A_{\text{total}}=1.5$, 50 g/l seed, x100 magnification)
Average size: 400 μm



a) seed;

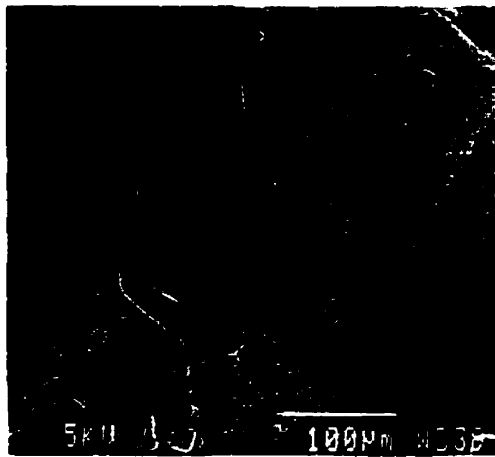
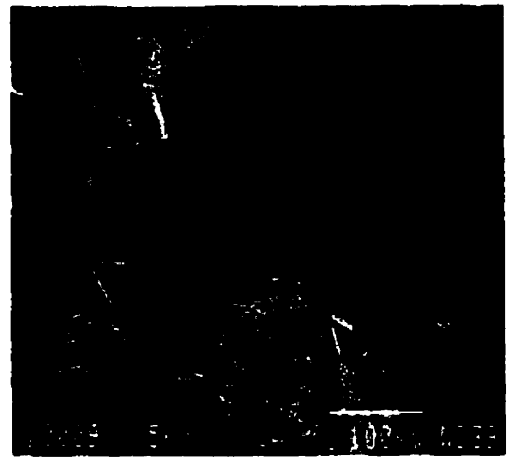
b) 1st recycle;c) 3rd recycle;d) 5th recycle

Figure 4.20 SEM images of $\text{NiSO}_4 \cdot 6\text{H}_2\text{O}$ produced from industrial solution via heterogeneous SDC (250 g/l H_2SO_4 , $T=20^\circ\text{C}$, $O/A_{\text{total}}=1.5$, 50 g/l seed, x200 magnification)
Average size: 200 μm

Heterogeneous crystallisation and product recycling favour growth in both cases; this effect is visible within the same system by comparing the product appearance after each recycle and also by comparing to the crystals obtained via homogeneous SDC (section 4.2.3.2, figure 4.16).

When the two systems are compared, crystals from industrial solution show moderate growth (average size: 200 μm) as opposed to the product from the synthetic electrolyte (average size: 400 μm), for the same number of recycles. Again the cause of this different result it seems to be the adsorption of impurities from the industrial solution onto the crystal's surface, blocking active growth sites (see also section 2.4.4).

Increased extent of recycling leads to polygonal particle shape (similar to reagent grade $\text{NiSO}_4 \cdot 6\text{H}_2\text{O}$ from Fisher), but while the particles from synthetic solution have smoother surfaces and rounder edges, crystals from industrial, impure electrolyte show dislocations, cracks and broken edges. As Mullin (1993) explains, certain impurities adsorb at defects on existing crystal surfaces, initiating thus crack propagation and subsequent fragmentation. Both systems present some decrease in particle size after the 3rd recycling, due to crystal fragmentation even under mild stirring. As the particles grow, they become susceptible to breakage by crystal-crystal, crystal-reactor or crystal-impeller collisions.

Acicular gypsum particles (regular shape for $\text{pH} < 1$, (Omelon, 1998)) separate from industrial electrolyte; even if part of gypsum is removed prior to nickel sulphate precipitation, the remaining calcium crystallises as gypsum during the entire SDC process. The gypsum problem will be addressed in some detail in section 4.4.

4.3.2.2 Settling Velocity

As the settling velocity is a function of solids content and not a definitive indication of increased particle size, the results were not used to evaluate the precipitation for each run. However, for equivalent solids loading, the settling velocities are considered as a semi-quantitative means to evaluate crystal growth (i.e. high settling velocity = large particle).

As expected, low supersaturation and use of seed/product recycling (heterogeneous crystallisation) favour growth for both systems, fact assessed by the

increasing trend in settling velocities when compared to the values issued by the homogeneous SDC tests.

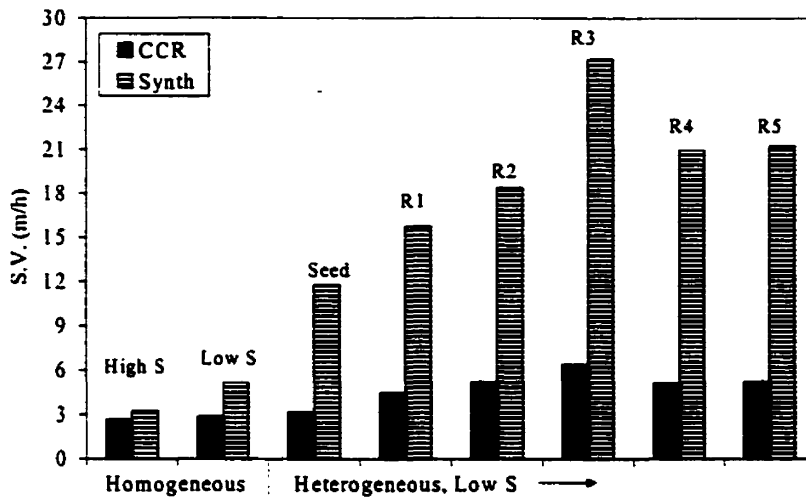


Figure 4.21 Influence of crystallisation strategy on settling velocities

The considerably lower settling velocities for the crystals produced from industrial solution are consistent to their SEM images (section 4.3.2.1) assessing a modest growth process, under the influence of impurities. The small drop in settling velocities for both systems after the 3rd recycle is related to the fragmentation process revealed by the SEM pictures; as the particles reach a critical size, they break due to cracks and collisions, the amount of fines increases resulting thus in lower settling velocities.

4.3.2.3 Solids Density

The solids density represents another semi-quantitative measure of the growth process. Large crystals have a smaller specific surface area hence retain less water form solution. Therefore, higher solids density indicates larger particles. After the slurry was allowed to settle by gravity, three aliquots of the solids were sampled from the settled mass and weighted. They were dried under ambient conditions and re-weighted. The following calculation was performed to check the solids density:

$$\text{S.D. (\%)} = (\text{dry sample mass})/(\text{wet sample mass}) \times 100 \quad (4.1)$$

The increasing trend in S.D. values for both systems proves the expected growth process, enhanced by the use of seed and product recycling under low S (figure 4.22).

The information offered by the chart below is again consistent to the information given by the SEM images concerning the crystals obtained from the industrial electrolyte: smaller S.D. indicate modest growth as compared to the product yielded by the synthetic system. As mentioned, it seems that the optimum recycles should be 3, since a larger extent of recycling triggers particle fragmentation in both solutions hence a drop in S.D.

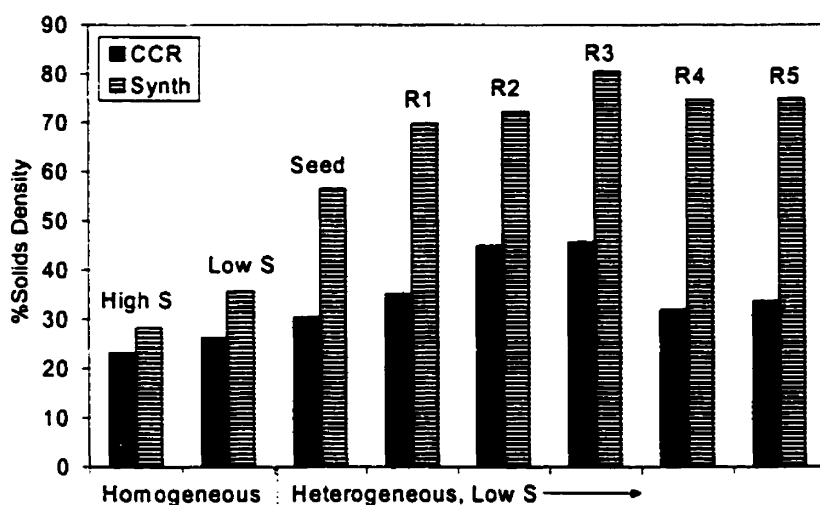


Figure 4.22 Influence of crystallisation approach on solids density

Partial Conclusions

- Use of seed/product recycling and $S < S_{cr,homo}$ (heterogeneous crystallisation) promote growth by secondary nucleation on crystal's surface rather than on reactor's walls or impeller for both electrolyte solutions, according to Crystallisation Theory principles.
- Different O/A ratios to initiate homogeneous crystallisation for the synthetic and industrial electrolyte respectively and non-similar behaviour during SDC tests are attributed to the presence of impurities in the industrial system.
- Gypsum precipitation interferes with nickel sulphate crystallisation from the industrial solution.

- For the same working conditions, heterogeneous SDC tests performed on the industrial system have a longer duration (since the selection of a low supersaturation could not rely on the critical supersaturation line, but by working with small O/A increments).
- SEM pictures confirm the growth process upon product recycling under low supersaturation for both systems. However, crystals from the industrial electrolyte exhibit a more modest growth and a rougher morphology than the particles crystallised from the synthetic one (effect of impurities discussed in section 4.4).
- Settling velocities and solids density have also been employed as semi-quantitative methods to evaluate the growth process (as they are related to particle size). These properties show an increasing tendency for both electrolyte solutions, always with smaller values for the industrial system, indicating moderate increase in particle size.
- The optimum recycling extent seems to be 3, after which a decrease in particle size occurs due to crystal fragmentation following collisions. This behaviour can be visualised through SEM images for each recycling test and by the corresponding values of settling velocities and % solids density as well.

4.4 Impurity Behaviour

The previous section demonstrated that supersaturation control and product recycling (heterogeneous crystallisation) favour particle growth so that solid/liquid separation is enhanced and impurity uptake reduced. The main objectives of this section are to assess the influence of impurities on crystal product quality both in terms of purity and size, with emphasis on calcium as the main interfering foreign element (precipitated as gypsum, $\text{CaSO}_4 \cdot 2\text{H}_2\text{O}$).

4.4.1 Effect of impurities on crystal growth

For this part of the work two feed solutions were used:

- (i) an industrial decopperised solution courtesy of Canadian Copper Refineries (CCR);
- (ii) a synthetic electrolyte simulating the composition of the industrial one in terms of nickel and sulphuric acid content (table 4.10).

Table 4.10 Chemical composition of nickel sulphate solutions

Element	Concentration in the Synthetic Solution (g/l)	Concentration in the Industrial Solution (g/l)
Ni	17-20	18-19
H_2SO_4	200-250	~250.5
Al	-	0.11
As	-	0.99
Bi	-	0.02
Ca	-	0.39
Cd	-	0.003
Co	-	0.02
Cu	-	1.14
Fe	-	0.29
Mg	-	0.08
Sb	-	0.002
Sn	-	0.11
Zn	-	0.14

The presence of impurities in a system can considerably affect crystallisation behaviour. The higher the charge on the impurity cation, the more powerful the inhibiting effect, e.g. $\text{Cr}^{3+} > \text{Fe}^{3+} > \text{Al}^{3+} > \text{Ni}^{2+} > \text{Na}^+$. The heteronuclei are rendered inactive by impurity

adsorption on their surfaces. Moreover, certain impurities adsorb at defects on existing crystal surfaces and initiate crack propagation and subsequent fragmentation.

As Mullin explains (1993), impurities can influence crystal growth rates in a variety of ways. They can change the structural properties of solutions or the equilibrium saturation concentration and hence the supersaturation. They can alter the characteristics of the adsorption layer at the crystal – solution interface and influence the integration of growth units or may be even built into the crystal (especially if there is some degree of lattice similarity). Impurities are often adsorbed selectively on to different crystal faces and retard their growth rates. To effect retardation, it is not necessary for the impurity to achieve total face coverage; three sites may be considered at which foreign species could adsorb and disrupt the flow of growth layers across the faces: a kink, a step or an edge.

Figures 4.19 and 4.20 (section 4.3.2.1) compare SEM pictures of crystals obtained via SDC from synthetic and industrial solutions, respectively, after 5 recycling experiments following seeding. The crystals from industrial solution show moderate growth (average size: 200 μm) as opposed to the product from the synthetic electrolyte (average size: 400 μm), for the same number of recycles. Retardation of crystal growth in the industrial solution may be attributed to impurity (in particular tri- and di-valent cations) adsorption.

Increased extent of recycling leads to polygonal particle shape but while the particles from synthetic solution have smoother surfaces and rounder edges, crystals from industrial electrolyte show dislocations, cracks and broken edges, suspected to be the effect of selective adsorption of impurities on their surface.

4.4.2 Behaviour of Calcium

Table 4.10 shows that the major impurities in the industrial electrolyte are copper (1.14 g/l), arsenic (0.99 g/l) and calcium (0.39 g/l). As described in section 4.1, IP addition initiate crystallisation of a white unknown precipitate at a critical O/A=0.2-0.22, prior to nickel sulphate separation (which occurs at O/A~0.3). These crystals (figure 4.23 a) were insoluble in water (even at high temperatures) but soluble in dilute HCl solutions. The process continues during the entire SDC experiment leading thus to impure nickel sulphate product (figure 4.23 b).

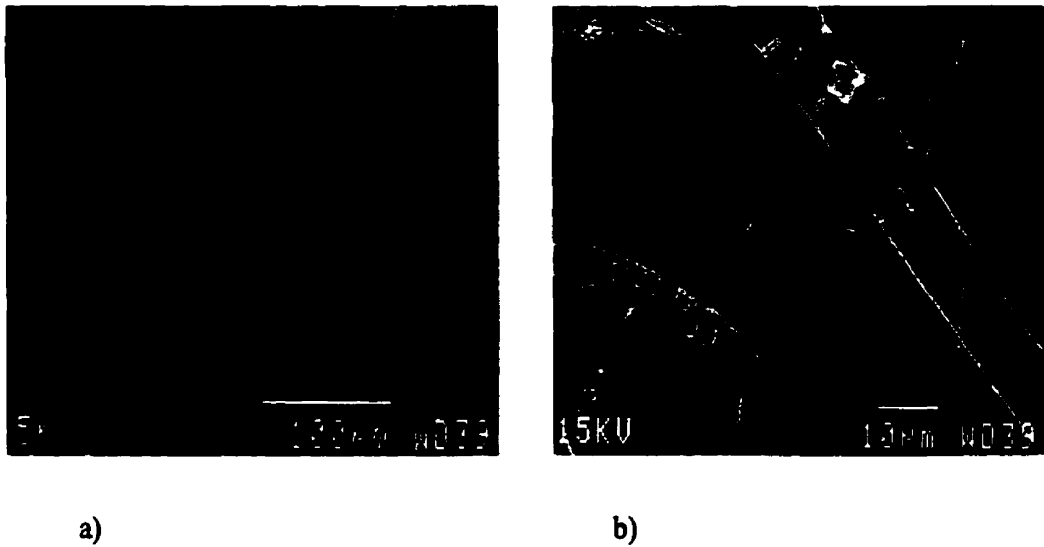


Figure 4.23 Gypsum particles separated during SDC process of nickel sulphate

- a) gypsum needles removed prior to nickel sulphate precipitation;
- b) gypsum needles co-precipitated with nickel sulphate (polygonal)

To confirm the identity of the white precipitate the Energy-Dispersive Spectroscopy (EDS) technique was employed. The detection limit of this method is quite high (~1%) but it was considered appropriate to give a first indication on the nature of the unknown product. The EDS spectrum of impure $\text{NiSO}_4 \cdot 6\text{H}_2\text{O}$ is presented in figure 4.24.

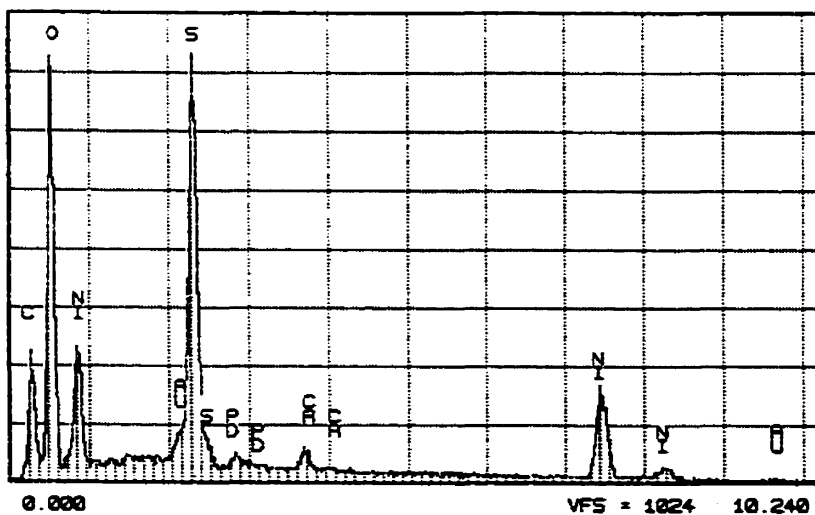


Figure 4.24 EDS spectrum of $\text{NiSO}_4 \cdot 6\text{H}_2\text{O}$ containing the white precipitate

Except the characteristic peaks coming from the coating material (Au, Pd and C), the main peaks of the spectrum indicate (as expected) Ni, O and S (hence nickel sulphate). In addition to Ni, S, and O, Ca was detected as well, revealing thus a *calcium compound*. A focused EDS spot analysis was then performed on the fine crystals, leading to a spectrum that indicated Ca, S and O (figure 4.25). Correlating this information to the solubility data found in literature, it appears thus that calcium co-precipitates with nickel sulphate under the form of **gypsum** ($\text{CaSO}_4 \cdot 2\text{H}_2\text{O}$), which is also in agreement with the fact that gypsum is a common impurity in most hydrometallurgical aqueous streams.

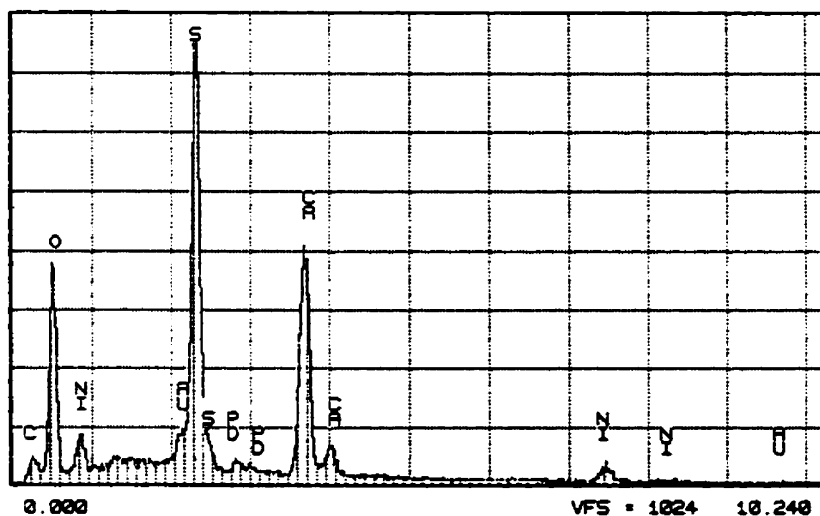


Figure 4.25 EDS spectrum of gypsum crystals (needles)

To sum up the facts, it seems that calcium present in the industrial electrolyte readily reaches its solubility limit when IP is added (O/A~0.2) and precipitates as gypsum prior to and then together with nickel sulphate, leading to an impure final product. As Omelon (1998) asserts, the acicular shape is the characteristic gypsum morphology at high acidity (250 g/l H_2SO_4); SEM pictures reveal very fine needles of < 100 μm in length (figure 4.21 a).

Apart of Ca, no other impurity was revealed by the EDS technique due apparently to its high detection limit (1%). To assess the impurity uptake process during SDC, a more sensitive method was employed, namely Inductively Coupled Plasma Spectroscopy (ICP), following dissolution of the crystals in 5% HCl.

4.4.3 Crystal quality: Solvent Displacement Crystallisation vs Evaporative Crystallisation

The previous sections discussed the quality of nickel sulphate crystals obtained via SDC from the industrial electrolyte by comparing them to those produced in a similar manner from a synthetic solution. It was demonstrated that supersaturation control and product recycling favour growth for both systems, although the product yielded by the industrial solution has a lower quality in terms of particle size and morphology. This behaviour was explained in terms of selective impurity adsorption onto the growing crystals' surface.

One of the main objectives of the present research work was to design a SDC procedure that yields clean, well-grown crystals and then to test the newly designed method with industrial electrolyte solutions and compare the product quality with that obtained Evaporative Crystallisation (EC) in CCR's Cu ER.

4.4.3.1 Particle size

Nickel sulphate crystals obtained via EC at CCR have a powdery appearance, indicating a fine particle size. Their greenish-yellow colour is characteristic to $\text{NiSO}_4 \cdot 2\text{H}_2\text{O}$ hydrate that forms at high temperature (Rohmer, 1939). These crystals have been produced by EC using the same industrial electrolyte that was employed in the present research project to perform SDC experiments.

SEM pictures of nickel sulphate crystals obtained via SDC and EC respectively are comparatively presented in figure 4.26.

Even under homogeneous crystallisation conditions, SDC produces crystals of average size $\sim 100 \mu\text{m}$ and with relatively regular shape (figure 4.26 a), indicating that the growth process was not hindered by a massive adsorption of impurities.

Under the same magnification (x200), crystals obtained via EC appear to be extremely small, tending to agglomerate in chunks (figure 4.26 b). For a better visualisation, a magnification of 1300 was required; the particles show an average size less than $10 \mu\text{m}$, irregular shapes and uneven edges which are the results of crystallisation under high supersaturation conditions (figure 4.26 c).

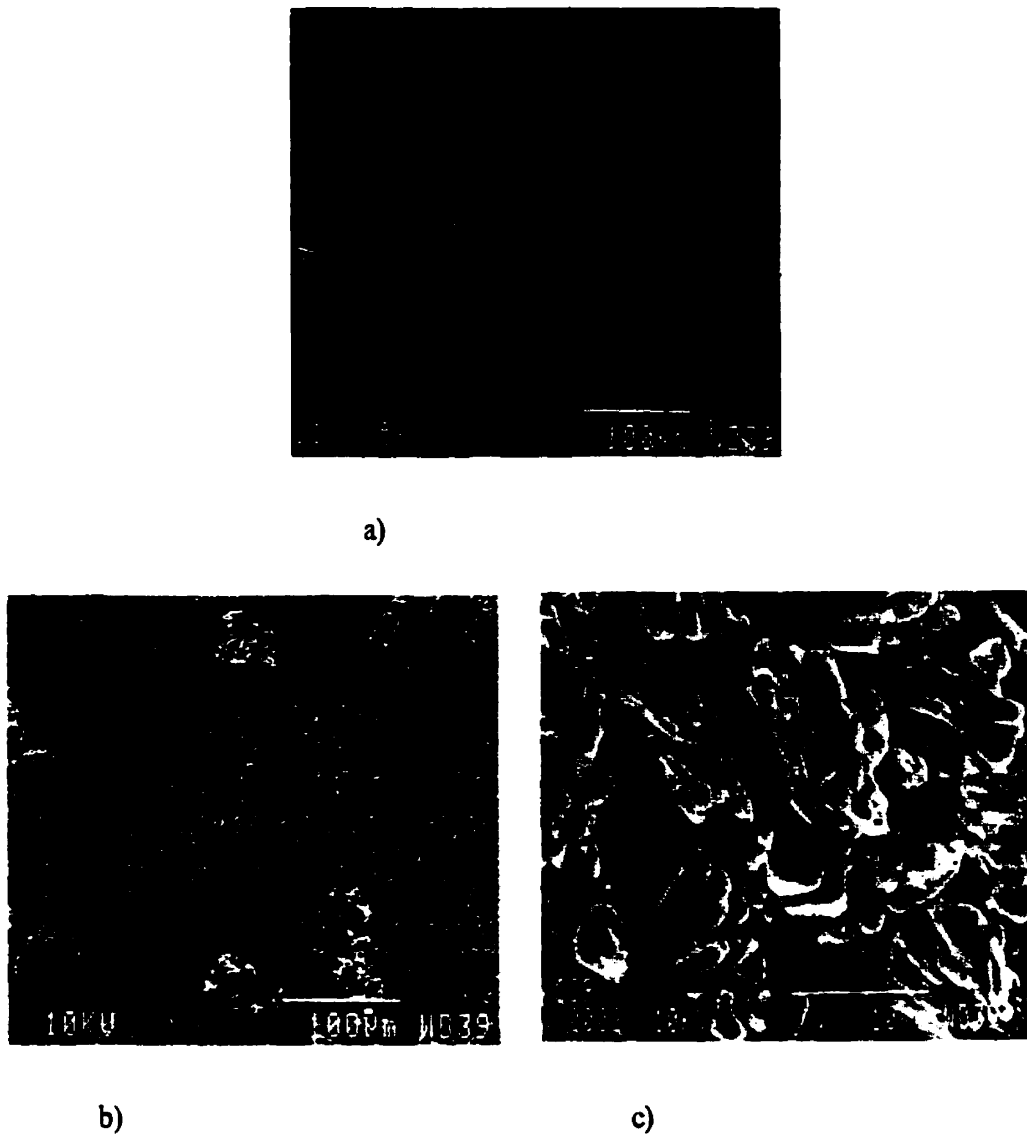


Figure 4.26 Particles of nickel sulphate produced from the industrial solution

- a) SDC method, homogeneous crystallisation, low supersaturation (20°C, x200 magnification, $O/A_{\text{total}}=1.5$)
- b) EC method (138°C, x200 magnification)
- c) EC method (138°C, x1300 magnification)

4.4.3.2 Crystal purity

The purity of crystals obtained via both techniques was determined with ICP analysis after dissolution in 5% HCl and the results are presented in table 4.11.

Table 4.11 Chemical composition of nickel sulphate crystals

ELEMENT (%)	NiSO ₄ ·6H ₂ O (SDC)	NiSO ₄ ·2H ₂ O (CCR)
Ni	18.6	31.4
Cu	0.14	1.25
Fe	0.02	0.59
As	< 0.02	0.05
Sb	0.01	0.10
Bi	0.02	0.02
Al	0.02	0.26
Ca	0.01	0.72
Na	0.05	0.2
Mg	-	0.16
H ₂ SO ₄	0.49	5.0

The impurity content is sometimes one order of magnitude lower for certain elements in the case of crystals produced via SDC, indicating thus a purer compound.

Copper represents the major impurity adsorbed in both cases, most probably due to high initial concentration in the aqueous solution and lattice similarity.

The most striking difference between the two methods lays in the sulphuric acid content: while the traditional EC yields a product containing 5% H₂SO₄, the precipitate obtained via SDC holds only 0.5%. This difference comes from the opposite techniques employed to generate supersaturation. EC removes water to increase nickel sulphate concentration above its solubility (but in the same time H₂SO₄ in solution will be thus concentrated) whereas SDC adds the miscible organic solvent to salt-out nickel sulphate but will dilute the H₂SO₄ in solution.

The XRD spectrum of nickel sulphate produced via EC indicates also a high impurity content, revealed by numerous small peaks and an irregular base line (figure 4.27).

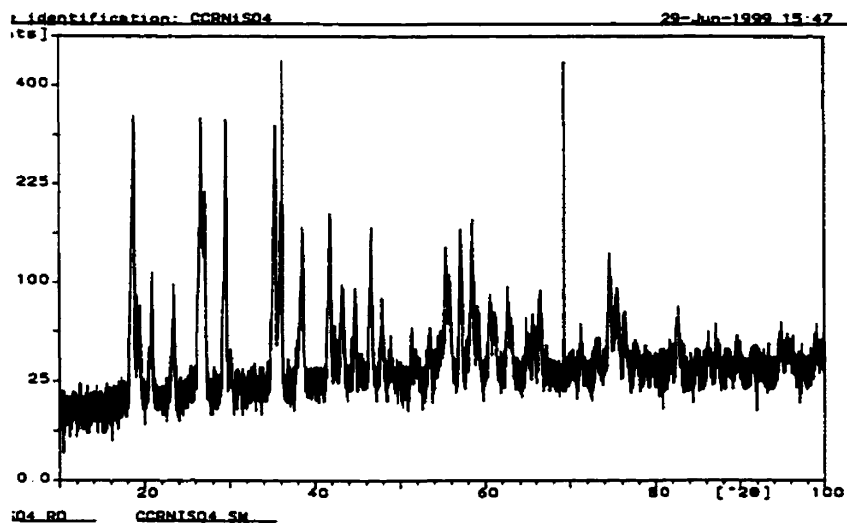


Figure 4.27 XRD spectrum of $\text{NiSO}_4 \cdot 2\text{H}_2\text{O}$ produced via EC at CCR

The XRD spectrum of nickel sulphate crystals obtained via SDC is comparatively presented in figure 4.28. The small number of peaks suggests less impurity uptake

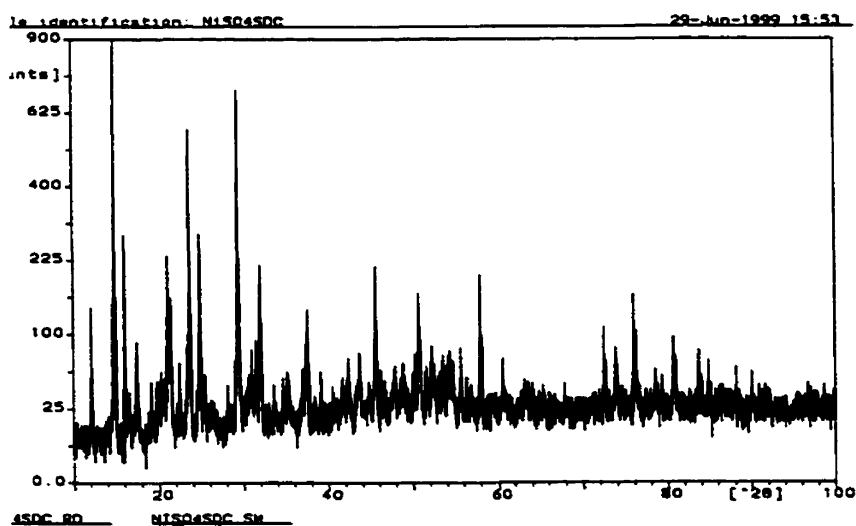


Figure 4.28 XRD spectrum of $\text{NiSO}_4 \cdot 6\text{H}_2\text{O}$ produced via SDC

Partial Conclusions

- The presence of impurities in the industrial solution leads to crystals that showed moderate growth as opposed to the product from the synthetic electrolyte for the same number of recycles. Moreover, crystals from industrial electrolyte show dislocations, cracks and broken edges, suspected to be the effect of selective adsorption of impurities on their surface.
- From the impurities contained in the industrial solution, Ca precipitates significantly as fine gypsum needles prior to and along with nickel sulphate during SDC.
- Nevertheless, SDC technique leads to better quality crystals (in terms of purity and particle size) than the traditional EC method.

4.5 Flowsheet Development

4.5.1 Production of $\text{NiSO}_4 \cdot 6\text{H}_2\text{O}$ from industrial electrolyte

One of the main objectives of the present research work was to design a SDC procedure that yields clean, well-grown crystals and then to test the newly designed method with industrial electrolyte solutions.

The results described so far in this thesis demonstrated that it is possible to use IP (or IP- H_2O azeotrope) to salt-out nickel sulphate from an industrial decopperised electrolyte, producing good quality crystals. Based on these results, a general schematic flowsheet was conceived for the treatment of an industrial decopperised electrolyte that leaves the cellhouse containing ~ 20 g/l Ni, ~ 250 g/l H_2SO_4 as principal components and minor impurities (figure 4.29).

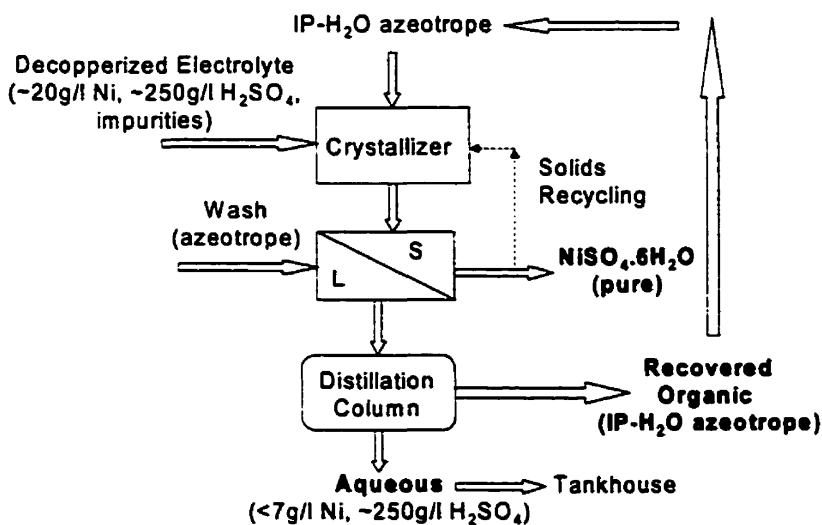


Figure 4.29 Nickel sulphate recovery from industrial decopperised electrolyte by SDC

In this process, the decopperised electrolyte leaves the cellhouse (where Cu, As, Bi and Sb have been removed by EW) at ~ 40 - 50°C and enters the crystalliser in the nickel recovery section. For practical purposes, IP- H_2O azeotrope as opposed to pure IP is preferred as salting-out agent; the azeotrope is added in a controlled manner, under moderate agitation, to the aqueous solution. The quantity of nickel precipitated at this stage depends on the O/A ratio and the temperature. A more elevated working temperature requires a higher O/A ratio. The crystalline product is separated by filtration or centrifuging, washed with azeotrope and

packaged. If larger $\text{NiSO}_4 \cdot 6\text{H}_2\text{O}$ particles are sought for, part of the solids can be recycled back to the crystalliser and used as seed in a heterogeneous SDC process; the solids recycling loop can be repeated until the required particle size is achieved.

The organic phase (azeotropic mixture) is recovered from the filtrate by fractional distillation at 80°C ; for high distillation efficiency, a packed column with 7-10 theoretical vaporisation-condensation plates would be required (Pavia et al., 1982). The distillate, exclusively azeotropic mixture, will be returned to the nickel recovery process for reuse.

The remaining aqueous phase contains less than 7 g/l Ni and the same amount of H_2SO_4 as the initial effluent (250 g/l). The solution can be returned to the Cu ER tankhouse to be mixed to the fresh electrolyte. Depending on the water balance requirements of the plant, pre-concentration of the acid solution to ~ 500 g/l H_2SO_4 by evaporating part of the water but without crystallising nickel sulphate may be practised.

4.5.2 Control of gypsum precipitation

As previously described (section 4.4), calcium is the only impurity whose significant co-precipitation as gypsum interferes with nickel sulphate crystallisation process during SDC, leading thus to an impure final product.

To avoid this problem, Ca removal from the industrial electrolyte before nickel crystallisation may be required. This can be achieved by removing part of gypsum prior to nickel sulphate crystallisation without introducing new substances to the system (except the salting out agent already employed), reducing thus to some extent the contamination of $\text{NiSO}_4 \cdot 6\text{H}_2\text{O}$.

A more detailed look on the nickel sulphate SDC process including a gypsum partial removal step is given in figure 4.30. The decopperised electrolyte, containing in principal Ni, sulphuric acid and minor impurities, enters the first crystalliser where azeotrope is added at a certain O/A ratio to precipitate the maximum possible amount of gypsum without initiating nickel sulphate crystallisation. After equilibration, gypsum is removed by filtration and the filtrate enters the second crystalliser where another O/A ratio is added to cause nickel sulphate separation. At this point azeotrope addition is performed in a controlled manner as to maintain a low supersaturation and seed can be used to favour growth; the process continues than as described in section 4.5.1.

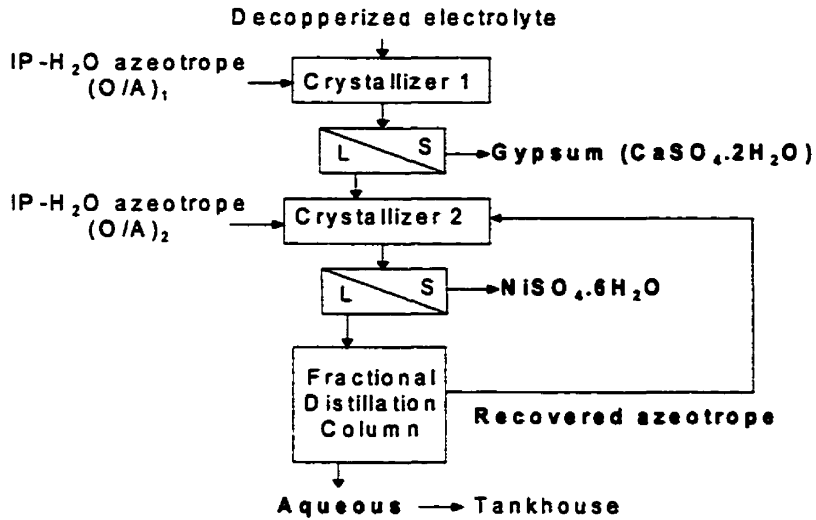


Figure 4.30 SDC of nickel sulphate with gypsum partial removal option

Although gypsum co-precipitation will still occur together with nickel sulphate, this process has the advantage of partially removing some gypsum and reducing thus the impurity content of the final product. Moreover, no additional reagents are introduced in the system, the same salting out principles being employed to precipitate gypsum prior to nickel sulphate, achieving thus some degree of selectivity.

5. CONCLUSIONS AND RECOMMENDATIONS

5.1 Conclusions

The goal of this research was to study the Solvent Displacement Crystallisation technique as described in literature (Cohen, 1987), by employing isopropanol (IP) as water-miscible organic solvent to homogeneously precipitate nickel sulphate from electrolyte solutions ($\text{NiSO}_4\text{-H}_2\text{O-H}_2\text{SO}_4$). The subsequent strategy was not only to design a SDC procedure that yields clean, well-grown crystals by maintaining low supersaturation and recycling the product as seed (heterogeneous crystallisation), but also to test the newly designed SDC method with industrial electrolyte solutions and compare the product quality with that obtained by the conventional procedure (Evaporative Crystallisation).

From the results of this work, the following conclusions can be drawn:

- Isopropanol was confirmed as an effective salting out agent to cause precipitation of $\text{NiSO}_4\cdot 6\text{H}_2\text{O}$ from synthetic and industrial electrolyte solutions.
- The amount of salt crystallised and the final nickel concentration in the aqueous phase depend on the organic to aqueous ratio (O/A). When O/A=1.5 was employed, ~74% of the initial nickel was precipitated as $\text{NiSO}_4\cdot 6\text{H}_2\text{O}$ and the final Ni concentration in the aqueous phase was comparable to that obtained in industry via evaporative crystallisation (~6 g/l Ni).
- Elevated working temperatures and use of azeotrope mixture as opposed to pure IP require the use of a higher O/A to achieve a similar final nickel concentration.
- Organic recovery is performed by fractional distillation, isopropanol being removed as azeotrope (88% IP wt/wt) at 80°C. In a potential industrial implementation of SDC, recycling of azeotrope as opposed to pure IP would be preferable.
- Critical solubility lines in water-isopropanol mixtures have been established for both synthetic and industrial solutions.
- Crystallisation kinetics is faster with the synthetic solution but high supersaturation (homogeneous crystallisation) leads to fine crystal product.

- Use of seed and product recycling in conditions of low supersaturation (heterogeneous crystallisation) promotes particle growth. However, crystals from the industrial solution exhibit a more modest growth and have a rougher morphology than those obtained from the synthetic one, due to adsorption of impurities on the surface.
- Calcium, in the form of gypsum ($\text{CaSO}_4 \cdot 2\text{H}_2\text{O}$), is the only impurity that significantly co-precipitates with nickel sulphate from the industrial electrolyte, yielding to contaminated final product.
- When the SDC and EC methods are compared from the standpoint of crystal quality, it appears that SDC produce cleaner particles (lower impurity uptake) and, if heterogeneous crystallisation conditions are maintained, the growth process is also favoured.

5.2 Recommendations for Future Work

- More SDC tests should be performed on the industrial electrolyte to match the actual plant conditions: temperature of 40-50°C, partial water evaporation prior to crystallisation in order to maintain the overall water balance and use of azeotrope.
- Although in theory all IP must be removed as azeotrope, traces of organic carry-over in the aqueous phase after distillation should be monitored and the effect of residual IP on Cu ER process (if any) should be studied.
- The optimal operating conditions must be perfected (O/A ratio, product recycles number, seed load, efficient distillation) and a procedure to avoid gypsum co-precipitation should be established and integrated to the SDC of nickel sulphate.
- Ultimately, consideration should be given to the selection of an appropriate crystalliser for this type of process.

REFERENCES

- Z. B. Alfassi, *The Separation of Electrolytes in Aqueous solution by Miscible Organic Solvents*, in "Separation Science and Technology", vol. 14(2), pp.155-161, 1979
- Z. B. Alfassi, S. Mosseri, *Solventing out of Electrolytes from their Aqueous Solutions*, in "AIChE Journal", vol. 30(5), pp.874-876, 1984
- K. Ando, N. Tsuchida, *Recovering Bi and Sb from Electrolyte in Copper Electrorefining*, in "JOM", vol. 49(12), pp. 49-51, 1997
- A.K. Biswas, W.G. Davenport, *Extractive Metallurgy of Copper*, 3rd edition, Pergamon, London, U.K., pp. 324-335, 1994
- T.B. Braun, J.R. Rawling, K.J. Richards, *Factors Affecting the Quality of Electrorefined Cathode Copper*, in "Extractive Metallurgy of Copper", vol. I "Pyrometallurgy and Electrolytic Refining", J.C. Yannopoulos and J.C. Agarwal, editors, The Metallurgical Society of AIME, New York, N.Y., pp. 511-524, 1976
- J.R.L. Bravo, *Aspects of Impurity Control at Caraiba Metais Electrorefinery*, in "EPD Congress 1997", B. Mishra, editor, TMS, Warrendale, Pa., pp. 403-412, 1997
- D.A. Busch, J.R. Stone, G. Chiszar, *Production of Refined Nickel Sulphate at Asarco's Perth Amboy Plant*, in "Extractive Metallurgy of Copper, Nickel and Cobalt", P. Queneau, editor, Interscience Publishers, New York, N.Y., pp. 469-474, 1961
- T.T. Chen, J.E. Dutrizac, *The Mineralogy of Copper Electrorefining*, in "JOM", vol. 42(8), pp. 39-44, 1990-a
- T.T. Chen, J.E. Dutrizac, *A Mineralogical Overview of the Behaviour of Nickel during Copper Electrorefining*, in "Metallurgical Transactions B", vol. 21B, pp. 229-238, 1990-b
- P.P. Chiang, M.D. Donohue, *Crystallization from Ionic Solution*, in "Fundamental Aspects of Crystallization and Precipitation Processes", AIChE Symposium Series, vol.

- 83(253), D.M. Briedis and K.A. Ramanarayanan, editors, AIChE, New York, N.Y., pp. 8-14, 1987
- J.M. Cohen, *Applications of Solvent Displacement Crystallization in Hydrometallurgy*, in "Separation Processes in Hydrometallurgy", G.A. Davies, editor, Ellis Horwood, London, pp. 265-273, 1987
- P.M. Cole, A.M. Feather, *A Solvent Extraction Process to Recover Copper and Nickel from a Tankhouse Effluent*, in "Copper 95-Cobre 95 International Conference", vol. III, "Electrorefining and Hydrometallurgy of Copper", W.C. Cooper et. al, editors, MetSoc of CIM, Montreal, PQ, pp. 607-616, 1995
- B. Conrad, *Impurity/Behaviour and Control in Cu ER*, from "Short Course on Fundamentals and Practice of Aqueous Electrometallurgy", MetSoc of CIM, Montreal, PQ, pp. 14-21, 1990
- G.P. Demopoulos, *Precipitation and Crystallization*, lecture presented at the "Workshop on Aqueous Processing of Inorganic materials", 9th CMSC, MetSoc of CIM, Montreal, PQ, June 17-20, 1997
- G.P. Demopoulos, D.J. Droppert, G. van Weert, *Hydrometallurgy*, vol. 38(3), pp. 245-262, 1995
- R.F. Dobner, *Bleed-off Treatment at Hutterwerke's Secondary Copper Electrorefinery*; in "EPD Congress 1997", B. Mishra, editor, TMS, Warrendale, Pa., pp. 413-424, 1997
- E.W. Flick, *Industrial Solvents Handbook*, 3rd edition, Publications Noyes, Parkridge, N.J., p. 223, 1985
- F. Franks, *The Properties of Aqueous Solutions of Non-Electrolytes*; in "Physico-Chemical Processes in Mixed Aqueous-Solvents", F. Franks, editor, Elsevier, New York, N.Y., pp. 50-69, 1967
- T. Havlik, M. Skrobjan, R. Kammel, J. Curilla, *Refining of Crude Nickel Sulfate Obtained from Copper Electrolyte*, in "Hydrometallurgy", vol. 41, pp. 79-88, 1996

- J.E. Hoffmann, *Process Options in the Treatment of Copper Refinery Electrolyte Bleed*; in "EPD Congress 1997", B. Mishra, editor, TMS, Warrendale, Pa., pp. 435-451, 1997
- V.T. Isakov, *The Electrolytic Refining of Copper*, Technicopy Ltd, Stonehouse, U.K., pp. 47-51, 1973
- W.F. Linke, A. Seidell, *Solubilities of Inorganic and Metal Organic Compounds (a compilation)*, 4th edition, Van Nostrand, Princeton, N.J., pp. 1219-1222, 1958
- J.A. Monick, *Alcohols: Their Chemistry, Properties and Manufacture*, Reinhold Book Corporation, New York, N.Y., pp. 119-125, 1968
- J.W. Mullin, *Crystallization*, 3rd edition, Butterworth-Heinemann, Oxford, U.K., pp. 172-263, 1993
- A.E. Nielsen, *Electrolyte Crystal Growth Mechanisms*, in "Journal of Crystal Growth", vol. 67, 1984, pp. 289-310
- R.L. Nyirenda, W.S. Phiri, *The Removal of Nickel from Copper Electrowinning Bleed-off Electrolyte*, in "Minerals Engineering", vol. 11(1), pp. 23-37, 1998
- S.J. Omelon, *High Solids Density Production through an Improved Neutralization Process for Zinc Plant Effluent*, (MEng Thesis), McGill University, Montreal, PQ, 1998
- D.L. Pavia, G.M. Lampman, G.S. Kriz, jr., *Introduction to Organic Laboratory Techniques (a contemporary approach)*, Saunders College Publishing, Philadelphia, Pa., pp. 514-635, 1982
- F.T. Principe, *Separation of Iron (III) from zinc sulfate-sulfuric acid using organophosphoric acid extractants* (MEng Thesis), McGill University, Montreal, PQ, 1999
- A. Rehioui, G. Johansson, *Electrochemical Behaviour of Isopropanol at Platinum Electrodes*, in "Talanta", vol. 18, pp. 329-337, 1971

- R. Rohmer, *Contribution a l'Étude du Sulfate de Nickel et du Sulfate de Cobalt*, in "Annales de Chimie", tome 11, pp. 611-721, 1939
- E. Rolia, J.E. Dutrizac, *The Determination of Free Acid in Zinc Processing Solutions*, in "Canadian Metallurgical Quarterly", vol. 23(2), pp. 159-167, 1984
- N. Sato, Y. Wei, M. Nanjo, M. Tokuda, *Recovery of Samarium and Neodymium from Rare Earth Magnet Scraps by Fractional Crystallization Method*, in "Metallurgical Review of MMIJ", vol 15(1), pp. 1-13, 1998
- H. Schneider, *The Selective Solvation of Ions in Mixed Solvents* in "Solute-Solvent Interactions", J.F. Coetzee and C.D. Ritchie, editors, Marcel Dekker, New York, N.Y., pp. 329-342, 1969
- D.A. Weingaertner, S. Lynn, D.N. Hanson, *Extractive Crystallization of Salts from Concentrated Aqueous Solution*, in "Ind. Eng. Chem. Res.", vol. 30(3), pp. 490-501, 1991

APPENDIX A

MODIFIED FREE ACID TITRATION METHODOLOGY

Acid-Measurement Problems

Free acid concentration in strong $\text{H}_2\text{SO}_4\text{-MSO}_4$ ($\text{M}=\text{Fe}, \text{Zn}, \text{Ni}, \text{etc.}$) solutions is impossible to be accurately determined using direct pH measurements; analysis by simple neutralisation with an alkaline titrant alone is very problematic also. For example, titrating with NaOH proves ineffective as neutralisation raises the analyte pH, causing result-distorting metal hydrolysis to occur. Consequently, a method utilising a complexing agent was considered.

Rolia and Dutrizac (1984) developed an analytical method that employed EDTA as a complexing agent; Mg_2EDTA solution is added to the diluted aliquot sample prior to neutralisation to exchange Mg^{2+} for the hydrolysable metals present in the analyte. This prevents any acid-producing metal hydrolysis to occur. However, since problems were encountered in applying this procedure to the experimental samples of interest, regardless of metal-acid medium, modifications to this methodology were necessary.

Principe (1999) modified and adapted the previously described technique in order to develop an accurate acid-measurement means in $\text{H}_2\text{SO}_4\text{-MSO}_4$ ($\text{M}=\text{Fe}$ and Zn) solutions based on the endpoint pH value without the risk of errors (5-20%) induced by the unmodified method.

The present research project adopts Principe's method and applies it to the system $\text{H}_2\text{SO}_4\text{-NiSO}_4$.

Preparation of Standards

Daily standardisation not only determines the endpoint pH, but also corrects for pH calibration error and $\text{Mg}_2\text{EDTA}^{2-}$ variations among batches. The procedure involved the preparation and use of one standard (solution A) of composition comparable to the experimental samples of interest. A second standard (solution B), also of comparable composition to experimental samples, was prepared and used to validate the standardisation with solution A. Acid levels of solutions A and B were different,

respecting upper and lower limits of a range in which the experimental samples fall (table A.1). A detailed description of this analytical method follows.

Table A.1 Preparation of H_2SO_4 - NiSO_4 standard solutions

Standard Type	1N NaOH (ml)	Endpoint pH (*)	$[\text{H}_2\text{SO}_4]_{\text{estimated}}$ (g/l)	$[\text{H}_2\text{SO}_4]_{\text{calculated}}$ (g/l)	Ni (g/l)
A	4.05	6.344	200	198.76	17.96
B	6.08	6.339	300	297.95	18.63

(*) value slightly differs upon daily standardisation

Titration Methodology

I. Titration Procedure

- (1) pour 50 ml of Mg_2EDTA solution into 150 ml beaker equipped with a magnetic stirring bar, mounted in auto-titration set-up;
- (2) pipet 1.00 ml of sample into same beaker, under mild agitation;
- (3) dilute with de-ionised water to 120 ml mark on beaker (by eye);
- (4) perform "standardisation" or "sample measurement".

II. Standardization

- (1) use the two standard solutions (A and B) previously described (sulphuric acid and nickel content may differ but should respect the concentration range of the experimental samples);
- (2) use solution A as the standardisation analyte and prepare the titration solution as in the "Titration Procedure" above;
- (3) set titrator to allow for a manual shutdown;
- (4) calculate the amount of NaOH 1N needed to neutralise analyte solutions A and B;
- (5) press RUN to start auto-titrator feeding 1N NaOH to solution A;
- (6) record the exact solution pH value at which the calculated titrant volume has been added (endpoint pH);
- (7) press STOP to end standardisation titration (manual shutdown);

- (8) program the titrator by setting the pH endpoint to the recorded value ($\text{pH}_{\text{endpoint}}$) and enable automatic predose to a set pH value ($\text{pH}_{\text{predosed}} < \text{pH}_{\text{endpoint}}$), to reduce overall titration time;
- (9) follow the "Titration Procedure" above using solution B as the analyte, to verify that standardisation just performed as valid;
- (10) follow "Sample Measurement" as detailed below;
- (11) the determined acid concentration should equal the known acid concentration:
 - (a) if not equal, redo standardisation with solutions A and B
 - (b) if equal, standardisation was properly performed; experimental samples may now be analysed ("Titration Procedure" then "Sample Measurement").

III. Sample Measurement

- (1) set to pertinent stored ENDPOINT methodology;
- (2) press RUN to add 1N NaOH titrant automatically;
- (3) following automatic shutoff, the total volume added to reach end-point is printed;
- (4) calculate the acid concentration:

$$m_a = N_a * E_g * V_{\text{sol}}$$

- where:
- $E_g = 98/2 = 49$: the gram-equivalent
 - V_{sol} = the total volume of solution
 - $N_a = V_b \cdot N_b / V_a$: acid's normal concentration
 - V_a = volume of analyte used in titration
 - V_b = volume of NaOH used in titration
 - N_b = NaOH normal concentration

APPENDIX B

PROPERTIES OF ISOPROPANOL

2-Propanol, $\text{CH}_3\text{CHOHCH}_3$, is the simplest secondary alcohol, also designated under the following conventional and non-conventional terms: isopropyl alcohol, secondary propyl alcohol, isopropanol, dimethylcarbinol, per-spirit, petrohol, avantine (Monick, 1968).

- **Physical Properties**

Isopropanol (IP) is a colourless, flammable liquid with a pleasant, characteristic odour, but has a bitter taste. It is stable under normal conditions and soluble in water (miscible) in all proportions. Solvent properties of IP are excellent with respect to natural fats and oils, essential oils, waxes, hydrocarbons, alkaloids, resins and organic compounds. It does not solvate most of inorganic compounds, for which acts as an effective salting-out agent. Physical constants of isopropanol are given in table B.1.

Table B.1 Physical properties of Isopropanol (Flick, 1985)

Property	Value	Property	Value
Acidity (as acetic acid)	0.002% (wt)	Max. Acceptable Conc.	200ppm in air
Boiling point (760mm)	82.3°C	Molecular weight	60.09
Dielectric constant (20°C)	18.62	Non-volatile matter	0.002g/100ml
Dipole moment	1.68 Debye	Purity	99.5%
Fire hazard	dangerous	Refractive index (20°C)	1.3772
Flash pt. (open cup)	15°C	Specific conductivity	$3.5 \cdot 10^{-6}$ mhos/cm
Freezing pt.	-87.7°C	Specific gravity (20°C)	0.786
Heat of combustion	7970 cal/g	Specific heat (20°C)	0.596 cal/g°C
Heat of fusion	21.08 cal/g	Surface tension (20°C)	21.7 dynes/cm
Heat of vaporization (b.p)	165 cal/g	Vapour pressure (20°C)	33 mmHg
Limit of flammability	2.65% (vol)	Viscosity (20°C)	2.4 cps

- **Toxicity**

Only slight to moderate toxic effects of IP on humans have been reported (Monick, 1968). Ingestion may have a small effect on respiration, but the pulse slows and the appetite is lost. However, prolonged ingestion of large doses causes coma at lower blood concentrations than ethanol.

Although IP has a narcotic effect on the central nervous system, the danger from inhalation is slight due to its low volatility and relatively high boiling point. The maximum allowable concentration of IP vapours for an 8-hr exposure has been estimated at 200 ppm, but no harmful intermediates are formed by the animal metabolism. Ingested IP diffuses into all the tissues and it is partially changed to acetone before elimination by lungs (detected in breath after 15 min) and kidneys (detected in urine after 1hr).

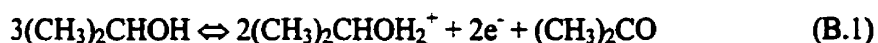
- **Electrochemical Behaviour of Isopropanol**

Since the present research project proposes the use of IP as a salting-out agent to be employed in conjunction with the Cu ER process, it is important to determine its electrochemical behaviour during electrolysis.

Rehioui and Johansson (1971) studied the reactions that limit the potential range of IP at a platinum electrode (Pt electrodes exhibit a high overpotential for O₂ evolution and are passive in almost any media), using 0.05M sodium perchlorate as supporting electrolyte.

I. Oxidation Limit

Anodic oxidation of IP solutions containing 0.05M sodium perchlorate occurs at 1.32 V (vs. SHE), resulting in an acidification of the medium and formation of acetone:



II. Reduction Limit

During electrolysis of IP-NaClO₄ solutions, H₂ evolved at the Pt electrode at - 0.98 V (vs. SHE):



When reactions (1) and (2) take place in the electrolysis cell, the net result is decomposition of IP according to the reaction:



Formation of water arises from a chemical side-reaction (acid-catalysed) between acetone and IP, assumed to be:



In conclusion, IP has a larger accessible potential range than water (from 1.32 to -0.98 V vs. SHE) and it should be electrochemically stable during Cu ER process.

APPENDIX C

FRACTIONAL DISTILLATION

When the boiling-point differences of two components are not large ($< 30^{\circ}\text{C}$), *fractional distillation*, as opposed to simple distillation, must be used to achieve a good separation. Pavia et al. (1982) give detailed information on distillation techniques and related theoretical background in their comprehensive book.

- ***Principles of Fractional Distillation***

When an ideal solution of two liquids (L1 and L2) is distilled by simple distillation, the first vapour produced will be enriched in the lower-boiling point component (say L1). Analysis of the condensed phase will determine that the distillate does not contain pure L1, since the boiling-point difference between L1 and L2 is below 30°C . Likewise, the liquid remaining in the distilling flask will contain a larger amount of the higher-boiling point component but will not be pure L2. However, if redistilled, each of these fractions would become enriched in the lower-boiling point component (L1). After a certain number of redistillations, one should obtain distillate that would be essentially pure L1 and a residue that would be pure L2.

Fractional distillation, by using a column inserted between the distilling flask and the distilling head, accomplishes all the redistillation cycles required in a single step. The column is insulated and filled with a suitable packing material (glass beads, glass helices, stainless steel sponge, etc.) that allows a mixture of L1 and L2 to be subjected continuously to many vaporisation-condensation cycles as it moves up the column (figure 3.2, chapter 3). With each cycle, the composition of the vapour is progressively enriched in the lower-boiling point component, thus nearly pure L1 emerges from the top of the column, condenses and passes into the receiving flask as the first fraction. The distillation must be carried out slowly to ensure numerous vaporisation-condensation cycles and to avoid column flooding (otherwise, the efficiency of separation decreases), but fast enough to maintain a constant rate at which material collects in the receiver. The temperature at the thermometer bulb should remain constant as a pure component is

removed; when most of the component is distilled, the distillation rate decreases and the temperature rises again.

- **Column Efficiency**

The number of *theoretical plates* gives a good measure of column efficiency (Pavia et al., 1982). Each theoretical plate corresponds to a simple distillation, or one vaporisation-condensation cycle. For example, if a liquid mixture requires five vaporisation-condensation equilibria within the column to be efficiently separated, a packed column with five theoretical distillation plates should be used (the first theoretical plate always corresponds to the initial vaporisation from the distilling flask).

The relation between the number of theoretical plates needed to separate a two-component mixture and the difference between the boiling points of the components are given in table C.1. However, since columns are seldom operated at equilibrium, more theoretical plates than listed may be necessary for a complete separation.

Table C.1 Theoretical plates required to separate liquid mixtures (Pavia et al., 1982)

Boiling-point difference (°C)	# Theoretical plates
108	1
72	2
54	3
43	4
36	5
20	10
10	20
7	30
4	50
2	100

As observed, the number of theoretical plates (efficiency) of the column must increase as the boiling-point differences between the components decrease for the separation to be adequate.

- **Fractional Distillation of Isopropanol-Water Azeotrope**

Many mixtures of compounds, because of intermolecular attractions or repulsions, do not show ideal behaviour and thus Raoult's law is not followed. The law states that the partial vapour pressure of component A in the solution (P_A) equals the vapour pressure of pure A (P_A^0) times its mole fraction (N_A) in the solution; same expression can be written for B.

The type of vapour-liquid diagram that results from such a non-ideal behaviour in the case of IP-H₂O system is a *minimum-boiling-point diagram*; the minimum point in such a diagram correspond to a constant-boiling point mixture called an *azeotrope*. The azeotrope has a fixed composition (88% IP, 12% H₂O wt/wt) which cannot be altered by fractional distillation and a fixed boiling point (80.4°C); hence, an azeotrope acts as if it were a pure compound (Pavia et al., 1982).

A minimum-boiling-point azeotrope results from a slight incompatibility of the substances, which leads to higher-than-expected combined vapour pressures from the solution; the higher combined vapour pressures bring about a lower boiling point for the mixture. The behaviour on fractional distillation of an isopropanol-water mixture of composition X can be described according to the phase diagram in figure C.1.

The phase diagram relates the composition of the boiling liquid (lower curve) and its vapour (upper curve) as a function of temperature. The *horizontal* lines represent the *vaporisation* step of a given vaporisation-condensation cycle and indicates the composition of the vapour in equilibrium with liquid at a given temperature. Each of the *vertical* lines represents the *condensation* step; the composition does not change as the temperature drops on condensation.

The mixture is heated (XL1) until is observed to boil (L1). The vapour (V1) will be richer in the lower-boiling point component (the azeotrope) than the original mixture. The condensate (L2) is vaporised again within the column to give V2. The process continues, following the lines to the right, until the *azeotrope* is obtained (V3). The distillate is not pure IP, but contains 88% IP and 12% water. The contents of the distilling flask become progressively richer in the higher-boiling point component as the distillation proceeds. When all the alcohol is removed as azeotrope, pure water remains, distilling at 100°C.

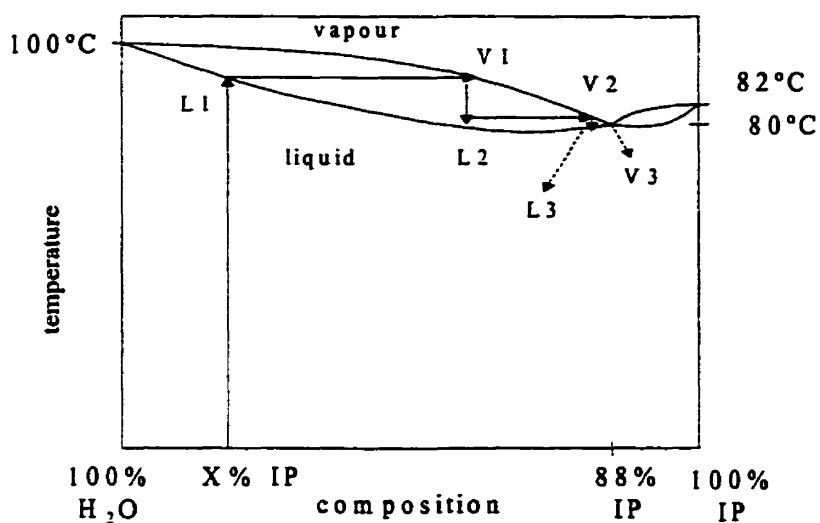


Figure C.1 Isopropanol-water phase diagram (adapted from Pavia et al., 1982)

If complete separation is required, an *azeotropic distillation* should be employed to obtain pure anhydrous isopropanol. However, this procedure is more complicated since it involves the addition of an inert solvent as a third phase and comprises two separate distillation sessions (Pavia et al., 1982).

As the azeotrope contains 88% IP, it is considered efficient enough to be employed as such as salting out agent for nickel sulphate in SDC tests. Therefore, the present research project considered only the fractional distillation as a simple means of separation.

APPENDIX D

NICKEL SULPHATE HYDRATES

Solvent molecules are frequently found in association with precipitated materials. For example, crystalline substances often form with water molecules located at specific sites, e.g. *water of crystallisation*, held in co-ordination complexes around lattice cations. These products are referred as *hydrates*; a certain substance may present several hydrates, depending on temperature and the presence of dehydrating agents in solution.

The transition between different hydrates (i.e. the solid phase changes) can be visualised as a break in the continuous solubility curve of a certain substance function of temperature. Such a break appears at the temperature at which the solution is saturated with respect to both solid phases (Mullin, 1993).

Usually, at temperatures below 85°C, NiSO₄ has two stable hydrates: one heptahydrate and one hexahydrate (dimorphs $\alpha \leftrightarrow \beta$). Both these hydrates can exist in unstable equilibrium with their saturated solution, even above the transition temperature between each of them. NiSO₄.7H₂O represents the form encountered from 0 to ~31°. The temperature of 31.2°C marks the transition NiSO₄.7H₂O \leftrightarrow α -NiSO₄.6H₂O, whereas at ~53.3°C the transformation α -NiSO₄.6H₂O \leftrightarrow β -NiSO₄.6H₂O happens. In the temperature range 85-100°C the β -hexahydrate becomes unstable and Rohmer (1939) reported the existence of unstable inferior hydrates (NiSO₄.5H₂O, 4H₂O, 3H₂O, 2H₂O and 1H₂O). Above 100°C the monohydrate is the only stable form. Table D.1 summarises the NiSO₄ hydrates as they are described in literature.

Table D.1 Nickel sulphate hydrates (adapted from Linke and Seidell, 1958)

Temperature (°C)	Hydrate	Description
0 - 31	$\text{NiSO}_4 \cdot 7\text{H}_2\text{O}$	stable; green; rhombic
31.2	Transition $\text{NiSO}_4 \cdot 7\text{H}_2\text{O} \leftrightarrow \alpha\text{-NiSO}_4 \cdot 6\text{H}_2\text{O}$	
31.2 - 53.3	$\alpha\text{-NiSO}_4 \cdot 6\text{H}_2\text{O}$	stable; greenish-blue tetragonal
53.3	Transition $\alpha\text{-NiSO}_4 \cdot 6\text{H}_2\text{O} \leftrightarrow \beta\text{NiSO}_4 \cdot 6\text{H}_2\text{O}$	
53.3 - 85	$\beta\text{NiSO}_4 \cdot 6\text{H}_2\text{O}$	stable; green; monoclinic
85 - 100 Unstable equilibria	$\beta\text{NiSO}_4 \cdot 6\text{H}_2\text{O} \leftrightarrow \text{NiSO}_4 \cdot 5\text{H}_2\text{O}$ $\beta\text{NiSO}_4 \cdot 6\text{H}_2\text{O} \leftrightarrow \text{NiSO}_4 \cdot 4\text{H}_2\text{O}$ $\beta\text{NiSO}_4 \cdot 6\text{H}_2\text{O} \leftrightarrow \text{NiSO}_4 \cdot 3\text{H}_2\text{O}$ $\beta\text{NiSO}_4 \cdot 6\text{H}_2\text{O} \leftrightarrow \text{NiSO}_4 \cdot 2\text{H}_2\text{O}$ $\beta\text{NiSO}_4 \cdot 6\text{H}_2\text{O} \leftrightarrow \text{NiSO}_4 \cdot \text{H}_2\text{O}$	$\text{NiSO}_4 \cdot 5\text{H}_2\text{O}$ - green $\text{NiSO}_4 \cdot 4\text{H}_2\text{O}$ - light green $\text{NiSO}_4 \cdot 3\text{H}_2\text{O}$ - greenish-yellow $\text{NiSO}_4 \cdot 2\text{H}_2\text{O}$ - yellow $\text{NiSO}_4 \cdot \text{H}_2\text{O}$ - light yellow
> 100	$\text{NiSO}_4 \cdot \text{H}_2\text{O}$	stable; light yellow;

The dehydration process stops at monohydrate, under relatively mild conditions ($T \sim 100^\circ\text{C}$, atmospheric pressure). The anhydrous salt can be obtained only at high temperatures and pressures or in the presence of a dehydrating agent.